UNIVERSITY OF CALIFORNIA

Radiation Laboratory

BERKELEY, CALIFORNIA

DISCLAIMER

UCRL-590
Unclassified Distribution

cy 2

UNIVERSITY OF CALIFORNIA

Radiation Laboratory

Contract No. W-7405-eng-48

THE RELATION OF PHOTOSYNTHESIS TO RESPIRATION

John W. Weigl

April 27, 1950

Berkeley, California

INSTALLATION	No. of Copies
Argonne National Laboratory	8
Armed Forces Special Weapons Project	1
Atomic Energy Commission, Washington	2
Battelle Memorial Institute	1
Brush Beryllium Company	1
Brookhaven National Laboratory	8
Bureau of Medicine and Surgery	1
Bureau of Ships	1
Carbide and Carbon Chemicals Div., Union Carbide and Carbon Corp. (K-25 Plant)	4
Carbide and Carbon Chemicals Div., Union Carbide and Carbon Corp. (Y-12 Plant)	4
Chicago Operations Office	1
Cleveland Area Office, AEC	1
Columbia University (J. R. Dunning)	2
Columbia University (G. Failla)	1
Dow Chemical Company	1
H. K. Ferguson Company	1
General Electric Company, Richland	3
Harshaw Chemical Corporation	1
Idaho Operations Office	1
Iowa State College	2
Kansas City Operations Branch	1
Kellex Corporation	2
Knolls Atomic Power Laboratory	4
Los Alamos Scientific Laboratory	3
Mallinckrodt Chemical Works	1
Massachusetts Institute of Technology (A. Gaudin)	1
Massachusetts Institute of Technology (A. R. Kaufmann)	1
Mound Laboratory	3
National Advisory Committee for Aeronautics	2
National Bureau of Standards	2
Naval Radiological Defense Laboratory	2
New Brunswick Laboratory	1
New York Operations Office	5
North American Aviation, Inc.	1
Oak Ridge National Laboratory	8
Patent Branch, Washington	1
Rand Corporation	1
Sandia Laboratory	1
Sante Fe Operations Office	1
Sylvania Electric Products, Inc.	1
Technical Information Division, Oak Ridge	15
USAF, Air Surgeon (R. H. Blount)	1
USAF, Director of Armament (C. I. Browne)	1
USAF, Director of Plans and Operations (R. L. Applegate)	1
USAF, Director of Research and Development (F. W. Bruner and R. J. Mason)	2
USAF, Eglin Air Force Base (A. C. Field)	1

INSTALLATION	No. of Copies
USAF, Kirtland Air Force Base (M. F. Cooper)	1
USAF, Maxwell Air Force Base (F. N. Moyers)	1
USAF, NEPA Office	2
USAF, Office of Atomic Energy (A. A. Fickel and H. C. Donnelly)	2
USAF, Offutt Air Force Base (H. R. Sullivan, Jr.)	1
USAF, Wright-Patterson Air Force Base (Rodney Nudenberg)	1
U. S. Army, Atomic Energy Branch (A. W. Betts)	1
U. S. Army, Army Field Forces (James Kerr)	1
U. S. Army, Commanding General, Chemical Corps Technical Command (J. A. MacLaughlin thru Mrs. G. Benjamin)	1
U. S. Army, Chief of Ordnance (A. R. Del Campo)	1
U. S. Army, Commanding Officer Watertown Arsenal (C. H. Deitrick)	1
U. S. Army, Director of Operations Research (Ellis Johnson)	1
U. S. Army, Office of Engineers (Allen O'Leary)	1
U. S. Army, Office of the Chief Signal Officer (Curtis T. Clayton thru G. C. Hunt)	1
U. S. Army, Office of the Surgeon General (W. S. Stone)	1
U. S. Geological Survey (T. B. Nolan)	1
U. S. Public Health Service	1
University of California at Los Angeles	1
University of California Radiation Laboratory	5
University of Rochester	2
University of Washington	1
Western Reserve University	2
Westinghouse Electric Company	4
University of Rochester (R. E. Marshak)	1
California Institute of Technology (R. F. Bacher)	1
Total	144

Information Division
Radiation Laboratory
University of California
Berkeley, California

TABLE OF CONTENTS

THE RELATION OF PHOTOSYNTHESIS TO RESPIRATION

UCRL-590
Unclassified Distribution

THE RELATION OF PHOTOSYNTHESIS TO RESPIRATION*

By

John Wolfgang Weigl

Radiation Laboratory and Department of Chemistry

University of California, Berkeley, California

April 27, 1950

ABSTRACT

The gas exchange by barley seedlings of O_2, CO_2, and added C^*O_2 has been measured in a closed system, with the following results:

1) The carbon of newly formed photosynthetic intermediates is not available for respiration while the light is on but becomes immediately respirable in the dark. The enhancement of dark respiration after a light period is very probably due to the built-up "photosynthates".

2) Photosynthesis proceeds at a measurable rate even at the lowest CO_2 pressures observed (.03 mm.Hg). There is no evidence for a "threshhold" concentration of carbon dioxide for the reaction. At the lowest comcentrations reached, respiration just equals assimilation, so that a CO_2- steady state ensues.

3) A curve showing the dependence of the rate of photosynthesis on partial pressure of CO_2 yields a "Michaelis Constant" of 0.79 mm.Hg; this corresponds to a free energy of carboxylation of -5700 cal./mol.

4) The mean rate of respiration in strong light is about half

* Work described in this paper was sponsored by the U.S. Atomic Energy Commission.

that in the dark. Re-assimilation of respiratory carbon dioxide probably accounts for part, but not all of this effect.

5) At low CO_2 pressures, molecular oxygen may be able to substitute for carbon dioxide as the oxidant of photochemically generated reducing agents.

6) The assimilation of $C^{14}O_2$ is about 17% slower than that of $C^{12}O_2$.

Backscattering appreciably raises the observed β-activity from the thick samples containing C^{14}. This effect must be subtracted if one wishes to determine the true self-absorption within the samples. The true self-absorption of carbon radioactive organic materials is the same as that of $BaC^{14}O_3$.

PREVIOUS INVESTIGATIONS

The relation of photosynthesis to respiration is, as yet, indadequately understood. Until recently, it was not even certain whether, in the light, there occurred any respiratory evolution of CO_2 simultaneously with the assimilation of carbon dioxide from the air, or whether, perhaps the path of carbon in photosynthesis was merely the reverse of that in respiration. The reason for this uncertainty is that the net overall reactions usually written for these two processes are opposite:

$$\text{Photosynthesis:} \quad CO_2 + H_2O \longrightarrow (CH_2O) + O_2$$

$$\text{Respiration:} \quad O_2 + (CH_2O) \longrightarrow H_2O + CO_2$$

where (CH_2O) represents carbohydrate, a typical photosynthetic product and respiratory substrate.

Without tracers, it is in principle impossible to distinguish kinetically between these simultaneous and opposing reactions while the light is on. Various attempts have been made by a great number of investigators to get approximate values for "light respiration." These have involved various assumptions:

1) Either photosynthesis or respiration may be poisoned selectively. Thus, Gaffron (1) used cyanide to "selectively" poison the respiration of Scenedesmus and found the quantity, (photosynthesis -- light resp. + dark resp.) to be constant over a range of degrees of poisoning; however, he could not determine whether light and dark respiration were equal. In

Chlorella, on the other hand, Myers and Burr (2) suppressed photosynthesis with cyanide; they found a strong increase in oxygen uptake with increasing light intensity ("photo-oxidation").

It seems hardly possible to poison one set of reactions in a complex organism without simultaneously upsetting other functions; this is expecially true for the case of two such closely related reactions as photosynthesis and respiration.

2) photosynthesis is known to be dependent on the concentration of CO_2 (below $\sim$1 mm. Hg.). One may measure the net gas exchange as a function of CO_2 pressure (light being held constant; the resultant curve can be extrapolated to zero (CO_2), where the intercept should be equal to the (light) respiratory rate (evolution of CO_2). Experiments at such low CO_2 pressure have to date, yielded data too poor to be analyzed in this fashion; neither Hoover, Johnston and Brackett (3) nor Gabrielsen (4) published extrapolations.

Very recently (11) the latter author has published the results of some interesting experiments, carried out in flowing gas initially free of CO_2. He collected and measured the CO_2 evolved into it by "sun leaves" (.23 mm. thick) and "shade leaves" (.13 mm.) of Sambucus nigra*. The "shade leaves" turned out to have the same rate of net CO_2 evolution in light or darkness, while the (five times greater) dark respiration of the "sun leaves" was reduced by about one-half in bright light.

---

* Elderberry

Gabrielsen interpreted this decrease as due to re-assimilation of respiratory carbon dioxide in the thicker "sun leaves" (which had a longer diffusion path for the CO_2). The fraction of carbon dioxide re-photosynthesized was found to decrease with decreasing respiratory rate and with increasing gas velocity. These results would indicate that respiratory intermediates must be converted into CO_2 before becoming available for re-assimilation (thus contradicting those of Miller and Burr, (12).

He further suggested that the "shade leaves" in the above experiment, as well as the "sun leaves" operating in a very rapid gas stream, showed no photosynthesis because the CO_2 pressure was below a "threshold" of .009%, supposedly necessary to "saturate" an acceptor.** We cannot understand this in terms of mass action or enzyme chemistry; on the contrary, it seems to us that at low concentrations, the acceptor would use the same fraction of CO_2 as at higher ones. Moreover, we feel that these data are adequtely explained by his picutre of CO_2 diffusion into the gas. At low respiratory rates, the diffusion from thin leaves into fast-moving gas could be sufficiently rapid to reduce the concentration in the cells to such a low value (far below the "threshold") that re-assimilation would be negligible.

** We feel that systematic experimental errors in his earlier work (4) invalidate similar conclusions reached then.

3) Photosynthesis also depends on light energy. A variety of experiments has been performed, involving the variation of either intensity or wave length and the resultant effect on gas exchange (for reviews, see Rabinowitch (5) and Weintraub (6)). For example, Moore and Duggar (8) followed photosynthetic evolution of oxygen in Chlorella by means of a platinum microelectrode, working in the neighborhood of the "compensation point". In calculating quantum yields, they corrected for light respiration first by subtracting an average value of dark respiration, then by comparing photosynthetic rates at different light intensities (and colors) and subtracting. They got the same value by both methods and concluded that dark and light respiration were equal. However, the same data could be interpreted to show merely that the light dependence of respiration near the compensation point is proportional to that of photosynthesis.

Kok (10) has, indeed, found some evidence to this effect. The solid line in Figure 1 represents the oxygen exchange of Chlorella as a function of light intensity, in the neighborhood of the compensation point, O. He considered the slope from K to S to show the true light dependence of photosynthesis, the extrapolation to B giving the correct value for respiration at high light intensities. As a result, he concluded that as the light was increased from darkness to intensity K, the rate of respiration decreased by about half.

Unfortunately, the same data can be interpreted to show almost the opposite effect if one considers the slope of $\overline{AK}$ to represent photosynthetic light dependence at a constant respiratory rate. From this it would

follow that beyond K an increase in light results in a linear increase in respiration. Furthermore, Kok made an error in graphing, which resulted in a two to four-fold exaggeration of his deviation.

4) External respiratory substrates can be added in the light and in the dark, and their relative rates of utilization measured. Thus Myers (13) found the "oxidative assimilation" of glucose and acetate (by dismutation) in Chlorella to be independent of the presence of light; however, this yielded no direct information concerning endogenous respiration.

5) The dark respiration may be measured as a function of light and dark pretreatment. Borodin (14) was the first to notice an increased rate of dark respiration after a period of active CO_2 assimilation; he also found that a light period in the absence of carbon dioxide produced no such enhancement. From this he concluded that the "stimulation" of dark respiration after active photosynthesis was indirect, and could be ascribed to the availability for (dark) respiration of freshly formed photosynthetic products. A great number of investigators have since worked on this problem (reviews: 5,6,15); these effects have been observed in a good many cases. In others they may have been hidden by large storage reservoirs; Spoehr and McGee (16) found a much stronger enhancement of dark respiration after photosynthesis in previously starved plants then in normal ones.

In addition to this "mass action" effect due to accumulated photosynthesis, there are undoubtedly some more direct effects, due to

"stimulation" by strong blue and ultraviolet light. Furthermore, reducing agents built up during photosynthesis can apparently use oxygen in place of their normal oxidant, CO_2, if the latter is lacking ("photo-oxidation" and its dark after-effects; Rabinowitch, 5). These phenomena do not appear to bear directly on the relationship between the photosynthetic and respiratory paths of carbon.

All these experiments still leave the following basic questions unsettled:

1) Are the enzymatic paths of carbon in photosynthesis and respiration closely linked? For instance, are recently photosynthesized compounds available for respiration while the light is still on?

2) Assuming the two processes to be truly independent, what is the rate of respiration during the photosynthesis of normal plants?

OUTLINE OF EXPERIMENTAL ATTACK

There is good evidence (17,18,19) that in plants the path of sugars to pyruvate follows the glycolytic sequence observed in yeast and muscle tissue; there is somewhat less conclusive evidence (18,19) that this pyruvate is degraded to CO_2 via the so-called "Krebs tricarboxylic acid cycle". In view of the close resemblance of the path of CO_2 assimilation to that of glycolysis and respiration (7,21-23) it was decided to start a series of kinetic experiments designed to distinguish between these processes.

The availability of tracer carbon-14 has made it possible, at least in principle, to settle the question of whether the respiratory

rates and paths of carbon are the same in the light and in the dark. One way to do this is to put some leaves in a sealed chamber which can be illuminated and darkened, to introduce a gas mixture containing C^*O_2 and to follow continuously, by means of non-destructive methods of analysis, the concentrations of radioactive and inactive carbon dioxide in the gas phase. If simultaneous photosynthesis and respiration are different reactions, at least the initial respiratory CO_2 will be inactive; the rate of reduction of the original specific activity of the added C^*O_2 should be a quantitative measure of the rate of respiration.

Since in these experiments we have been mainly concerned with the exchange of carbon dioxide in the gas phase we have used the following terminology:

Photosynthesis: assimilation of CO_2 from the gas

Respiration: evolution of CO_2 into the gas

These definitions imply that even in strong light all respired carbon leaves the cells as CO_2, is mixed with the entire gas phase and can only then be re-assimilated. Hence the quantitative evaluation of the rate of respiration in the light will yield not the total rate, but only that fraction of it which actually appears in the atmosphere as CO_2. This problem will be taken up further in the Discussion of Results.

INSTRUMENTATION

General Description of Apparatus

Figures 2 and 3 show the experimental set-up. At the beginning

of a run the leaves of 1-2 week old barley shoots were cut and placed into a one liter glass chamber. This was closed, the entire system evacuated and filled with the desired gas mixtures (containing C^*O_2). A rubber tubing pump took a continuous sample of the gas in the chamber and cycled it through a series of three instruments: an ionization chamber to measure C^*O_2; a paramagnetic-type oxygen analyzer; and a selective-detector infra-red CO_2 analyzer. Within less than a minute (from experiment Barley 14 on) the sample was returned to the chamber, the flow rate being >500 cc/min. Time lags between the individual instruments were found to be less than half a minute at these pumping rates. The whole system was connected by 3/16" i.d. Tygon tubing.

The plant chamber (Figure 4) was immersed in a tank of running water, which kept the temperature constant at about 15° C $\pm$ 1° C; infra-red filters were placed in the ($\sim$2 in. deep) water above the chamber. A bank of spot lights provided approximately 14,000 f.c. from above.

Biological Material

In most experiments we used 1-2 week old barley leaves (var. Sacramento). Typical pretreatment was one week's greenhouse growth to 3-4 in. in height, followed by a day or two under a 60-watt light bulb. The leaves were cut about half an hour before the experiment, moistened, placed in the glass chamber. During evacuation and gas mixing, they were generally kept in the dark, in order to minimize gas exchange as long as the instrument readings were unsteady.

In three experiments (only one of which is recorded in this thesis),

succulent plants were investigated: Aegeum sp. and Crassula multicava. Again we used only green leaves and otherwise followed the procedure outlined above.

Gas Circulation

The little "rubber tubing" pump has been the only piece of equipment which has never given us any trouble. Its mode of operation is easily recognized from the picture in Figure 4: one after another, the four rollers at the corners of the square spider pass over the rubber suction tubing, pushing the gas ahead of them and pulling more in from behind, each roller blocking a new air pocket before the last has been lifted off. Speed can be varied from 50 to 600 cc./min. by means of a set of step-pulleys (not shown) and the adjustable hinged tubing race. The resulting flow (as measured continuously by a calibrated rotameter, Figure 7) is quite smooth above $\sim$200 cc./min. and only slightly bumpy ($\pm$ 10%) below this rate.

The main virtues of this type of circulating pump are the smooth flow and negligible "hold-up", the lack of moving parts and lubricant in contact with the gas, its rugged construction and ability to withstand evacuation without leakage around shafts and bearings. It has found many other uses around this laboratory, such as CO_2 precipitation in barium hydroxide (see below,) supplying air to algae cultures, and pulling a slow, well-controlled vacuum to 10 mm. Hg pressure or better.

The rest of the tubing in the system was 3/16 in. tygon and glass, with greased, standard taper joints to make quick connections. The

rate of diffusion of carbon dioxide through tygon and rubber (pump) tubing was measured (see below,) and found to be negligible.

Up to experiment Barley 12 inclusive, the circulation rate was only $\sim$ 100 cc./min. because the capacity of the oxygen meter was limited. At this point it was realixed that time lags between instruments of the order of 1-2 minutes could greatly affect, (though not eliminate) an observed rise in specific activity (presumed due to an isotope effect, (see below). Two steps were taken to eliminate this source of error:

1) The Pauling meter was removed from the circuit and the pump rate stepped up to $\geq$ 500 cc./min.

2) The direction of gas flow was reversed, in order to invert the order of passage of the gas sample through CO_2 analyzer and ionization chamber. (As expected, this did not affect the results).

In some later experiments (Barley 26, 28), the Pauling meter was again put into the system; the gas was pumped through all other instruments first, then through a Y connection into another flowmeter and the oxygen analyzer, a second Y, and finally back into the plant chamber. The bypass took 400 cc./min, so that the flow through the Pauling meter was again only about 100 cc./min.

One or two drying tubes, $\sim$6 in. long, were inserted in the gas stream between the plant chamber and the first instrument. They contained $CaCl_2$ with Drierite ($CaSO_4$ with CO^{++}) as indicator.

Plant Chamber

The barley chamber (Figure 4) consisted of a one-inch thick rectangular brass frame with greased neoprene gaskets, sandwiched between two 1-inch glass panes (24). After the plants were inserted, the windows were clamped against the gaskets and the chamber exhausted through three-way stopcocks. A vacuum of 3 in. Hg was just sufficient to hold it together and keep it leak-proof. The whole assembly was now submerged in the running water of the cooling tank and attached to the rest of the system by means of ground joints.

Lights

Illumination was provided from above by a bank of four spot lights (G.E. 150 watt Projector or 300 watt Reflector Spots) usually about 3 in. above the water level (Figure 4). The average intensity reaching the plants through water, infra-red filters and glass was measured by means of a calibrated, water-proof Weston Photronic Cell. It turned out to be about 14,000 f.c. (150,000 lux) (midday sunlight in Berkeley being about 16,500 f.c.)*

Oxygen Analyzer

The Pauling Oxygen Analyzer (25) is a small magnetic torsion balance. A vertical quartz fiber carries a mirror and a horizontal pair of metallized glass dumbbells, free to rotate between the poles of a permanent magnet. The gas sample passes through a diffusion barrier into the 2 cc.

* Measured on May 5, 1949)

cell surrounding the test body; a change in the volume magnetic susceptibility of the gas will upset the balance and cause dumbbells, fiber and mirror to come to a new equilibrium position. The beam from a stationary small light bulb is reflected off the mirror onto a translucent scale; since oxygen is the only commonly encountered paramagnetic gas, the instrument can be calibrated directly by the manufacturer* in terms of partial pressure of oxygen. The total pressure of other gases present exerts a negligible effect on the scale reading. At normal flow rates, the instrument indicates 90% of a sudden change within one minute.

The particular instrument used in these experiments (Figure 5) was Beckman's Model C, calibrated in units from zero to 100 mm. partial pressure; with care it could be read to ± 0.2 mm. (The range of this particular instrument, incidentally, accounts for the fact that most of our experiments were carried out at oxygen concentrations between one quarter and one-half that in the normal atmosphere; in future experiments we hope to employ an instrument of greater range).

Determination of Radioactivity

Radioactive C^*O_2 was measured continuously by means of an ionization chamber and Lindemann electrometer.** The basic techniques were worked out at the Radiation Laboratory by Dr. C.D. Janney and B.J. Moyer (26), to whom

---

* Arnold O. Beckman Co., Pasadena, California.

** Electrometer built at the Ryerson Laboratory, University of Chicago.

we are indebted for the loan of equipment and much valuable advice. Figures 5 and 6 show the set-up. Two ionization chambers were used in different experiments: a 10 cc. chamber of simplified design (Figure 5) and a standard, 100 cc. model (Figure 6) which had nearly ten times the other's sensitivity but also contained a greater portion of the total volume of the system. Both were provided with two connections and needle valves, to facilitate an efficient and continuous gas circulation through them. It was found that gas movement at the velocities used in these experiments has no measurable effect on the ionization current; i.e., electrometer readings for a given activity were the same with the pump on or off.

Since we desired to get instantaneous and continuous measurements of the radioactivity, the usual rate-of-drift fashion of reading the electrometer was replaced by a null method. The condenser system of the circuit was replaced by the large resistor R ($10^{11}\Omega$, Figure 9); the central ionization chamber probe was initially grounded, and the electrometer fiber set to the center of the miscrope scale. After the electrometer was ungrounded, the ionization current, I_i had to travel through Resistor R, past junction V and through the decade resistance box (0-9999Ω) to ground. A relatively large opposing current (0-1 milliampere) was made to travel in the external circuit sketched below V; its magnitude was controlled by the 10,000-Ω potentiometer and 45 v battery.

The potential this "bucking" current developed across the (variable) decade box appeared at point V; when this voltage just equaled that developed by the very small ionization current I_i through the very large resistor R, the electrometer needle appeared at the center (null) position.

In practice, all changes in ionization were quickly followed by continuous adjustment of the potentiometer and occasional changes on the decade resistance box. The opposing current was measured by a recording Esterline-Angus milliammeter, so that the operator merely had to keep a record of changes on the resistance box. Later, after the experiment, the ammeter data could be read off the chart and multiplied by the prevailing decade box resistances to yield "millivolts" of radioactivity.

In some recent experiments, such high ionization currents were expected that it was necessary to add 10,000 Ω of the 50,000 Ω "current-limiting" resistor (of the opposing circuit) to the decade box. This was done with a multiple-position switch and wire-wound precision resistors.

The response of this circuit is linear with respect to radioactivity; that is a plot of "millivolts" of activity against microcuries of C^*O_2 contained in the chamber is a straight line. This has been shown true for the large chambers by serial dilution experiments (26,27); and for our little chamber by the injection of several measured aliquots of radioactive C^*O_2. Readings show a strong dependence on total gas pressure, since the radii of both chambers are considerably smaller than the median range of the β-particles. They also show a somewhat smaller dependence on the kind of gas present in the chamber; thus, Otvos (28) has found that for C^{14} beta radiation of a given strength, oxygen yields only 0.76 as many ions as pure CO_2, and nitrogen 0.57 as many. In our experiments these effects were negligible since at most 4% CO_2 were exchanged for 4% O_2, the

rest of the gas composition remaining constant. The corresponding change in "ionization probability" is just outside experimental error for the 4% CO_2 experiments but negligible for those starting with less than 1% (e.g. Barley 28):

$\%CO_2$	"Ionization Probability"
4%	103.0
2%	101.5
1%	100.8
.5%	100.4
0%	100.0

It is an excellent feature of this circuit that it in itself never limits the precision of the ionization current readings. The reason for this is that the decade box can be kept so adjusted that the milliammeter always reads at midscale or above; hence, so far as the circuit is concerned, the same precision of readings is available over an ionization current range equivalent to 1-50,000 mv. full scale.

Needless to say, other factors limited the instrument. The substitution of resistor R for the usual condenser-charging circuit involved the sacrifice of a factor of sensitivity between 10 and 100. Since the highest stable sensitivity of the electrometer was about 1000 div./volt, this meant that fairly high percentages of radio-C^*O_2 had to be used, and that the 100 cc. chamber was preferred to the smaller one. On the other hand, "background" due to cosmic rays, neutrons from the neighboring 60 in. cyclotron and α-contamination from the brass chamber walls were all too

small to be seen and never gave any trouble at all.

"Memory" effects due to previously adsorbed radioactive carbonates on the inside walls have never been definitely seen in these experiments. Although it is not uncommon for a chamberful of activity a hundred times background to leave behind it a carbonate film counting twice background (26), the sensitivity of our circuit was too low to see such small differences. In special experiments in which large amounts of C^*O_2 were quickly displaced by air, over 99.9% of the radioactivity was lost within a couple of minutes.

On the other hand, occasional trouble was encountered in the form of leakage currents across the main insulator in the chamber (between central probe and ground). This looked like background and we attempted to correct for it in the usual manner (by subtracting the "residual ionization" left when all CO_2 had been removed from the chamber). This was not very satisfactory, and no quantitative evaluation was made of any results obtained in this manner. In experiments, Barley 11 and 26 for instance, the small, resp. large, ionization chamber gave such troubles. The central insulators were carefully cleaned or replaced before subsequent experiments.

Two experiments were designed to determine the rate of response of this apparatus to quick changes in radioactivity. The rubber tubing pump (operating at ~500 cc./min.) and the chamber to be tested were connected in series; both could be connected alternately to large reservoirs containing radioactive C^*O_2 or to the atmosphere by means of three-way stopcocks.

(The "time constant" for the electrometer itself was only 2 seconds). The small chamber (10 cc.)* underwent essentially 100% of each change in less than 5-6 seconds, although the operator sometimes took 15 seconds to find the exact new steady value. The large (100 cc.) chamber, as might be expected, took longer; about 80% of a sudden decrease in activity was complete in 15 seconds, 90% in half a minute and 99% or better in a minute; two or three minutes were required for the last half percent or so. Increases in radioactivity were, for some reason, followed even more quickly; more than 99% of the activity was recorded less than half a minute after the stopcocks were turned. At any rate, all changes were 90% complete in 30 seconds, even in the large chamber. These experiments were rather important as confirmation of the "Isotope Effect" (see Discussion).

Stray Currents in Ionization Chambers

The worst troubles generally encountered with ionization chambers due to "stray currents" of the order of magnitude of the ionization current to be measured (10^{-16} - 10^{-13} amperes). Most often these are found to cross the main insulator between central probe and ground, thus by-passing the measuring circuit and causing what appears like a "background" reading. Three distinct effects may cause such currents:

1) true leakage through the insulator, rarely encountered with

---

* Used in all experiments up to Barley 14, inclusive.

good materials such as polystryrene plastic or Kovar glass;

2) surface leakage, due to a film of moisture, or grease, fingerprints, etc., which can usually be avoided by careful machining, cleaning and handling of the insulator;

3) strain and piezoelectric currents.

The latter effects are usually the most troublesome because they are large and quite unpredictable. It is necessary to avoid even mild shocks to the insulator; after carefully setting a chamber on the electrometer head one usually has to wait from 15 minutes to 3 hours to let the strains and their currents die out. Slight temperature changes in the room can cause sufficient expansion and contraction of "poly" or Kovar insulators to overshadow small ionization currents completely.

Recently, two polyfluoroethylenes, Teflon and Fluorothene, have become generally available. In view of their reportedly excellent electrical properties (29) we decided to try these materials for our central insulator. Mrs. Jane Krone of the Donner Laboratory has tested a number of chambers with Teflon insulators, using the highly sensitive Vibrating Reed Electrometer. Thermal and shock strain currents were found to be negligibly small compared to real background (α's, cosmic rays, neutrons). In addition, these materials can be cleaned safely by the most drastic chemical methods and are too hydrophobic to permit the formation of surface water-films. As a result, chambers with the new insulators can be made to yield nearly ten times their former sensitivity.

Vibrating Reed Electrometer

The main virtue of the "Vibrating Reed" electrometer* (30) for this work is the fact that it records automatically and continuously the rate of charge accumulation in its condenser. Since α-rays cause far more ionization per particle than β's, each pulse due to α-contamination in the walls will show up as a distinct discontinuity in the record. Such "jumps" are then disregarded when one measures the rate of drift in order to calculate β-radioactivity in the ionization chamber.

In the case of the Lindemann electrometer, on the other hand, the operator cannot adequately distinguish α-jumps from normal drift rate; as a result, the (often considerable) α-background is included in the averaged value for β-radioactivity.

Now that piezoelectric currents in the insulators appear to have been eliminated, it may become possible to use a Vibrating Reed electrometer to push the lower limit of sensitivity of our ionization chambers 10-100-fold beyond that presently available.

Carbon Dioxide Analyzer

Introduction

In recent years three different methods have been developed for the analysis of gas mixtures for single polyatomic components by means of infra-red radiation. All three were applicable to the determination

---

* Manufactured by Applied Physics Corporation, Pasadena, California.

of CO_2, since this gas absorbs strongly in the 4.3 μ region, as well as less strongly near 2.7 μ.

McAlister (31) passed the radiation from a black-body source through his absorption cell, then separated the 4.3 μ band by means of a rock salt spectrograph and measured its intensity by means of a vacuum thermocouple and galvanometer. The sensitivity was very high; about 0.0002% CO_2 per millimeter galvanometer deflection. Unfortunately his galvanometer was subject to d.c. drift (for which, however, he could correct periodically). The response time was 5 seconds; during experiments galvanometer readings were usually taken every 30 seconds.

Pfund and his coworkers (32), as well as Wright and Herscher (33), developed gas analyzers based on the negative-filter principle of Schick (34). Radiation from a homogeneous source passes through the sample chamber, then through two parallel filter cells, and is measured by parellel bolometers. One filter cell is filled with the pure gas to be determined, so that its detector receives none of the radiation absorbed by this gas (4.3 μ for CO_2); the other filter contains a non-absorbing gas which permits the corresponding bolometer reading to vary with the concentration of the gas to be measured in the absorption cell. The difference in the readings of the two bolometers is characteristic only of this concentration, and the instrument may be calibrated with known gas mixtures. This method of analysis is the least sensitive of those discussed here, being most useful in the 0-20% range of CO_2 concentration.*

* The Wright-Herscher type of instrument is commercially available from Baird Associates, Inc. of Cambridge, Mass.

A third method, utilizing a selective detector, was developed independently by American and German workers during the second World War. The principle is letting black-body radiation pass through the "unknown" absorption cell into a detector containing the very gas for which one is analyzing. The gas in the detector absorbs all that remains of its characteristic bands and converts the energy into heat. Pfund (35) measured this without much success by means of a shielded thermocouple.

Luft (36) ingeniously "chopped" his radiation at the source, thus generating an audio-frequency expansion and contraction in his detector gas, whose amplitude was proportional to the "characteristic" radiation transmitted by the absorption cell. Parallel optical paths, containing "standard" and "unknown" gas samples ended in parallel detector cells filled with CO_2. A microphone diaphragm between the detectors picked up the differences in their amplitudes of vibration and converted them into electrical signals. This instrument could be made very sensitive; for instance, .03% CO_2 full scale is attained in a currently available commercial version.**

In the winter of 1946 a special arrangement was made with Drs. O. Beeck and D.J. Popeo of the Shell Development Co. whereby they

---

** Sir Howard Grubb Parsons and Co. of Newcastle-upon-Tyne, England now manufacture Infra-red Gas Analyzers based on Luft's "U.R.A.S."

permitted us to copy their basic design for a new version of the Luft infra-red gas analyzer. An instrument was built at the Radiation Laboratory under the direction of Robert Olsen and P.M. Warrington.* Both Shell Development and we have considerably changed our respective instruments since then; they to make theirs more versatile and stable (for plant control of CO_2 or hydrocarbons), we to make ours more sensitive to carbon dioxide.** The main difference between the current Shell Development Co. model and ours lie in the electronic circuits and in the fact that we retained the "resonant cavities" while they were not versatile enough for Shell's hydrocarbon analyses. The following sections will describe our apparatus only.

Description

Figures 7 and 8 show the chassis carrying the optical and acoustic components of the instrument. Radiation passes from each glower source (at the left) through an absorption cell, in which the carbon dioxide present takes out a certain amount of the radiation at 4.3 μ. The remaining light passes through lithium fluoride windows into the detector cell, which is filled with enough pure CO_2 to completely absorb the rest of the 4.3 μ band. As a result, the detector gas becomes hot and expands slightly. If a shutter is now placed in front of the source, all radiation is shut off and the CO_2 cools and contracts rapidly.

---

* Mr. Warrington has been working with us ever since, mostly on the operation and improvement of the CO_2 analyzer.

** The most recent Shell Development Co. model of the infra-red gas analyzer will be commercially available from the Applied Physics Corporation of Pasadena, California.

A rotating shutter can be made to open and close 120 times per second; there results a 120-cycle acoustical vibration whose amplitude is a measure of the per cent transmission of the gas in the absorption cell. A condenser microphone in the rear of the detector cell is used to convert this vibration into an electrical signal. Each detector consists of two CO_2-filled chambers connected by an "induction tube" of such shape and size as to make the whole cell a Helmholtz resonant cavity, giving a threefold acoustical amplification for this gas at atmospheric pressure.

The absorption cell on the left contains nitrogen or some other unchanging reference mixture, while the "sample" cell on the right is connected to the rest of the instruments by the Tygon leads shown in the pictures.

The two microphone signals are run through pre-amplifiers onto the opposite ends of the "Helipot" slidewire of a Brown Electronik recording potentiometer. Since the shutter geometry is such that light is alternately transmitted through the two optical paths, the two signals are 180° out of phase and will produce a "null" point of minimum amplitude somewhere on the slidewire. The rest of the circuit (Figure 10) serves to drive the recording pen to this null point.

Calibration

The CO_2 analyzer was calibrated with gas mixtures previously analyzed for CO_2 by $BaCO_3$ precipitation (see below). Two tanks were used; one of them contained nitrogen, the other a nitrogen-CO_2 mixture

corresponding to the full-scale percentage of carbon dioxide desired (4%, resp. 0.75% for the experiments reported here.). Parallel streams of these gases were measured by calibrated rotameters (see below) and flushed through the sample cell. The valves on the latter were closed and the steady scale reading noted on the Brown chart.*

We now attached the rubber tubing pump to one valve and used it to pull a vacuum of about 10 cm. Hg below atmospheric pressure (measured to $\pm$ 1 mm. by a mercury manometer). After a reading at this pressure, others were taken at 20 cm. and 30 cm. The whole procedure was now repeated with eight or nine other gas mixtures. From these data we could plot a family of calibration curves (Figures 11 and 12) of scale reading as a function of CO_2 partial pressure, each curve being valid at the selected total pressure. Since most photosynthetic experiments were run at a 10 in. vacuum (mainly to hold the plant chamber together), the "10 in. vacuum" curves were the ones actually used in the calculation of kinetic data.

A similar pressure-broadening effect on the calibration has been observed by Fastie and Pfund (32) with the selective-filter type of CO_2 analyzer. Although surprisingly large, it is certainly related to perturbation of the CO_2 stretching vibrations by neighboring molecules. Cross and Daniels (37) were able to correlate analogeous effects on the infra-

---

* The instrument reading for a given gas mixture was independent of its rate of flow over the range covered in these experiments (0-600 cc./min.)

red absorption of H_2O with the gas kinetic diameters of the perturbing molecules (as calculated from viscosity measurements). Hertz (38) found differences in the effects of hydrogen gas and air on the absorption of carbon dioxide; however, nitrogen and air should, for practical purposes, act identically.

In order to eliminate any possible systematic errors in the flowmeter method of calibration, the following confirmatory experiment was run for the 0.00-0.75% CO_2 scale. A number of 1-2 liter flasks were filled with a series of gas mixtures by attaching the flasks to a manometer (read to $\pm$ 1 mm.), exhausting them to a few microns pressure and filling them with various proportions of .75% CO_2 mixture and nitrogen. Three satisfactory sets of check points were obtained on the flowmeter calibration (see Figure 12), which meant that the curves were valid within about $\pm$ 1 division below 2 mm. partial pressure and, at most, $\pm$ 2 divisions above 2 mm.

Expansions of the scale of the CO_2 analyzer were effected simply by adding variable resistors to the "Helipot" slidewire (see circuit, Figure 10). This decreased the fraction of total resistance comprised by the slidewire and magnified the effect on pen position of a given change in the ratio of the two signals. On the other hand, the simultaneous equivalent increase of one of these resistors and decrease of the other resulted in a shift of the calibration without expansion of contraction. Thus the circuit permitted almost indefinite expansion and shifting of the scale, the only limitation on sensitivity being the

smallest stable change obtainable in signal ratio from one end of the scale to the other.

Interference by Other Gases

Carbon dioxide has a secondary absorption band at 2.7 μ, with a peak extinction about one-fifth that at 4.33 μ. Although no common gas has a band in the latter region, water does absorb strongly in a narrow band at 2.6 μ. We have calculated the degree of overlapping of the water and CO_2 bands and found that the CO_2 analyzer "sees as carbon dioxide" only 4% of the water vapor in the absorption cell. In calibration runs we used dry tank gases while during kinetic experiments water vapor was removed by $CaCl_2$ drying tubes. The water vapor pressure over the latter is .025 atmospheres (39); thus, at the usual 10 in. vacuum we had .025 x 30/20 = .0375% H_2O. The detector gas responded to 4% of this, giving a CO_2 equivalent reading of .0375% x .04 = $1.5 \cdot 10^{-3}$% (or ~ .01 mm.). This was just within experimental error at the very low CO_2 pressures prevailing in Barley 28; in all other experiments to date this "background" was of no consequence at all. If, in the future, we decide to work at even higher sensitivities, we may have to insert "negative filters" of water vapor into our light paths in order to take out all 2.7 μ radiation before it reaches the detectors.

This calculation assumed complete absorption of 2.7 μ band radiation by the CO_2 of the detectors. If this were not true, the contribution of water vapor would be even less.

Isotope Shift of Absorption Spectrum

One interesting property of the CO_2 detector cells is their ability to distinguish between $C^{12}O_2$ and $C^{14}O_2$ - that is, $C^{12}O_2$ in the cavities "sees" only abosrption by $C^{12}O_2$ and apparently none by $C^{14}O_2$. This was not realized until recently, when we were able to obtain some C^*O_2 of very high specific activity ($\sim$ 27% $C^{14}O_2$) and measure its absorption in the infrared region (40). At the low pressure prevailing in the test cell, the main CO_2 bands near 4.3 μ appeared completely resolved. It does not seem likely that pressure broadening makes them overlap noticeably at the normal pressures used in the CO_2 analyzer.

Instead of reading "total CO_2" then, the analyzer yields only "inactive $C^{12}O_2$", and what was thought to be Specific Activity $\left(\frac{C^{14}O_2}{\text{total } CO_2}\right)$ is really an Isotopic Ratio $\left(\frac{C^{14}O_2}{\text{total } CO_2}\right)$. This however, introduces no difficulties whatever, for the maximum specific activity of the C^*O_2 used in all experiments up to Barley 26 was only $\sim$ 1% $C^{14}O_2$ or less, i.e. within the error of measurement. In Barley 28 we used 4.75% $C^{14}O_2$ and re-calculated the data accordingly; even in this case, neither the qualitative nor the quantitative results were affected.

Response Time

Since the recording potentiometer had a cross-scale travel time of only 4 seconds and the detectors and electronic circuit responded within microseconds, the only limiting factor was the circulation rate of gas through the 80 cc. absorption cell. At a flow of 500 cc./min.

it took less than 15 seconds from the time of a sudden change in the sample until a steady reading was obtained corresponding to the new gas mixture.

Troubles

The difficulties encountered in the construction and use of such a complex instruments as this can readily be imagined. The sequence of electrical, optical, acoustic and electronic components invites troubles of many kinds. Rather than discuss them one by one, we have grouped them according to their overall effect on the operation of the instrument, the three main difficulties being "Phase Shift", "Drift", and "Wandering". Dozens of minor mechanical and electronic difficulties need not be mentioned.

Phase Shift

One of the most crucial adjustments which have to be made affects the precision with which the null point is defined. The recorder pen travels over a one-foot chart marked with 200 divisions; hence its position can be read to the nearest 1/400 of full scale. However, a finite voltage gradient is required to drive the pen motor, and the larger the "null" amplitude, the wider the range within which the pen may sit without moving. It is thus clear that this amplitude directly determines the precision of CO_2 analysis.

If one takes the "standard" signal as basis, the "unknown" signal should be exactly 180° out of phase with it in order for the "null" amplitude to be zero (and for the pen to drive directly to the

null point). In practice, the effective relative timing of the two microphone signals is quite difficult to adjust. Two factors determine their phase relationships:

a) The relative positions of the shutter and the windows of the absorption cells.

Since the shutter rotates upwards in front of one of the absorption cells and downwards in front of the other, the first signal will be retarded somewhat and the second advanced if the absorption cell windows are raised. Conversely, a lowering of the cells produces a reverse phasing shift. In view of this fact, we have used a thumb screw adjustment for the level of the absorption cells in order to obtain a minimum null signal.

b) Time lags in the response of the cavities.

It often happens that the phase angle between signals changes significantly as the amount of CO_2 in the sample cell is varied - i.e. that the null point widens from $\pm$ 1/2 division at one end of the range to $\pm$ 5 or more at the other end. We have performed a variety of experiments in order to better understand this "phase shift" and the origin of the "90° component". It is most noticeable on the highest scale, where one of the signals remains steady while the other decreases by nearly 50% when 4% CO_2 is run into the sample cell.

The introduction into the light path of an equivalent area of opaque paper has essentially the same effect. The phase shift appears to be related to the relative (not absolute) signal sizes, as

well as to the tension on the condenser microphones.

In his book, Vibration and Sound, Philip M. Morse (41) mentions that condenser microphones, undergoing strong forced vibration near their resonant frequency are apt to get out of phase with the exciting signal. This seemed like a reasonable explanation; however, a number of runs were tried with different microphone tensions (and hence different resonance frequencies) without any improvement. On the other hand, recharging the cavities with fresh 100% CO_2 did seem to help temporarily. The nature of this effect is as yet poorly understood; if and when we return to CO_2 concentrations where "phase shift" is a serious problem, we shall have to tackle it once more.

Drift

"Drift is the slow change of scale reading while there is a given sample in the absorption cell. Clearly it is due to a progressive change in one or both of the signals. Both ends of the scale usually drift in the same direction and at approximately the same rate. This seems to indicate that the drift does not involve the simultaneous increase or decrease of both signals but rather the increase of one at the expense of the other or, more likely, the change of only one of them. This phenomenon has been most noticeable on the most sensitive scales tried.

Several possible causes have been found and eliminated.

a) Temperature changes could exert an effect on the resonance of the cavities (but only a slight one, since in a closed system the

gas bulk modulus, $\propto \sqrt{\frac{\text{pressure}}{\text{density}}}$, remains constant at reasonable temperatures and pressures). This was eliminated by means of a thermostated box, surrounding the whole chassis.

b) Slight variations in source intensities or temperatures could be caused by variable voltage or by the ageing of the light sources. The silicon carbide Clo-bars originally used were found to wear unevenly and rapidly; they were replaced by platinum wire glow-coils wound on baked ceramic (designed in this laboratory by P.M. Warrington). The input voltage of the sources and, in fact, of the whole instrument was closely regulated ($\pm$ 1/2 v.) by a Sola constant voltage transformer.

c) The electronic circuit was throroughly checked for stability by testing individual components and by injecting a steady "dummy" signal at the pre-amplifiers. There was no sign of drift. In the near future we hope to put a constant output control on one or the other signal; if any variation persists it will be due to the other "side" of the instrument.

d) Changes in the detector gas may have been responsible for relatively rapid drift on some occasions. Very slight leaks were found in the cavities. These occurred mostly in the wax seals around the salt windows; the leaks were fixed, the cavities re-charged with CO_2 and most of the drift eliminated. There may have been a continuous, very slow diffusion of CO_2 through some gaskets which held

the cavities together; unfortunately neither neoprene and gum rubber nor lead gaskets proved to be entirely successful.

c) The response of the microphones themselves may have changed with time. A recent checkup revealed, for instance, that the lead gaskets which hold the diaphragms taut had become worn smooth and that, as a result, the tension had slackened. Other parts of the microphone had to be resurfaced at the same time the gaskets and diaphragms were replaced. We feel that these are probably the major causes of our trouble with drift, and expect that they will be largely eliminated in future experiments.

Wandering

By "wandering" we defined a random fluctuation in the readings, averaging at the proper value for a given sample but taking excursions from $\pm$ 1 to $\pm$ 10 divisions, depending on conditions. We felt that vibration, electrical pickup, and CO_2 fluctuations in the atmosphere were responsible.

a) Vibration was mainly generated by the shutter motor and shaft and received, of course, by the microphones. In order to cut down the direct connection between them, the motor was backed off onto a special mount and connected to the shaft by means of a flexible coupling and special ball bearings.

All components and both mounts were individually mounted on rubber pads. In additions, the vulnerable pre-amplifier tubes have been replaced by "non-microphonic" tubes emplaced in gimbals.

A closely related problem was that of twisting and distortion of the entire chassis. The originally designed Duralumin base (Figures 7 and 8) turned out to be too light and flexible; it was replaced by a very rigid mount based on parallel steel pipes.

b) Thirty-cycle electrical pickup originated in the shutter motor, while plenty of 60-cycle background came from the rest of the equipment, fluorescent lights, etc. All vulnerable parts of the large circuit (in cabinet at far left of Figure 2) and of the chassis had to be carefully "shielded"; furthermore a selective feed-back filter was introduced into the voltage amplifier in order to cut out all frequencies but the desired 120-cycle signal.

c) The third source of wander became noticeable only when the instrument was set to its most sensitive ranges (0.2, 0.1, 0.03% full acale - not used in photosynthetic experiments, to date). Clouds of atmospheric CO_2 were free to drift in and out of the short air spaces between glower, absorption cell, and detector windows. A momentary high local concentration of CO_2 (due to a breath, a puff of smoke, the gas from a Bunsen burner) could absorb enough radiation in one or both light paths to offset the pen temporarily. The constant temperature box was of great help in reducing drafts of this kind.

MISCELLANEOUS TECHNIQUES

Tank Gases

Commercial nitrogen ("oil pumped" or "high pure", oxygen free grades), and CO_2 nitrogen mixtures (usually 4% CO_2, 96% purified nitrogen) served to calibrate the CO_2 analyzer and were used in photosynthetic experiments. Other mixtures were derived from them by the use

of a high-pressure manifold and the appropriate gages. Each gas was analyzed by one of the two carbonate precipitation methods described below.

Flow Meters (see Figure 5)

All rotameters were calibrated with the same gases which they were to measure, by letting the latter flow through at a steady rate, catching the gas and measuring the volume per unit time. Due corrections were applied for hydrostatic and water vapor pressures. The calibrations appeared to be quite stable; we had no trouble in reproducing the manufacturer's original calibrations, where applicable.* We had to design and use a new float for one of these flowmeters in order to be able to read the desired high gas velocities.

In the course of some early work with the oxygen polarograph (see below), glass orifice meters were used. These were not found to be very satisfactory, as small bits of grease or dust often obstructed orifices and gave erroneous readings.

Barium Carbonate Precipitation

Two methods were used to precipitate CO_2 as barium carbonate. The first, described by Dauben, Reid and Yankwich (42), involves the bubbling of CO_2 through "carbonate-free" sodium hydroxide, followed by precipitation with $BaCl_2$. This procedure has certain disadvantages when very small quantities of CO_2 are involved:

---

* Fischer and Porter Co., Hatboro, Pennsylvania.

a) A small Na_2CO_3 "blank" (of the order of 0.1 mg. $BaCO_3$ per mmol. NaOH) is present in the absorbing NaOH.

b) A fair amount of handling and pouring of the absorbing solution in the open atmosphere is required while excess base is still present. As a result appreciable amounts of atmospheric CO_2 are often absorbed and precipitated along with the C^*O_2 from an experiment. This is not objectionable when one is interested only in the <u>total</u> activity fixed, regardless of its dilution. However, it becomes very difficult to measure the specific activity of the experimental sample.

To overcome these problems, an entirely different procedure was developed. The sample bulb containing some percentage of C^*O_2 was attached to the tubing as shown in Figure 13. A centrifuge cone of appropriate size was half filled with carbonate-free saturated $Ba(OH)_2$ solution, while being flushed by a stream of nitrogen. It too was attached to the system. All tubing to both sides of the sample bulb was now alternately exhausted by an aspirator and flushed with nitrogen for a few times, in order to remove traces of atmospheric carbon dioxide.

Finally the system was closed off, the sample stopcocks opened, and the rubber tubing pump started. While the gas was recycled over the $Ba(OH)_2$ the centrifuge tube was shaken to allow the $BaCO_3$ to settle to the bottom as it was formed. Absorption was complete in 5-15 minutes, depending on the size of the sample bulb; this point was recognized by the failure of 2-3 minutesof recycling to produce a new

film of $BaCO_3$ on the surface of the solution.

At this point, the pump was stopped and the barium hydroxide tube taken off under a continuous nitrogen stream, stoppered, and centrifuged.

The precipitate was washed three times (under N_2) with boiling water, once with ethanol, once with ether. It was dried *in vacuo* for 15 minutes at 70°C. An alternate method of drying was to wash with water and ethanol as above, then dry overnight at 110°C.

Needless to say, the specific activity of the original C^*O_2 sample was faithfully preserved by this method. Straight exchange of BaC^*O_3 with CO_2 was the only possible source of dilution of the activity; under the conditions of our experiments this should have been negligible (43).

The two methods were compared by measuring equal samples from a "0.75% CO_2" cylinder (prepared by adding an appropriate amount of nitrogen to analyzed 4% CO_2 gas.) The results were:

a) NaOH, $BaCl_2$ precipitations: 0.78%*

b) $Ba(OH)_2$ precipitation: 0.73%*

c) Gas mixing (pressures): 0.75%

At these low percentages of CO_2, this is excellent agreement; we feel that, if anything, the sodium hydroxide procedure is in error, due to absorption of ~ 1/200 mmol. of CO_2 from the atmosphere.

---

* Barium carbonate precipitates obtained were 65.7 mg., resp. 64.9 mg.

Leaks and Vacuum Testing

Gas leaks in various parts of the experimental system were a constant source of trouble. Most often they ocurred in the wax seals around ionization chamber insulators and absorption cell windows, rarely in the plant chamber gaskets (once the latter had been properly seated and greased). The connecting tubing itself gave little difficulty, although the Tygon readily cracked or formed pinholes when pinched excessively.

The vacuum testing techniques varied considerably depending on the problem at hand. At various times we have used Bourdon gages, a mercury manometer, a differential mercury manometer, pressure- and-soap-bubble tests, the helium-spray technique and a flow-meter method.

The latter, to our knowledge, has not been described before. One attaches a fast vacuum pump (Cenco Hyvac) to a sensitive rotameter and exhausts various portions of the system through it. If the section tested leaks, the flowmeter will show a steady deflection; if it is tight, the flow will drop to zero within a minute or so. This is perhaps our most sensitive and rapid method of leak detection.

CO_2 Diffusion through Rubber and Tygon

Three 100 ml. pear-shaped flasks were flushed with nitrogen; a 10 ml. aliquot of carbonate-free, saturated $Ba(OH)_2$ was added to each. They were stoppered with three well-greased ground joints, at ends of which was attached a nitrogen-flushed length of the tubing to be tested:

1) a 1 cm. rubber connection, as control

2) 60 cm. of brown gum rubber suction tubing, used in the pump

3) 85 cm. of 3 mm. i.d. Tygon tubing.

All flasks were filled with nitrogen and inserted into a large desiccator containing an atmosphere of CO_2. The far ends of all these pieces of tubing were doubly closed by tight pinch clamps and sealed-off pieces of glass tubing.

After 48 hours, all three flasks were taken out, the barium carbonate precipitate removed, washed and dried under nitrogen. Estimated recovery was ~95% in this case. The results are presented below:

	Blank	Brown Rubber 3/16"	Tygon 3 mm.	Tygon 5 mm.
Total $BaCO_3$ recovered (uncorr.) - mg.	1.9	242	104	(calc.)
ml. CO_2 (S.T.P.)/hr/ft. length/atmos. CO_2	---	0.18	.09	.125

In a typical experiment, less than 10 ft. of 5 mm. Tygon was used with a total gas volume of ~1000 ml.; hence the rate of CO_2 diffusion was .125 x 10/1000 x 100 = 0.13% of CO_2 present per hour. In the presence of 4% CO_2 (e.g. Barley 14) this would amount to .03 mm./hr. (partial pressure), the corresponding photosynthetic and respiratory changes occurring at rates of 40, resp. 4 mm./hr. Clearly, carbon dioxide diffusion through our tubing was negligible.

*CO_2 Generation

Since carbon 14 supplied is in the form of BaC^*O_3, it is readily converted to C^*O_2 by concentrated sulfuric acid dropped from a pressure-equalizing funnel. It is then trapped in a glass spiral

immersed in liquid nitrogen. If the trap is sufficiently large to hold the C^*O_2, it may be removed from the liquid nitrogen and stored indefinitely (42,44). Dried organic tissue is readily converted to CO_2 by means of a simple variation of the above procedure: a chromic acid "van Slyke" (47) combustion mixture is dropped on the organic matter and heated to boiling for a few minutes. The CO_2 is collected in a cold trap, as above. When properly carried out, the reaction appears to be quantitative.

Geiger Counting

Radioactive samples were "plated" and counted by means of thin mica end-window counters. (for details, see 42,45; also section on Self-Absorption, below).

Extraction of Radioactive Products from Barley Seedlings.

After certain experiments (Barley 3,4,5) involving various periods of photosynthesis and respiration in the presence of C^*O_2, the barley was frozen, dried and extracted. The resulting overall distribution of radioactivity among various fractions has been published (7). This work is not closely enough connected with the topic of this thesis to warrant its repetition here.

SPECIAL EXPERIMENTS ON ISOTOPE EFFECT

A number of experiments was carried out in order to check the rise in the specific activity of the C^*O_2 observed during photosynthesis (see Results)

1) The most obvious potential cause was a difference in

response times the order of 2-3 minutes, between CO_2 analyzer and ionization chamber. In order to eliminate it, we increased the flow rate to 500 cc/min. (from Barley 14 on) and measured the individual response times of the individual response times of the instruments themselves (see above). The latter turned out to be negligibly short.

2) Conceivably some volatile radioactive product, other than C^*O_2 was evolved during the experiments. The only way to determine this was to collect samples of the gas over the plants from time to time, precipitate the C^*O_2 as BaC^*O_3, and measure the specific activity of the carbonate samples.

Barley 15, 19, and 25 were three such runs. In the former two, gas samples were pulled into evacuated flasks. In the latter, a series of flasks formed part of the gas system; one by one they were cut out and by-passed by means of T-connections and stopcocks. In these experiments the gas volumes had to be very large in order to give us enough carbonate to weigh and to make good "plates" for counting.

Each sample was precipitated with $Ba(OH)_2$ by the rubber tubing pump method (see above,). Its radioactivity was then measured by two independent methods:

a) Plating and counting with a thin-window Geiger tube, and

b) Transformation into C^*O_2 and measurement in "standardized" ionization chambers*.

* We are indebted to Mrs. Ruth Scott and Mrs. Jane Krone for the ionization chamber measurements; Miss Marie Haumeder and Mrs. Yvonne Stone "plated" and counted many of the carbonate samples.

The results are plotted in Figures 14, 15, and 16. Considering the experimental difficulties involved, they appear quite satisfactory. Although two or three points are out of line, they do show the rise and fall of specific activity observed in the (better) "instrumental" runs. Unfortunately, at very low specific activities of the order of 70 c./min./mg. $BaCO_3$ had to be used for convenient counting; as a result our continuous-reading ionization chamber and electrometer circuit could not be used to provide a direct cross-check between the two methods.

The ion chamber values in experiment Barley 25 looked rather discouraging. However, we found out later that the chamber insulators used at the time had sufficiently large random "transient" currents to mask any signs of the isotope effect. One of the four Geiger counts on Sample 1 is high; however, the other three are close together and presumably define the correct initial specific activity. The appearance of these results also indicates the great experimental difficulties involved in handling C^*O_2 and carbonate outside a closed system, without contamination, dilution, or exchange with the atmosphere.

One further experiment was performed in order to confirm the reality of the isotope effect. A 200 mg. "isotope farm" of algae was grown from a 2 mg. inoculum in a large quantity of dilute C^*O_2 (4 liters; $\sim$1570 dis/min/mg or $\sim 0.2 \cdot 10^{-6}\%$ $C^{14}O_2$; initial CO_2 pressure, 20 mm. hg). When 70% of this carbon had been converted into organic matter, the reaction was stopped, the three "phases" (air, solution, and algae) separated and the carbon in each converted into BaC^*O_3 under an

inert atmosphere. The carbonate was counted; also, 10 mg. aliquots were re-converted to CO_2 for the purpose of measuring the $C^{13}O_2$ in the same samples by means of a mass spectrometer*. The results were:

	$C^{13}O_2$**		$C^{14}O_2$
Air CO_2	1.195	1.209	99
Water CO_2 and carbonate	1.206	1.207	106
Algae	1.160	1.153	83, 79, 82 (corr. for inoculum: 81)

It is interesting to note the unexpectedly large difference in isotope effects for $C^{13}O_2$ (4%) and $C^{14}O_2$ (20%). The selectivity by which plants discriminate against $C^{13}O_2$ in nature has been measured by Nier (48) and Urey (49); since they were dealing with steady states rather than with kinetic systems, the net effects they observed were considerably smaller than those reported here.

RESULTS

Our experimental results will be presented in the form of graphs and tables. Although a number of similar experiments was performed (Barley 4.5.6.10.11.12.26 with radio-C^*O_2, the others without), the behavior of the plants is most clearly shown in the two best runs, Barley 14 and 28. The discussion in the next section will center about these two.

Each of the other "hot" runs suffered from some experimental

---

* The $C^{13}O_2$ peak (mass 45) was observed; unfortunately, "background" obscured mass peak 46, corresponding to $C^{14}O_2$.

**We are indebted to Dr. William Siri of the Division of Medical Physics for these measurements.

difficulty, such as inaccurate data at low CO_2 concentrations (due, for instance, to insensitivity of the CO_2-analyzer or "background" currents in the ionization chamber) or time lags between instruments (due to slow pumping rate). Knowing the corrections to be applied, we have drawn more or less quantitative curves for each of these experiments. In no case have they contradicted the conclusions drawn from the "best" runs.

As mentioned above (under General Description of Apparatus,), all "hot" experiments were started with the addition of a gas mixture containing C^*O_2 to the complete system (plant chamber, plants and instrument circuit). After the first four or five minutes of cycling required to mix the "slug" of C^*O_2 with the rest of the gas, all instrument readings became steady and meaningful.

The experiment proper was not started. Generally, it involved one or more periods of photosynthesis, preceded and/or followed by periods of dark respiration. Oxygen partial pressures were read directly as often as desired; both CO_2 analyzer and ionization chamber readings were automatically graphed on the record charts.

After each experiment, these data were read off the charts and converted to "partial pressures of CO_2", respectively "millivolts of radioactivity". The specific activity of the C^*O_2 present at any time was obtained by dividing millivolts of radioactivity by millimeters of CO_2 pressure.

In order to graph the radioactivity most conveniently, we arbitrarily set the initial specific activity equal to 1.00. This enabled

us to calculate and plot "millimeters (Hg) of original C^*O_2" from the experimental "millivolts". We could then compare the time course of the two lines, "partial pressure of total CO_2" and "partial pressure of C^*O_2"; when $C^*O_2 >$ total CO_2 the specific activity was greater than unity, when $C^*O_2 <$ total CO_2, it was less.

It should be mentioned here that for the purposes of certain calculations it was necessary to used the true specific activity (the mol percent of $C^{14}O_2$ in total CO_2). This was readily obtained from the arbitrarily defined value above by multiplying it by the actual per cent radiocarbon dioxide present in the original gas mixtures (Table I, col. 7).

It is difficult to present these data adequately on a few small graphs because their precision is very much greater than is implied. For example, between times 275 and 375 in Barley 28 (Figure 24), the "Radioactive CO_2" curve barely rises off the abscissa; yet, a very excellent smooth curve may be drawn through the data points even if the vertical scale is magnified 200-300 fold. Needless to say, our "working curves" have been drawn to such large scales; on them we can measure the slopes and other quantities required for quantitative discussion. It seems to us that the best way to present the precision of the measurements is in table form (see Tables 1-5).

TABLE I

EXPERIMENTAL CONDITIONS

Experiment	Plants			Initial gas mixture			Average conditions		
	Age days	Weight grams ± .5 g.	Pre-treatment before 1st light (with times)	P_{CO_2} mm.Hg	P_{O_2} mm.Hg	$\%C^{14}O_2$ in CO_2	Vacuum in. Hg ± .2 in.	Temp. °C. ± 1°	Light f.c.	Pump rate cc./min.
Barley 4	28	(7)	Dim 24 h., dark 1 h.	22	16	0.01	5	16	(7000)	100
Barley 5	11	13.5	Dim 6 h., dark 5 m.	19	12	0.05	5-3	20	(7000)	100
Barley C-7	13	16	Light 36 h., dark 10 m.	13	~46	0.0	10	16	(7000)	100
Tobacco C-1	--	--	Dark 2h.	15	8	0.0	10	16	(7000)	100
Barley C-9	(10)	6.5	(Dark 30 m.)	18	2	0.0	10	15.5	(7000)	100
Barley 10	7	10	Dark 30 m.	17	7.5	0.13	10	16	(7000)	100
Barley 11	(7)	24	(Dark 30 m.)	17	5.5	0.25	10	15	(7000)	100
Barley 12	7	20	Dim 24 h., dark 25 m.	19	77	1.1	11	16	(7000)	100
Barley 14-1	8	20	Light 24 h., dark 40 m.	17	(10)	1.1	10	22	(7000)	500
Barley 14-2			Light 40 m., dark 65 m.	3.6	(23)	0.14	10	22	(7000)	500
Barley 14-3			Light 15 m., dark 70 m.	3.3	(23)	0.082	10	22	(7000)	500
Barley 15	8	30	Light 24 h., dark 60 m.	22	--	$0.7 \cdot 10^{-4}$	3.5-14	25	(7000)	500
Barley 19	6	14	Light 24 h., dark 25 m.	33	--	$1.6 \cdot 10^{-3}$	10	24	(7000)	500
Barley 25	10	15	Light 6 h., dark 90 m.	21	--	$1.8 \cdot 10^{-3}$	10	21	(7000)	500

TABLE I (cont.)

Experiment	Plants: Age days	Plants: Weight grams ± .5 g.	Plants: Pre-treatment before 1st light (with times)	Initial gas mixture: P_{CO_2} mm Hg	Initial gas mixture: P_{O_2} mm Hg	Initial gas mixture: $\%C^{12}O_2$ in CO_2	Vacuum in Hg ± .2 in.	Temp. °C. ± 1°	Light f.c.	Pump rate cc./min.
Barley 26-1	9	10	Light 24 h., dark 65 m.	16.3	30.5	0.78	10	20	8700	500
Barley 26-2			Light 75 m.	(.01)	48	(0.16)	10	20	3500	500
Barley 26-3			Light 85 m.	(.01)	48	(0.16)	10	20	200	500
Barley 26-4			Dim Light 10 m.	.10	48	(0.16)	10	20	9800	500
Barley 26-5			Dark 145 m.	(.01)	45.5	(0.16)	10	20	9800	500
Succulents C-2-1	--	45	Dim light	1.65	16.8	0.0	10.2-9.7	16.5	(8700)	500
Succulents C-2-2	---		(Dark respiration)	6.0	31.3	0.0	9.7	14.5	---	500
Succulents C-2-3			Dark 60 m.	6.6	33.0	0.0	9.6-8.2	17.5	(8700)	500
Succulents C-2-4			Dark 140 m.	15.8	35.8	0.0	11.2	6± 2	(8700)	500
Barley 28-0	14	(15)	Light, dark 15 m.	3.4	11.2	0.0	10	13.5	9800	500
Barley 28-1			Dark 60 m.	4.2	39.9	4.75	9.8	14.5	9800	500
Barley 28-2			Dark 80 m.	1.16	49.0	.23	8.5±.5	15.5	9800	500

Table 2

Experiment	? CO_2 at steady state mm Hg	Length of time at steady state min.	Initial specific activity	Min. spec. act. obtained during photosynthesis	Length of time in dark min.	Relative rates of evolution of C^*O_2/CO_2 in dark average	Notes
Barley 4	.1 ± .1	5	1.0	.0 ± ?	350	.09	Slow mixing; 3 div. drift of CO_2 analyzer
Barley 5	--	--	1.0	--	--	--	Slow mixing; leak
Barley C-7	.0 ± .1	30	0.0	--	30	--	Slow mixing; 12 div. drift of CO_2 analyzer
Tobacco C-1	.0 ± .1	10	0.0	--	65	--	" " 5 div. drift of CO_2 analyzer
Barley C-9	.0 ± .1	15	0.0	--	--	--	
Barley 10	.0 ± .1	5	1.0	.0 ± ?	190	1.0	Time lags, ion chamber background
Barley 11	.1 ± .1	8	1.0	.0 ± ?	335	.087	" " " " "
Barley 12	.15 ± .1	10	1.0	.0 ± ?	235	.14	" " " " "
Barley 14-1	.1 ± .1	10	1.0	.00 ± .05	65	.125	
Barley 14-2	.1 ± .1	6	.122	.00 ± .015	70	.078	Very slight ion chamber drift
Barley 14-3	.1 ± .1	2	.082	.00 ± .018	85*	.066*	
Barley 15	---	--	--	---		--	Sampling experiment; large volume (5 liters)
Barley 19	---	--	--	---		--	" " " " (13 liters)
Barley 25	---	--	--	---		--	" " " " "

* - Obtained by flushing out respiratory C^*O_2, weighing and counting BaC^*O_3

Table 2 (cont.)

Experiment	PCO_2 at steady state	Length of time at steady state	Initial specific activity	Min. spec. act. obtained during photodynthesis		Relative rates of evolution of C^*O_2/CO_2 in dark	Notes
	mm Hg.	min.		min.		average	
Barley 26-1	.01 ± .05	20	1.0	.2 ± .2	--	--	
Barley 26-2	.01 ± .05	10	.2 ± .2	.2 ± .2	--	--	
Barley 26-3	.10 ± .05	10	.2 ± .2	.2 ± .2	--	--	Ionization chamber "background"
Barley 26-4	.015 ± .05	5	.2 ± 2	.2 ± .2	145	.20	
Barley 26-5	---	--	.2 ± .2	.2 ± .2	35	.19	
Succulents C-2-1	.01 ± .05	40	0.0	---	--	--	Crassula multicava
Succulents C-2-2	---	--	0.0	---	60	--	
Succulents C-2-3	.05 ± .05	45	0.0	---	140	--	
Succulents C-2-4	---	--	0.0	---	--	--	
Barley 28-0	.02 ± .01	5	0.0	---	30	--	
Barley 28-1	.03 ± .01	70	1.0	.065 ± .032	80	.049	Very slight CO_2 analyzer drift (2-1/2 div.),
Barley 28-2	.04 ± .01	5	.049	.025 ± .012	25	.035	(Corrected during experiment)

TABLE 3

Fastest Gas Exchange in Light*

Experiment	Carbon Dioxide		Oxygen		Photosynthetic Quotient**
	$\frac{\text{mm Hg}}{\text{min.}} \times 100$	$\frac{\text{mm Hg}}{\text{min. gram}} \times 100$	$\frac{\text{mm Hg}}{\text{min.}} \times 100$	$\frac{\text{mm Hg}}{\text{min. gram}} \times 100$	$-\frac{d(O_2)}{d(CO_2)}$
Barley 4	44	6.3	49	7.0	1.1
Barley 5	42	3.1	(33)	(2.45)	.79
Barley C-7	35	2.2	(64)	(4.0)	(1.8)
Tobacco C-1	21	--	31	---	---
Barley C-9	26	4.0	27	4.15	1.0
Barley 10	22	2.2	26	2.6	1.2
Barley 11	85	3.55	85	3.55	1.0
Barley 12	69	6.9	77	7.7	1.1
Barley 14-1	110	5.5	--	---	---
Barley 14-2	50	2.5	--	---	---
Barley 14-3	34	1.7	--	---	---
Barley 15	22	3.65	--	---	---
Barley 19	5.3	4.9	--	---	---
Barley 25	3.1	2.7	--	---	---

* 1 mm Hg $\cong$ .069 mmols CO_2 $\cong$ 1.55 ml. CO_2 at S.T.P.

** R_Q and PS_Q values were variable within each experiment

TABLE 3 (cont.)

Fastest Gas Exchange in Light*

Experiment	Carbon Dioxide		Oxygen		Photosynthetic Quotient**
	$\frac{\text{mm Hg}}{\text{min.}} \times 100$	$\frac{\text{mm Hg}}{\text{min. gram}} \times 100$	$\frac{\text{mm Hg}}{\text{min.}} \times 100$	$\frac{\text{mm Hg}}{\text{min. gram}} \times 100$	$-\frac{d(O_2)}{d(CO_2)}$
Barley 26-1	57	5.7	49	4.9	.86
Barley 26-2	0	---	0	---	---
Barley 26-3	--	---	--	---	---
Barley 26-4	--	---	--	---	---
Barley 26-5	5.9	.59	9.4	.94	1.6
Succulents C-2	see graph				
Barley 28-0	23.5	1.55	15.5	1.03	.66
Barley 28-1	12.5	.83	11	.7 3	.88
Barley 28-2	7.0	.47	10	.66	1.4

* 1 mm Hg $\cong$ .069 mmols CO_2 $\cong$ 1.55 ml. CO_2 at S.T.P.

** R_Q and PS_Q values were variable within each experiment.

TABLE 4

Average Gas Exchange in Dark**

Experiment	Carbon Dioxide: $\frac{\text{mm Hg}}{\text{min.}} \times 100$	Carbon Dioxide: $\frac{\text{mm Hg}}{\text{min. gram}} \times 100$	Oxygen: $\frac{\text{mm Hg}}{\text{min.}} \times 100$	Oxygen: $\frac{\text{mm Hg}}{\text{min. gram}} \times 100$	Resp. Quotient*** $-\frac{d(CO_2)}{d(O_2)}$	Initial PO_2 mm Hg
Barley 4	3.9	.56	3.5	.50	1.1	33
Barley 5	--	--	--	--	--	--
Barley C-7	2.0	.125	5.5	.345	.36	61
Tobacco C-1	.83	--	.86	--	.97	29.5
Barley C-9	--	--	--	--	--	--
Barley 10	1.5	.15	.36	.036	4.2	29
Barley 11	2.9	.12	2.5	.10	1.2	23
Barley 12	1.7	.17	2.2	.22	.78	29.5
Barley 14-1	6.2	.31	--	--	--	(27)
Barley 14-2	4.6	.23	--	--	--	(27)
Barley 14-3	4.9*	.245	--	--	--	~4 mm*
Barley 15	--	--	--	--	--	--
Barley 19	--	--	--	--	--	--
Barley 25	--	--	--	--	--	--

* Obtained by flushing out respiratory C^*O_2 with "oil-pumped N_2" and weighing BaC^*O_3

** 1 mm Hg $\cong$ .069 mmols CO_2 $\cong$ 1.55 ml. CO_2 at S.T.P.

*** R_Q and PS_Q values were variable within each experiment

TABLE 4 (cont.)

Average Gas Exchange in Dark**

Experiment	Carbon Dioxide		Oxygen		Resp. Quotient***	Initial
	mm Hg / min. x 100	mm Hg / min. gram x 100	mm Hg / min. x 100	mm Hg / min. gram x 100	$-\frac{d(CO_2)}{d(O_2)}$	P_{O_2} mm Hg
Barley 26-1	---	---	---	---	---	---
Barley 26-2	---	---	---	---	---	---
Barley 26-3	---	---	---	---	---	---
Barley 26-4	1.45	.145	1.45	.145	1.0	46
Barley 26-5	1.45	.145	0.85	.085	1.7	48
Succulents C-2	see graph					
Barley 28-0	1.07	.071	---	---	---	14.5
Barley 28-1	1.28	.085	---	---	---	43
Barley 28-2	1.85	.123	---	---	---	53

** 1 mm Hg $\cong$ .069 mmols CO_2 $\cong$ 1.55 ml. CO_2 at S.T.P.

*** R_Q and PS_Q values were variable within each experiment.

Table 5 UCRL-590

Precision of Measurements

Barley 14

Time	Event	CO_2 Analyzer	Ioniz. Chamber	Specific Activity
0	Start of respiration before PS No. 1	17.0 ± 2%	1160 ± 1%	1.00 ± .03
20	Start of photosynthesis No. 1	18.8 ± 2%	1160 ± 1%	.903 ± .03
40	Specific activity peak No. 1	3.2 ± 3%	240 ± 1%	1.09 ± .04
48-60	Steady state No. 1	0.1 ± 50%	0.0 ± .05mv	0.00 ± .05
100	Middle of respiration after PS No. 1	2.7 ± 4%	20.4 ± 1%	0.11 ± .005
125	Start of photosynthesis No. 1	3.6 ± 3%	30.0 ± 1%	0.12 ± .004
135-140	Steady state No. 1	0.1 ± 50%	0.0 ± .05mv	0.00 ± .015
185	Middle of respiration after PS No. 2	2.3 ± 4.5%	12.2 ± 1%	0.078 ± .002
210	Start of photosynthesis No. 3	3.3 ± 3%	18.4 ± 1%	0.082 ± .003
225	Steady state No. 3	0.1 ± 50%	0.0 ± .05mv	0.00 ± .015
255-310	Average of respiration after PS No. 3	--	--	0.066 ± .01*

* Obtained by flushing out C^*O_2 with N_2, precipitating and counting as BaC^*O_3

Barley 28

Time	Event	CO_2 Analyzer	Ioniz. Chamber	Specific Activity
120	Start of respiration before PS No. 1	3.96 ± 1%	20,000 ± 1%	1.00 ± .02
140	Start of photosynthesis No. 1	4.20 ± 1%	20,000 ± 1%	0.935 ± .02
180	Specific activity peak No. 1	.27 ± 5%	1950 ± 1%	1.09 ± .06
200	Start of steady state No. 1	.03 ± 30%	47 ± 1%	0.31 ± .12
270	End of steady state No. 1	.03 ± 30%	9.5 ± 5%	.065 ± .032
320	Middle of respiration after PS No. 1	.60 ± 5%	148 ± 1%	.049 ± .003
355	Start of Photosynthesis No. 2	1.16 ± 2%	248 ± 1%	.043 ± .002
370	Specific activity peak No. 2	.29 ± 5%	83 ± 1.5%	.056 ± .004
390	Steady state No. 2	.04 ± 25%	5.0 ± 10%	.025 ± .012
420	End of respiration after PS No. 2	.46 ± 4%	78.5 ± 1.5%	.034 ± .002

TABLE 6

UCRL-590

Dark Respiration

Experiment	Time min.	Dark Respiration mm Hg/min x 100 Oxygen	Dark Respiration mm Hg/min x 100 CO_2	P_{O_2} mm Hg	Pre-treatment
Barley 4	66-90	9.5		33.5-31	45 m. PS (3 m. steady state)
	90-230	3.5		31-24	25 m. dark
	230-360	2.6		24-21	65 m. dark
	70-90		9.1	33-31	45 m. PS (3 m. steady state)
	95-140		5.1	31-29	30 m. dark
	150-360		3.9	28-21	85 m. dark
Barley 10	185-230	2.1		29-28	155 m. PS (5 m. steady state)
	240-360	0.36		28	55 m. dark
	187-192		5.3	29	155 m. PS (5 m. steady state)
	200-360		1.5	29-28	15 m. dark
Barley 11	95	19.6		22	40 m. PS (10 m. steady state)
	100	7.6		21.5	5 m. dark
	105-250	2.9		22-18	10 m. dark
	300-450	1.3		16-15	205 m. dark
	95-300		2.5	22-17.5	40 m. PS (10 m. steady state)
	300-450		1.7	17-15	205 m. dark

Table 6 (cont.) UCRL-590

Dark Respiration

Experiment	Time min.	Dark Respiration mm Hg/min x 100 Oxygen	Dark Respiration mm Hg/min x 100 CO_2	P_{O_2} mm Hg	Pre-Treatment
Barley 12	95	34		29.5	45 m. PS (10 m. steady state)
	100	14.5		28.5	5 m. dark
	105	8.7		28	10 m. dark
	110	6.1		27.5	15 m. dark
	115	4.7		27.3	20 m. dark
	130	4.1		26.5	35 m. dark
	150-250	3.1		26-24	45 m. dark
	250-330	2.2		24-22	55 m. dark
	97		9.0	29.5	45 m. PS (10 m. steady state)
	105		5.1	28	10 m. dark
	110-150		3.4	27-26	15 m. dark
	150-220		3.4	25	55 m. dark
	300-330		1.15	23-22	85 m. dark
Barley 14	0-20		9.8	(10)	40 m. dark
	60		10.6	(27)	40 m. PS (15 m. steady state)
	65		7.6		5 m. dark
	70-85		6.6		10 m. dark
	100		5.2	(24)	40 m. dark
	110		4.4		50 m. dark
	120		3.0		60 m. dark
	140		9.6	(27)	15 m. PS (5 m. steady state)
	145		6.8		5 m. dark
	150		6.4		10 m. dark
	160-210		5.0	(26)	20 m. dark
	225-310		6.0*	(27)	15 m. PS (2 m. steady state)

*Obtained by sweeping out CO_2 and weighing $BaCO_3$

TABLE 6 (cont.)

Dark Respiration

Experiment	Time	Dark Respiration mm Hg/min x 100 Oxygen	Dark Respiration mm Hg/min x 100 CO_2	P_{O_2} mm Hg	Pre-Treatment
Barley 26	181-185	(5.8)	2.35-2.15	48	100 m. PS (45 m. low CO_2)
	200-220	2.5	1.66-1.5	47	20 m. dark
	230-235	1.45	1.45	46	50 m. dark
	405-410	12.4	1.45	49	80 m. PS (0 m. steady state)
	420-440	.85	1.45	48	15 m. dark (note: no initial enhancement)
Barley 28	72-80		1.07	14	30 m. PS (5 m. steady state)
	90-110		0.8	14	20 m. dark
	120-142		1.45	40	50 m. dark
	275-325		1.28	44-48	135 m. PS (75 m. steady state)
	350-355		1.91	49	75 m. dark
	395-400		1.85	53	40 m. PS (10 m. steady state)
	400-420		1.68	53	5 m. dark
Tobacco C-1	105-170	.86	.83	29.5	100 m. PS (15 m. steady state) (Note: no initial enhancement)

DISCUSSION

Figure 23 shows the changes in (CO_2) and (C^*O_2) which took place in experiment Barley 14. At time 0 a uniform gas mixture containing 1.1% $C^{14}O_2$ was introduced into the plant chamber. The barley respired inactive CO_2 in the dark, thus reducing the specific activity. When the light was turned on, the specific activity first dropped briefly, due to induction effects (see below, page 86) then rose to about 1.2 times its value at the time the lights were turned on, or 1.3 times the minimum which occurred about time 65. The fact that this peak was some 10% higher even than the specific activity of the original C^*O_2 left no other explanation than an isotope effect (50)*. Finally the continuous respiratory evolution of inactive CO_2 caught up to the photosynthetic isotope concentration and quickly reduced the specific activity to a very low value.

Photosynthesis was CO_2-limited below about 1 mm. partial pressure and became exactly equal to respiration when the only carbon dioxide avaliable for assimilation was provided by respiration. (In strong light at 45 mm. oxygen, this steady state CO_2 pressure was .04 ± .01 mm., well below the figures reported by Gabrielsen (4) and by Miller and Burr (51) - See Barley 28.

After 10 minutes at this steady state, the lights were turned off. Both radio-C^*O_2 and inactive CO_2 were evolved immediately and,

---

* See section on Special Experiments on Isotope Effect,

after five minutes, in a steady ratio. As a result, as both C^*O_2 and CO_2 increased, the specific activity of the gas rose, then remained constant over long periods of time. Clearly, in the dark recently assimilated radioactive compounds became immediately respirable in a constant ratio to the evolution of "dead" CO_2, whereas they were not respirable while the light was on.

The light was now turned on again; at low CO_2 pressures the respiratory dilution overtook the isotope effect more rapidly and the specific activity did not actually rise, but merely failed to drop immediately. Shortly after the CO_2 steady state was reached, the lights were turned off once more and the specific activity found to rise again, to a slightly lower level than that observed after the first light period. As a check on the instruments, this procedure was repeated once more; this time, after the lights were turned off, the entire system was swept for 85 minutes by tank nitrogen (containing about 4 mm. O_2) through a NaOH bubbler. The resultant carbonate was precipitated and counted by means of a Geiger counter; when its specific activity was converted to ionization chamber units, it was found again to be slightly lower than the preceding level; the average rate of respiration was close to that of the preceding dark periods.

This level of specific activity in the dark was roughly inversely proportional to the total light period from the time the first major assimilation of radio-carbon dioxide took place. This merely signified that the photosynthetic intermediates were transformed into non-respirable

products more quickly in the light than in the dark.

Dr. A.A. Benson of this laboratory has shown (52) that algae assimilating C^*O_2 in the light turn less than 0.35% of it into "Krebs cycle respiratory intermediates", such as glutamic acid--although these compounds are present inactive in considerable quantity. If, after some minutes of photosynthesis, the lights are turned off and the C^*O_2 swept out, the radioactivity in the glutamic and isocitric acids is increased more than tenfold. This shows again that the sources of respiratory carbon in the light differ from those in the dark.

We have usually found that after a period of intense photosynthesis in the presence of plenty of CO_2 the dark respiration rate (CO_2 evolution and O_2 absorption) is enhanced by factors of 2-3 or more for varying periods (10-200 minutes - see Table 6). On the other hand, in a couple of experiments (Barley 26, Barley 28-1) this temporary rise did not appear; in these cases, the plants had been kept in the light at the low, steady-state pressure of CO_2 for long periods of time.

It is a great temptation to think of all these results in terms of the mass action effect first suggested by Borodin (14); the building up of photosynthetic intermediates, which become respirable in the dark. If the plants are kept in the light with little CO_2 for long periods, these intermediates are further transformed into more stable storage and structural materials and are no longer readily available for the enhancement of respiration. This reasoning might lead one to expect to see no rise in the specific activity of dark respiration after such a long period

of light and low CO_2 (most of the latter originating from dead, respiratory carbon, at that). Barley 26 and Barley 28-1 whow striking examples of this (see Table 2 and Figures 21,25*).

We may summarize these results, then, by saying they all support the point of view which attributes enhanced dark respiration after a light period to built-up photosynthetic intermediates.

A few photosynthetic and respiratory quotients($-\frac{d(O_2)}{d(CO_2)}$, respectively $-\frac{d(CO_2)}{d(O_2)}$) computed from simultaneous O_2 and CO_2 slopes are listed in Table 3 and 4. They are representative of the surprisingly wide variation in values we have observed in these experiments. It seems that the only conclusion one can safely draw is that carbon dioxide and oxygen changes are equivalent only when averaged over long periods, and quite independent at any given moment. The loose linkage of the oxidation-reduction systems connecting CO_2 and oxygen is particularly evident in succulent plants (Figure 22;) Bonner and Bonner (53) and others have shown that this is closely connected to their variable organic acid reservoirs. The particularly rapid drop of oxygen pressure at low P_{CO_2} after the light is turned off may indicate that molecular oxygen can take the place of carbon dioxide as oxidant of light-generated reducing power.

---

* Note however, that in Barley 28-2 (time 395) the specific activity did rise, as usual, after a short time at low CO_2 pressure. This seems to eliminate unusual behavior on the part of instruments or plants earlier in this experiment.

It was mentioned above that we have observed certain induction effects. For example, in Barley 28-1 (time 140), the direct measure of assimilation, $-\frac{d(C^* O_2}{dt}$, increased to a nearly steady value in about five minutes, while the CO_2 slope did not reach its maximum for nearly fifteen minutes (see Figure 24*). In addition, in some experiments (e.g. Barley 14-1, Barley 28-1) we have seen a slight net rise in P_{CO_2} which may or may not be real. This means that inactive CO_2 was being evolved most quickly for the first few minutes in the light (actually faster than in the dark), and more slowly later on**.

The magnitude of the isotope concentration observed was rather surprising at first. The best experiment (Barley 28, see below) gave us a value of about 0.83 for the ratio of assimilation rates of $C^{14}O_2$ and $C^{13}O_2$. It is possible to derive such large differences even for a single step from a simple bond-vibration calculation if one assumes:

1) the effect occurs in the breaking of a bond between the carbon and a large molecule (such as an enzymatic CO_2-acceptor).

2) the zero point energies of the R-C^{12} and R-C^{14} bonds differ, but the energy levels of the "activated states" are the same.

3). the relative activation energies of the two complexes are the only factor involved.***

---

* Unfortunately it is rather difficult to see these effects on the small scale we had to use for these reproductions.

** Compare the "gush" of CO_2 observed by Emerson and co-workers (57).

*** Recently, Bigeleisen (54) has made more rigorous calculations in which he found that the amximum attainable ratio of rate constants for C^{12}- and C^{14}-containing species at 25°C was as great as 1.5.

It was mentioned above that we have observed certain induction effects. For example, in Barley 28-1 (time 140), the direct measure of assimilation, $-\frac{d(C^*O_2)}{dt}$, increased to a nearly steady value in about five minutes, while the CO_2 slope did not reach its maximum for nearly fifteen minutes (see Figure 24*). In addition, in some experiments (e.g. Barley 14-1, Barley 28-1) we have seen a slight net rise in P_{CO_2} which may or not be real. This means that inactive CO_2 was being evolved most quickly for the first few minutes in the light (actually faster than in the dark), and more slowly later on**.

The magnitude of the isotope concentration observed was rather surprising at first. The best experiment (Barley 28, see below) gave us a value of about 0.83 for the ratio of assimilation rates of $C^{14}O_2$ and $C^{12}O_2$. It is possible to derive such large differences even for a single step from a simple bond-vibration calculation if one assumes:

1) the effect occurs in the breaking of a bond between the carbon and a large molecule (such as an enzymatic CO_2-acceptor).

2) the zero point energies of the $R\text{-}C^{12}$ and $R\text{-}C^{14}$ bonds differ, but the energy levels of the "activated states" are the same.

3) The relative activation energies of the two complexes are the only factor involved.***

---

* Unfortunately it is rather difficult to see these effects onthe small scale we had to use for these reproductions.

** Compare the "gush" of CO_2 observed by Emerson and co-workers (57).

***Recently, Bigeleisen (54) has made more rigorous calculations in which he found that the maximum attainable ratio of rate constants for C^{12}- and C^{14}-containing species at 25° was as great as 1.5.

It is, of course, more likely that several successive bond formations and ruptures are responsible. If these occur in a series of equilibrium steps followed by a slow reaction all the isotope effects will be cumulative, so far as the CO_2-reservoir is concerned. (The last, slow, step would be likely to be the main contributor, since it has no opposing reaction.)

It is interesting to note that the total isotope effect (as seen in the gas above the plants) is hence probably greater when the acceptor enzymes are "saturated" with carbon dioxide than when the CO_2-pressure is low; with plenty of CO_2-exchange the plants have more choice of isotopic species, as it were.

In only one experiment, so far, (Barley 28-1) has the precision of the data justified a detailed kinetic analysis to show the rate of "light respiration". Unfortunately the isotope effect introduces a third variable (in addition to photosynthetic and respiratory rates). This makes an explicit solution impossible; however, one can pick a very sensitive function of these three parameters and try to fit it to the experimentally determined values. The function chosen was the time rate of change of specific activity, $d/dt\ (\frac{C^*O_2}{CO_2})$, or of isotopic ratio, $d/dt\ (\frac{C^*O_2}{CO_2})$ - depending on which of these quantities of the CO_2 analyzer furnished. (See section on CO_2 analyzer,).

The same expression can be derived for it from straight mass action kinetics (any order of reaction) of from a "Michaelis"-type

equation (enzyme limiting** - (55).

The mass action approach merely assumes the rate of assimilation to be proportional to some power of the CO_2 partial pressure; since the same result is obtained for any power (including zero), the equation obtained for the rate of change of specific activity whatever variation in the CO_2 dependence is found experimentally.

The "Michaelis" assumptions are a little more detailed. One considers the atmospheric CO_2 to be in rapid reversible equilibrium with an (enzymatic) acceptor A:

$$CO_2 + A \rightleftharpoons CO_2 \cdot A$$

The complex then decomposes slowly into further products:

$$CO_2 \cdot A \xrightarrow[\text{slow}]{} P_1 + P_2$$

The net rate is proportional to the concentration of the complex, $CO_2 \cdot A$, which is, in turn, given by the equilibrium constant for the first reaction, as well as the concentration of CO_2 and enzyme. At very high CO_2 concentrations, the acceptor is "saturated", i.e., essentially all the enzyme is in the complex form, and a further increase in carbon dioxide does not enhance the rate. On the other hand, at very low CO_2 pressures,

---

** In the latter case one has to assume that the isotope effect occurs in the rate-limiting step after the equilibrium - i.e. that the Michaelis constant is the same for the substrates $C^{12}O_2$ and $C^{14}O_2$.

most of the acceptor is available for combination, and assimilation increases linearly with CO_2 pressure. The "Michaelis constant" is the inverse of the equilibrium constant, as usually defined, i.e.,

$$K_M = \frac{(CO_2)\ (A)}{(A.CO_2)}\ .$$

It can readily be shown to be equal to the CO_2 concentration at which the net rate is one half the maximum rate attainable with a given amount of enzyme.

We have called

(C^oO_2) - partial pressure of inactive CO_2

(C^*O_2) - " " " radioactive CO_2

(CO_2) - " " " total CO_2

R_D - rate of respiration in the dark

$R_L \equiv R$ - rate of respiration in the light

$k_o \equiv k$ - photosynthetic rate constant for C^oO_2

k^* - " " " " C^*O_2

$V_o \equiv V$ - " " maximum rate for C^oO_2 (Michaelis eq.)

V^* - " " " " " C^*O_2 (" ")

$U^* \equiv \frac{k^*}{k} = \frac{V^*}{V}$ - ratio of rate constants for C^*O_2 to C^oO_2; an isotopic "utilization factor".

$S \equiv \frac{C^*O_2}{CO_{*2}}$ - specific activity of the CO_2 in the gas

$s \equiv \frac{C\ O_2}{C^oO_2}$ isotope ratio " " " " " "

Rate Equations from Mass Action Point of View
(CO_2 Analyzer reading $C^{o}O_2$ only)

$$d/dt(C^{o}O_2) = R\,\frac{[C^{o}]}{[C]} = k\,(C^{o}O_2)$$

$$d/dt(C^{*}O_2) = R\,[s] = kU_{*}(C^{*}O_2)$$

$$d/dt(CO_2) = R - k(C^{o}O_2) - kU_{*}(C^{*}O_2)$$

$$s = \frac{(C^{*}O_2)}{C^{o}O_2} = \text{Isotopic Ratio}$$

$$\frac{ds}{dt} = \frac{(C^{o}O_2)\;d/dt(C^{*}O_2) - (C^{*}O_2)d/dt(C^{o}O_2)}{(C^{o}O_2)^2}$$

$$= \frac{d/dt(C^{*}O_2)}{(C^{o}O_2)} - \frac{s}{(C^{o}O_2)}\left[R - R\,[s] - K(C^{o}O_2)\right]$$

$$= \frac{d/dt(C^{*}O_2)}{(C^{o}O_2)} - \frac{sR}{(C^{o}O_2)}\,(1-[s]) + sk(C^{o}O_2)$$

$$kU_{*}\,(C^{*}O_2) = -d/dt(C^{*}O_2) + R\,[s]$$

$$k = \frac{d/dt(C^{*}O_2)}{U_{*}(C^{*}O_2)} + \frac{R\,[s]}{U_{*}(C^{*}O_2)}$$

$$\frac{ds}{dt} = \frac{d/dt(C^{*}O_2)}{(C^{o}O_2)} - \frac{sR}{(C^{o}O_2)}\,(1-[s]) + \frac{R\,[s]}{U_{*}(C^{o}O_2)} - \frac{d/dt(C^{*}O_2)}{U_{*}(C^{o}O_2)}$$

$$= \frac{d/dt(C^{*}O_2)}{(C^{o}O_2)}\left(\frac{U_{*}-1}{U_{*}}\right) - \frac{Rs}{(C^{o}O_2)}\,(1-[s]) + \frac{R[s]}{U_{*}(C^{o}O_2)}$$

Notes: The same results are obtained for an n'th order reaction.

Rate Equations from Michaelis Point of View
(CO_2 Analyzer reading $C^{o}O_2$ only)

$$d/dt(CO_2)\ PS = \frac{V\ (CO_2)}{K_M + (CO_2)}$$

$$d/dt\ (C^{o}O_2) = -\frac{V(C^{o}O_2)}{K_M + (CO_2)} + R(1-[s])$$

$$d/dt(C^{*}O_2) = \frac{VU_* (C^{*}O_2)}{K_M + (CO_2)} + R[s]$$

$$d/dt(CO_2) = R - \frac{V}{K_M + (CO_2)} \left[(C^{o}O_2) + U_* (C^{*}O_2)\right]$$

$$\frac{V}{K_M + (CO_2)} = \frac{R[s]}{U_* (C^{*}O_2)} - \frac{d/dt(C^{*}O_2)}{U_* (C^{*}O_2)}$$

$$s = \frac{C^{*}O_2}{(C^{o}O_2)} = \text{Isotopic rate}$$

$$\frac{ds}{dt} = \frac{d/dt(C^{*}O_2)}{(C^{o}O_2)} - \frac{s}{(C^{o}O_2)} \left[R(1-[s]) - \frac{V(C^{o}O_2)}{K_M + (CO_2)} \right]$$

$$= \frac{d/dt(C^{*}O_2)}{(C^{o}O_2)} - \frac{Rs}{(C^{o}O_2)} (1-[s]) + s\left[\frac{R[s]}{U_*(C^{*}O_2)} - \frac{d/dt(C^{*}O_2)}{U_*(C^{*}O_2)}\right]$$

$$= \frac{d/dt(C^{*}O_2)}{(C^{o}O_2)} - \frac{Rs}{(C^{o}O_2)} (1-[s]) + \frac{R[s]}{U_*(C^{*}O_2)} - \frac{d/dt(C^{*}O_2)}{U_*(C^{o}O_2)}$$

$$= \frac{d/dt(C^{*}O_2)}{(C^{o}O_2)} \left(\frac{U_*-1}{U_*}\right) - \frac{Rs}{(C^{o}O_2)} (1-[s]) + \frac{R[s]}{U_*(C^{o}O_2)}$$

Note: This is the same equation as that obtained from Mass Action point of view.

Rate Equations from Mass Action Point of View
(CO_2 Analyzer reading Total CO_2)

$$d/dt(C^{o}O_2) = R\frac{[C^{o}]}{C} - k(C^{o}O_2)$$

$$d/dt(C^{*}O_2) = R[s] - kU_{*}(C^{*}O_2)$$

$$d/dt(CO_2) = R - k(C^{o}O_2) - kU_{*}(C^{*}O_2)$$

$$k = \frac{R[s] - d/dt(C^{*}O_2)}{U_{*}(C^{*}O_2)}$$

$$d/dt(CO_2) = R - \frac{R[s] - d/dt(C^{*}O_2)}{U_{*}(C^{*}O_2)}\left[(CO_2) + (U_{*} - 1)(C^{*}O_2)\right]$$

$$S = \frac{C^{*}O_2}{CO_2} = \text{Specific Activity}$$

$$\frac{dS}{dt} = \frac{d/dt(C^{*}O_2)}{(CO_2)} - \frac{(C^{*}O_2)R}{(CO_2)^2} + \frac{(C^{*}O_2)}{(CO_2)^2}\left[\frac{R[s] - d/dt(C^{*}O_2)}{U_{*}(C^{*}O_2)}\right]\left[(CO_2) + (U_{*}-1)(C^{*}O_2)\right]$$

$$= \frac{d/dt(C^{*}O_2)}{(CO_2)} - \frac{SR}{(CO_2)} + \frac{R[s] - d/dt(C^{*}O_2)}{(CO_2)U_{*}} + \left(\frac{U_{*}-1}{U_{*}}\right)\left(\frac{S}{(CO_2)}\right)\left[R[s] - \frac{d}{dt}(C^{*}O_2)\right]$$

Note: This is valid for an n'th order equation.

Rate Equations from Michaelis Point of View
(CO_2 Analyzer reading Total CO_2)

Again, answer is same as for Mass Action Derivatives:

$$\frac{dS}{dt} = \frac{d/dt(C^{*}O_2)}{(CO_2)} - \frac{SR}{(CO_2)} + \frac{R[s] - d/dt(C^{*}O_2)}{(CO_2)U_{*}} + \left(\frac{U_{*}-1}{U_{*}}\right)\left(\frac{S}{(CO_2)}\right)\left[R[s] = d/dt(C^{*}O_2)\right]$$

$[C^{\circ}]$ - inactive respirable carbon

$[C^{*}]$ - radioactive " "

$[C]$ - total " "

$[S]$ $\left[\frac{C^{*}}{C}\right]$ - specific activity of respirable carbon

From these quantities we have derived expressions for ds/dt and for dS/dt, the former valid if the CO_2 analyzer records only $C^{\circ}O_2$, the latter if it reads "total CO_2".

We first considered the CO_2 analyzer as reading total CO_2, took the data for $d/dt(C^{*}O_2)$, CO_2, and S obtained in Barley 28, assumed various values for parameters $U_{\frac{1}{2}}$, R and s and plotted a family of curves of dS/dt against time. In addition, we graphed $\frac{dS}{dt}$, as obtained directly from the slope of the experimental "specific activity" curve and compared it to the "calculated" graphs (see Figures 26,27,28,29).

Figure 30 shows a similar set of curves, as obtained for the more likely case that the CO_2 analyzer "sees" only $C^{\circ}O_2$. This time "rate of change of isotopic ratio" was the experimental graph; again, $d/dt(C^{*}O_2)$, $C^{\circ}O_2$, and s provided the data for calculating ds/dt.

The main features of the experimental curve can be represented only by setting $U_{\frac{1}{2}} = .83 \pm .03$ and $R_L = 0.5\ (\pm .1) \times R_D$ (where R_D is the respiration rate in the preceding dark period). A finite value was assumed for the specific activity of respired carbon after an hour or so in the light; however, this factor was used ad hoc. It may be more reasonable to think of R_L as a variable, decreasing from $\sim 2 \times R_D$ when the

light is first turned on, to well below 0.5 R_D after an hour or more - averaging at about the latter figure.

This variation in CO_2 evolution was alluded to already in connection with "induction effects". One may consider the disappearance of C^*O_2 to be directly proportional to the rate of assimilation; the curve fitting above, provided a value of the isotope utilization factor to be used in the calculation. The difference in rates of disappearance of the isotopic species was then an instantaneous measure of R_L:

$$R_L = d/dt(CO_2) + k(C^oO_2) + kU_*(C^*O_2)$$

$$\text{where } k = \frac{d/dt(C^*O_2)}{U_*(C^*O_2)} + \frac{R\ [s]}{U_*(C^*O_2)}$$

A third method to determine R_L is to extrapolate the curve of net rate of CO_2 change to zero CO_2 pressure:

$$-d/dt(CO_2) = k(C^oO_2) + kU_*(C^*O_2) - R_L$$

$$-d/dt(CO_2) = k(0) + kU_*(0) - R_L = -R_L$$

Figure 34 shows the extrapolations obtained from the data of Barley 28-1 and 28-2. They correspond to

$$R_L = (.65 = .7)\ x\ R_D$$

If one subtracts R_L (determined by any of the above three methods) from the net change in CO_2 one gets a series of values for the rate of photosynthetic gas assimilation. Plotted against CO_2 partial pressure,

these yield a hyperbola closely approximating a theoretical Michaelis curve for K_M = .79 ± .05 mm. CO_2. From this association constant for carboxylation, one can calculate a ΔF = -5.7 k. cal./mole, but the significance of this figure cannot as yet be judged.

It was mentioned in the Introduction that gas phase measurements alone cannot give us a true value for either total respiration or total photosynthesis in the light, but only the fractions of gas actually exchanged with the atmosphere above the plants. Some portion of respired CO_2 must certainly remain dissolved in the cells, and be re-assimilated* from solution. Once it is evolved into the intercellular air spaces, it should diffuse quickly into the main gas body where a 500 cc./min. wind provides excellent mixing.

A part of the observed depression of light respiration could be due to this effect. The diffusion calculations of McAlister (31) and of Linderström-Lang (56), as well as the experiments of Gabrielsen (11) seem to show, however, that diffusion equilibria in our ~0.1 mm. thick barley leaves are rapid enough to keep it small compared to chemical processes.

---

* Gabrielsen (11) has shown fairly convincingly that respiratory intermediates are not re-assimilated as such but only after conversion to carbon dioxide.

SUMMARY

The gas exchange by barley seedlings of O_2, CO_2, and added C^*O_2 has been measured in a closed system, with the following results:

1) The carbon of newly formed photosynthetic intermediates is not available for respiration while the light is on but becomes immediately respirable in the dark. The enhancement of dark respiration after a light period is very probably due to the built-up "photosynthates".

2) Photosynthesis proceeds at a measurable rate even at the lowest CO_2 pressures observed (.03 mm.Hg). There is no evidence for a "threshold" concentration of carbon dioxide for the reaction. At the lowest concentrations reached, respiration just equals assimilation, so that a CO_2-steady state ensues.

3) A curve showing the dependence of the rate of photosynthesis on partial pressure of CO_2 yields a "Michaelis Constant" of 0.79 mm.Hg; this corresponds to a free energy of carboxylation of -5700 cal./mol.

4) The mean rate of respiration in strong light is about half that in the dark. Re-assimilation of respiratory carbon dioxide probably accounts for part, but not all of this effect.

5) At low CO_2 pressures, molecular oxygen may be able to substitute for carbon dioxide as the oxidant of photochemically generated reducing agents.

6) The assimilation of $C^{14}O_2$ is about 17% slower than that of $C^{12}O_2$.

APPENDIX A

Construction and Operation of an Oxygen Polarograph

(May - August 1947)

INTRODUCTION

In the spring of 1947 it was suggested to the author that he design a polarograph for the continuous determination of O_2 in a flowing gas stream. This instrument was to be used in conjunction with others in the measurement of rates of photosynthesis and respiration; hence, a wide range of CO_2, as well as of O_2 partial pressures was to be encountered. A polarograph is essentially an electrolytic cell, one of whose electrodes is very small. When a current passes through the cell, the reactant at the micro-electrode becomes quickly depleted in its vicinity; hence, a diffusional gradient is established across a "film" from the concentration of the reactant in the main body of solution to that at the micro-electrode, which is essentially zero. The rate of oxidation or reduction at this electrode, and the resultant cell current, thus become limited to the rate of diffusion of reactant across the film, which in turn is proportional to its concentration in the main body of the liquid.

Figure 32 shows an idealized polarogram for the reduction of O_2 (of a given concentration) at the micro-cathode (58). The first rise in current is associated with the reduction to H_2O_2, then a plateau is reached, where the reaction is diffusion limited.

$$H_2O_2 \rightleftharpoons 2H^+ + O_2 + 2\,e^- \quad E^\circ = .68$$

Beyond this, the second rise of current indicates the further reduction to H_2O:

$$2\ H_2O \rightleftharpoons 2H^+ + H_2O_2 + 2\ e^- \quad E^\circ = -1.78$$

Anywhere along the plateau, the "diffusion current" should be proportional to the concentration of dissolved oxygen. This has been found to be the case by a number of investigators, using stationary and rotating platinum, as well as dropping mercury micro-electrodes (59-63).

An examination of the literature revealed the following information:

1) No polarograph had ever been described for the continuous oxygen analysis of a gas stream.

2) The rotating platinum micro-electrode did not yield the misleading "maxima" in the current-voltage curves of the dropping mercury electrode, was much more sensitive than the stationary-wire electrode (due to larger diffusion currents) and responded much more quickly than both other types. As a result, it was chosen as the instrument to be used.

Design of Equipment

Rotor "B" described by Laitinen and Kolthoff (58,63) was modified as shown in Figure 33. The "dead" gas space was minimized to about 5 cc.; the mercury cup and Wilson seal gave a gas tight closure (which, however, could not be subjected to evacuation). The shaft bearing the platinum wire electrode was coated with Glyptal or Ceresin wax; although some trouble was experienced with pinholes in the former and cracking the latter insulation, either of these coatings worked well if applied carefully. A vertical stirring motor rotated the shaft at a steady 886 r.p.m.

The anode cell (Figures 34,35) consisted of a quiet pool of mercury ($\sim$1 cm^2. large enough to show no concentration polarization), covered by the "supporting electrolyte", usually 0.1 N KCl. This, in effect, constituted a "0.1 N calomel half cell", and the "applied e.m.f." accordingly included the (steady) potential of .335 $\pm$ .005 v. (depending on the partial pressure of oxygen). (64). A wire in a mercury well provided electrical contact to the anode, and a sintered glass disk allowed a rapid stream ($\sim$ 100 cc./min.) of fine gas bubbles to be pumped through the cell.

Figure 36 shows the electrical circuit. AG.E. recording potentiometer across a standard resistance box acted as microammeter (reading to $\pm$ 2 %). The "applied potential" was equal to that across R_3, since the drop across the potentiometer resistance was always small compared to that across the polarographic cell. This potential could be varied by means of rheostats R_3 and R_4, in order to obtain a "plateau curve" of cell current vs. potential. The voltage could then be held constant at some value within the diffusion-limited plateau region, and the current measured as a function of dissolved oxygen concentration.

OPERATION

Figure 37 shows a typical "plateau curve." It resembles the plots of Laitinen and Kolthoff (63) but has a shorter and more slanted "plateau". The explanation for this very probably lies in disturbed diffusion, caused by the rapid gas bubbling.

Current-concentration calibrations were usually carried out in .1 N KCl solution, at -.75 v. near the center of the "plateau". Commercial tank gases ("water-pumped" oxygen; "oil-pumped" nitrogen containing 0.5% O_2; and purified helium) were metered through glass orifices, mixed in the tubing leads, all excess discarded to the atmosphere through a bypass, and a constant flow of the mixture passed through the cell. The percent concentration of oxygen in the gas could be readily calculated: it appeared safe to assume a very rapid equilibrium of gaseous and dissolved oxygen (90% change in 15 sec. - 61,63).

Individual calibration curves looked excellently linear (see Figure 38). Although reproducibility was, at first, very poor, it improved when the cell was held at 0.0 $\pm$ .5°C by an ice bath; however, stirring conditions were still rather unstable and could not be reproduced from day to day. In fact, in some experiments, the curves for increasing and decreasing series of O_2 concentrations differed by as much as 10-20% (see Figure 39). Still, it seems to the author that, if necessary, this polarograph could have been made to work reproducibly and stably for the determination of O_2 in N_2, He, or other inert gases.

Unfortunately, it was the purpose of the instrument to measure rates

of photosynthesis, which necessitated the presence of variable amounts of CO_2 in the gas mixture. A great number of experiments was run to compare the readings of the instrument in the presence and in the absence of 4% CO_2 in the nitrogen. With CO_2 results became even less reproducible than before. It appeared reasonable that this might be due to changes in the pH of the electrolyte. Two methods were tried to overcome this:

1) substitution of .1 M H_2SO_4 (with and without KCl), to keep the solution too acidic to be affected by the solution of CO_2;

2) the use of a pH 5 phosphate buffer.

Neither of these methods improved matters; in both cases, slow electrode reactions (such as the formation of Hg_2SO_4 at the anode and some sort of corrosion at the cathode) may have been responsible for variable results. Cleaning the platinum electrode by filing seemed to help only temporarily.

Two other electrodes were prepared in the following fashion:

1) Silver was plated on to the platinum wire from an $Ag(CN)_2^-$ solution (5 minutes at 3 volts, resulting in a fairly uneven layer).

2) The silver was removed with nitric acid and a small amount of mercury deposited from sodium amalgam. This yielded a "rotating mercury micro-electrode". Neither of these cathodes was stable especially in the presence of CO_2. Recent work by v. Rysselberghe (65) has shown that if O_2 is reduced at a dropping mercury cathode in the presence of CO_2, percarbonic acid is formed by the H_2O_2 at a half-wave potential intermediate between the two oxygen waves. The percarbonate also catalyzes

the further reduction of the peroxide. These observations may well explain the failure of this polarograph in the presence of carbon dioxide.

By this time (August 1947) the Pauling paremagnetic-type oxygen analyzer had become available. It possessed many advantages over the polarograph: simplicity, stability, small volume, absence of water, direct calibration -- against the polarograph's sole virtue of greater sensitivity at low partial pressures. Two photosynthetic experiments were carried out, with the two oxygen analyzers operating in series. Figure 40 shows a portion of one of these runs. The instability of the polarograph is clearly shown; in addition to "wandering" far above and below its mean line of trend, it also read high by many millimeters, although it had been calibrated only some hours before the photosynthetic run. Clearly, the Pauling Meter was far superior to the polarograph and it alone was used in all subsequent photosynthetic experiments.

APPENDIX B

Self-Absorption and Backscattering Effects in the Measurement of Soft Beta Radiation

The "Self-Absorption" of Organic Materials

By way of introduction to the use of tracer carbon, the author was asked to determine the degree of self-absorption of Carbon-14 beta rays in organic meterials. Up to this time, organic compounds and tissues had usually been burned to CO_2 and precipitated and counted at $BaCO_3$ (42). A self-absorption curve had been prepared for this compound (66).

About this time it became frequently necessary to count organic substances as such, because,

a) Usually the substance had to be recovered for further study,

b) There was often too little material for adequate recovery and precipitation of the CO_2,

c) Combustion was too time-consuming.

It was expected that the self-absorption of the organic material at equal surface density (in mg./cm^2.) would be less serious than that of $BaCO_3$, in which the large electron cloud of the Ba^{++} ion should play a dominant role in the slowing of electrons.

The experiments were carried out in the following manner: empty, weighed aluminum plates were mounted on a small turntable; they were marked with a circle of radius 1.91 cm., within which the substance to be counted was spread as evenly as possible by means of pipette and stirring rod. A blower quickly dried the deposit (46), Figure 41. The plates were now weighed again and counted under a thin mica window Geiger counter, at approximately 30% geometry.

A sample of carboxyl-labeled phenylacetic acid (specific activity about 500 c./min./mg.) (67) was dissolved in benzene and used for the first two runs. Another portion was neutralized and deposited from water solution as the sodium salt, and a third as the barium salt. A fourth was esterified with p-phenyl phenacyl bromide and the p-phenyl phenacyl phenylacetate deposited from alcohol.

The results are shown in Figure 42. The ordinate represents the fraction of maximum specific activity, normalized to unity at zero plate thickness for all runs. The previously known $BaCO_3$ curve is also plotted to the same scale. Two things are immediately apparent:

a) the wide scattering of the data (the Ba^{++} salt data were so bad they were not even plotted)

b) the unquestionably steeper curves for all the organic substances tried, indicating a far stronger (if poorly reproducible) self-absorption.

At first this seemed puzzling; however, a close examination of all organic "plates" soon revealed the explanation that all deposits were more or less granular, with relatively large empty spaces between crystals. Clearly, the effective thickness of the deposit was three to four times greater than the "average thicknesses" obtained by dividing the weight of deposit by the <u>total</u> surface area. As a result, the average β-particle had to travel a much longer absorber path and had correspondingly less chance of getting as far as the counter. This explanation also accounts for the wide scattering of experimental points.

From these curves, one may conclude that crystalline deposits

containing C^{14} should have a surface density of less than .05 mg./cm^2., counting inert, as well as radioactive material; on the large disks used in this laboratory this amounts to 0.5 mg. per 11.5 cm^2. plate.

Some months later, in connection with the problem of back-scattering, a series of really smooth organic plates was prepared. Methyl-labeled sodium acetate (1.75×10^5 c./min./mg.) was esterified with p-phenyl phenacyl bromide and the resultant ester dissolved homogeneously in another (long-chain) ester, artificial Ceresin wax, the resultant specific activity of the solution being about 20 c./min./mg. This mixture was readily melted and deposited on the aluminum disks, yielding very smooth and uniform layers of a wide range of thickness.

The "relative specific activities as counted at 30% geometry by a G-M tube and at 50% efficiency in a window-less Nucleometer are recorded in Table 7 and plotted in Figure 43. One may consider these curves to represent the effective self-absorption (including scattering effects, see below) for any smooth organic deposit on an aluminum backing plate.

TABLE 7

Ceresin Wax -- p-phenyl-phenacylacetate plates

Plate	Geiger Counter Data			Nucleometer Data	
	X	A	A/mg.	A	A/mg.
114	0.8	96.3	10.39	932.2	100.6
115	1.15	127.2	9.60	1185.3	89.5
116	2.76	216.2	6.81	1777.8	56.0
118	7.96	339.4	3.70	2555.8	27.9
113	9.87	354.7	3.12	2647	23.7
117	1.71	172.6	8.76	1428.9	72.5
111	0.34_5	42.5	10.71	393.6	99.1
110	0.35_2	49.7	12.24	423	104.2
112	2.21	184.8	7.27	1595	62.7
106	0.207	21.7	9.08	228.2	95.5
107	0.637	27.3	3.72	249.8	34.0
125	14.64	357.2	2.12		
126	13.62	350.2	2.23		
124	16.95	362.8	1.85_5	2528.2	12.9
120	2.12	187.1	7.65	1560.5	63.8
128	3.01	219.4	6.35		
123	6.14	312.8	4.43	2472.3	35.0
199	6.02	302.5	4.37		
198	11.04	309.7	2.44		
121	17.6	417.2	2.06	3428.3	16.9
103	1.07	111.4	9.02	1137.3	92.2

TABLE 7 (cont.)

Plate	X	A	A/mg.
129	0.72_5	72.1	8.64
20_1	7.09	286.5	3.51
133	4.84	282	5.05
134	4.63	278.8	5.23
136	3.68	222.9	5.26
139	3.89	260.8	5.83
137	4.27	226.8	4.62
127	2.99	207.7	6.04
132	3.76	248.5	5.74

Note: X = surface density in mg./cm^2.

A = total counts/minute on plate

A/mg. = specific activity in cts./min./mg.

The Relation of Backscattering to Self-Absorption

At about this time, Dr. Peter E. Yankwich of this laboratory* became interested in the scattering of β-particles by various substances. It was decided to compare the backscattering from a variety of backing materials with the self-scattering of the electrons by the radioactive deposits themselves.**

The enhancement of observable activity caused by reflection processes is said to be due to "backscattering". The intrinsic activity of a thin sample is increased by "exterior reflection" from the sample mount; that of a thick sample is further raised by "interior reflection" due to multiple scattering processes taking place within the sample itself. The latter effect is always observed as part of self-absorption and therefore one compensates for it automatically when self-absorption corrections are derived from data obtained experimentally under conditions identical with those used in routine counting.

Beta radiations subjected to interior reflection can be divided arbitrarily into two groups: (a) some particles which start toward the counter are deflected away from the sensitive volume; (b) others start away from the detector but are reflected back into the counter from some point in the sample. These two processes differ only in direction. Deflection has always been measured as part of the complex

---

* Present address: Department of Chemistry, University of Illinois, Urbana, Illinois.

** The remainder of this section is quoted from "Relation of Backscattering to Self-Absorption in Routine Beta-Ray Measurements."(70).

beta-ray absorption phenomenon; reflection, on the other hand, effectively adds more particles to the measurable flux and thus enhances the observed activity. At the surface of a thick sample the enhancement of the activity is due entirely to internal reflection, since deflection is negligible in the short air path between sample and counter. It can be shown that in deeper-lying layers of the sample this net enhancement is maintained despite the increasing importance of deflection processes.

The magnitude of the backscattering effect depends upon the nature of the sample and mounting and upon the energy of the radiations involved. When thick samples or mounts are used, the effect increases with their atomic numbers and with increasing beta-particle energy. The activity increase due to the mount is kept small by using backings which contain only the lighter elements, such as paper, Cellophane, Nylon, etc. (Accurate determinations of backscattering factors as functions of the solid angle subtended by the detector at the source have not been made. It is known that the size of the effect observed is dependent upon the geometry of the detection system, increasing with increasing geometric efficiency). In order to gain information on the effect of backscattering upon self-absorption data, some experiments were performed which were designed to yield information concerning the relative backscattering powers of a number of substances at two different detection geometries.

A 4 μg. sample of C^{14} active barium carbonate was mounted over an area of 0.040 cm^2. in the center of a plastic film circle 20 cm. in diameter and 0.07 mg./cm^2. thick; the sample layer was not heavier than 0.15 mg./cm^2. The aluminum equivalent thickness of the counter

window and air path was 3.4 mg./cm^2. at the lower geometry (12%) and 2.3 mg./cm^2. at the higher (36%). The sample was first counted over 25 cm. of air; then thick layers of various materials were maneuvered to within 0.05 mm. of the back of the sample spot and the activity again measured. This enhanced activity, divided by that first observed, is taken as being equal to the backscattering factor of the substance in the thick backing layer at the geometric efficiency with which detection was carried out. The data are collected in Table 8.

TABLE 8

Backscattering of C^{14} Beta-Particles

Scatterer	Relative observed activity 12% geometry	30% geometry
Air	1.00	1.00
Platinum	1.43 ± 0.02	1.51 ± 0.02**
Barium carbonate	1.30 ± .01	1.35 ± .01
Glass	1.16 ± .01	1.17 ± .01
Aluminum	1.15 ± .01	1.16 ± .01* **
Paper (unsized)	1.04 ± .015	1.07 ± .015
Wax (artificial ceresin)	1.05 ± .015	1.07 ± .015

* Compare with L.D. Norris and M.G. Ingram (68).

** Compare with J.R. Hogness, et al. (69).

From these data it is possible to make certain statements about interior reflection in samples of various thicknesses. Consider, first, a sample of radioactive barium carbonate mounted on aluminum and counted

at 36% geometry. If one envisions the sample as made up of many thin layers, it is apparent that the observed activity of the first lamina (counting from the mount) is 1.16 times the intrinsic activity because the aluminum mount contributes an additional radiation flux to the measurement by exterior reflection. The activity observable from the next lamina is increased by slightly more than 1.16, for although fewer radiations can reach the backing, they are more powerfully reflected from the first barium carbonate lamina. Thus, as the sample thickness is increased, the activity rises from 1.16 to 1.35 times that observed when all reflection effects are neglected. If samples of active wax were used, the activity observable would fall from 1.16 to 1.07 times the "no-reflection" strength because the interior reflecting power of wax is less than the exterior reflecting power of aluminum.

Backscattering effects saturate very rapidly because they involve double transit of radiations through absorbing layers. The maximum penetration thickness of C^{14} beta-particles is about 28 mg/cm^2; yet the reflection effects reach 80% of their maximum at a sample thickness of 6 mg./cm^2. and 97% at 12 mg./cm^2.

It has been assumed by many investigators that the effective self-absorption corrections for several sample substances are very nearly the same as those for barium carbonate, for which most such determinations have been made. That this is not the case can be seen by reference to Figure 44, where data for wax and barium carbonate samples, all mounted on aluminum, are graphed.

A consideration of the reflection enhancement of the observed

radiation leads one to expect that, at sample thicknesses where the backscattering effects are saturated, the curves for the two sample materials will be related to each other by the quotient of the proper reflection coefficients. The value predicted is $1.35 \pm 0.01/1.07 \pm 0.015 = 1.26 \pm 0.02$; that observed is 1.27.

SUMMARY

Backscattering appreciably raises the observed β-activity from the thick samples containing C^{14}. This effect must be subtracted if one wishes to determine the true self-absorption within the samples. The true self-absorption of carbon-radioactive organic materials is the same as that of $BaC^{14}O_3$.

BIBLIOGRAPHY

1. Gaffron, H., Biochem. Zeits., 292, 241 (1937).

2. Myers, J. and Burr, G.O., J. Gen. Physiol., 24, 45 (1940).

3. Hoover, W.H., Johnston, E.S. and Brackett, F.S., Smithsonian Miscell. Collect., 87, No. 16 (1933).

4. Gabrielsen, E.K., Nature (London) 161, 138 (1948).

5. Rabinowitch, E.I., Photosynthesis, N.Y., Interscience, Vol. 1 ((1945).

6. Weintraub, R.L., Botan. Reviews, 10, 383 (1944).

7. Benson, A.A., Calvin, M., Haas, V.A., Aronoff, S., Hall, A.G., Bassham, J.A., and Weigl, J.W., Photosynthesis in Plants, ed. by J. Franck and W.E. Loomis (Iowa State College Press, Ames, (1949) chapter 19.

8. Moore, W.E. and Duggar, E.M., ibid, Chapter 11.

9. Loomis, W.E., ibid., Chapter 1.

10. Kok, B., Enzymologia, 13, No. 1 (1947).

11. Gabrielsen, E.K., Nature 163, 359 (1949).

12. Miller, E.S. and Burr, G.O., Plant Physiology, 10, 93 (1935).

13. Myers, J., J. Gen. Physiol., 30, 217 (1947).

14. Borodin, I., Mem. Acad. Imp. Science VIII, 28, (4), 1 (St. Petersburg, 1881).

15. Mothes, K., Baatz, I. and Sagronsky, H., Plants, 30, 289 (1939).

16. Spoehr, H.A. and McGee, J.M., Carnegie Inst. Wash. Pub., No. 325, (1923).

17. James, W.O., Ann. Rev. Biochem., 15, 417 (1946).

18. Bonner, J. and Wildman, S.G., Arch. Biochem., 10, 497 (1946).

19. Bonner, J., Arch. Biochem., 17, 311 (1948).

20. Calvin, M. and Benson, A.A., Science, 109, 140 (1949).

21. Calvin, M. and Benson, A.A., Science, 107, 476 (1948).

22. Benson, A.A. and Calvin, M., Science 105, 648 (1947).

23. Benson, A.A. and Calvin, M., Proc. Cold Spring Harbor Symp. Quant. Biol. 13, 6 (1948).

24. Aronoff, S., Benson, A.A., Hassid, W.Z. and Calvin, M., Science, 105, 664 (1947).

25. Pauling, L., Wood, R.E. and Sturdivant, J.H., J. Am. Chem. Soc., 68, 795 (1946).

26. Janney, O.D. and Moyer, B.J., MDDC 621; MDDC 1303; Rev. Scient. Inst., 19, (Oct. 1948).

27. Krone, J., Private Communication.

28. Otvos, J.W., Report to Amer. Phys. Soc., Los Angeles, (Jan. 1948); also Private Communication.

29. Glass, F.M., Oak Ridge, Nat. Lab. Report 191.

30. Palevsky, H., Swank, R.K. and Grenchik, R., Rev. Sci. Inst., 18, 298 (1947).

31. McAlister, E.D., Smithson. Miscell. Collect., 95, No. 24 (1937).

32. Pfund, A.H., U.S. Pat., 2, 212, 211 (1940) Fastie, W.G., and Pfund, A.H., J. Opt. Soc. Amer., 37, 762 (1947).

33. Wright, N. and Herscher, L.W., J. Opt. Soc. Amer., 36, 195 (1946).

34. Schmick, H., U.S. Pat. 1,758,088 (1930).

35. Pfund, A.H., Science 90, 236 (1939).

36. Luft, K.F., Zeits. f. Physik, 24, 97 (1943).

37. Cross, P.C. and Daniels, F., J. Chem. Phys., 2, 6 (1934).

38. Hertz, G., Verh. d. Dout. Phys. Ges., 13, 617 (1911).

39. Handbook of Chemistry and Physics, 30th Ed., Chem. Rubber Publ. Co., page 1367 (1947).

40. Sheline, R.K. and Weigl, J.W., J. Chem. Phys. 17, 747 (1949).

41. Morse, P.M., Vibration and Sound, New York, McGraw-Hill and Com. (1942).

42. Dauben, W.G., Reid, J.C. and Yankwich, P.E., Anal. Chem., 19, 828 (1947).

43. Yankwich, P.E., Science 107, 681 (1948).

44. Calvin, M., Heidelberger, C., Reid, J.C., Tolbert, B.M. and Yankwich, P.E., Isotopic Carbon, John Wiley and Sons, N.Y. (1949).

45. Ibid., pages 68, 104 ff.

46. Ibid., page 111.

47. Van Slyke, D. D. and Folch, J., J. Biol. Chem., 136, 509 (1940).

48. Nier, A.O. and Gulbransen, E.A., J. Am. Chem. Soc., 61, 697 (1939).

49. Urey, H.C.Science 108, 489 (1948).

50. Weigl, J W. and Calvin, M., J. Chem. Phys., 17, 210 (1949).

51. Miller, E.S. and Burr, G.O., Plant Physiology, 10, 93 (1935).

52. Calvin, M., Benson, A.A., et al. (to be published).

53. Bonner, W. and Bonner, J., Am. Jour. Bot., 35, 113 (1948).

54. Bigeleisen, J., in Brookhaven Conference Report (BNL-C-8), Isotopic Exchenge Reactions and Chemical Kinetics, (Dec. 1-3, 1948).

55. Michaelis, L. and Menten, M.L., Biochem. Zeits., 49, 333 (1913).

56. Linderström-Lang, K., Compt. Rend. Lab. Carlsberg, ser. Chimique, 25, No. 11 (1946).

57. Emerson, R. and Lewis, O.M., Am. Jour. Bot., 26, 808 (1939).

58. Kolthoff, I.M. and Lingane, J.J., Polarography (New York, Interscience, 1946).

59. Kolthoff, I.M. and Miller, O.S., J. Am. Chem. Soc., 63, 1013 (1941).

60. Vitek, V., Coll. Czechoslov. Chem. Commun., 7, 537 (1935).

61. Kolthoff, I.M. and Laitinen, H.A., Scinece 92, 152 (1940).

62. Petering, H.G. and Daniels, F.J., J. Am. Chem. Soc., 60, 2796 (1938).

63. Laitinen, H.A. and Kolthoff, I. M., J. Phys. Chem., 45, 1079 (1941).

64. Latimer, W.M., Oxidation States of the Elements and their Potentials in Aqueous Solutions (New York, Prentice-Hall, 1938) page 162.

65. v. Rysselberghe, P., Report to the American Chemical Society Meeting, San Francisco, March 1949.

66. Yankwich, P.E., Norris, T.H., and Huston, J., Anal. Chem., 19, 439 (1947).

67. Dauben, W.G., Reid, J.C., Yankwich, P.E. and Calvin, M., J. Am. Chem. Soc., 68, 2117 (1946).

68. Norris, L.D. and Inghram, M.G., Phys. Rev., 73, 350 (1948).

69. Hogness, J.R., Roth, L.J., Leifer, E. and Langham, W.H., J. Am. Chem. Soc., 70, 3840 (1948).

70. Yankwich, P.E. and Weigl, J.W., Science 107, 651 (1948).

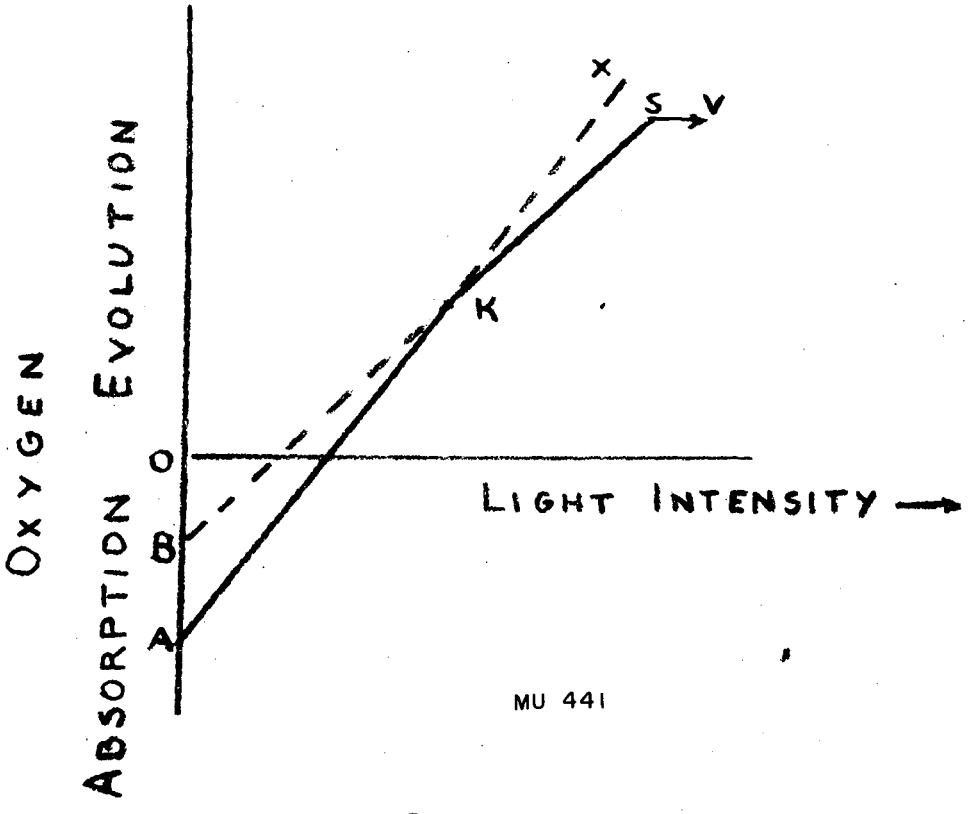

Figure 1

Dependence of Respiration on Light
According to Kok (10)

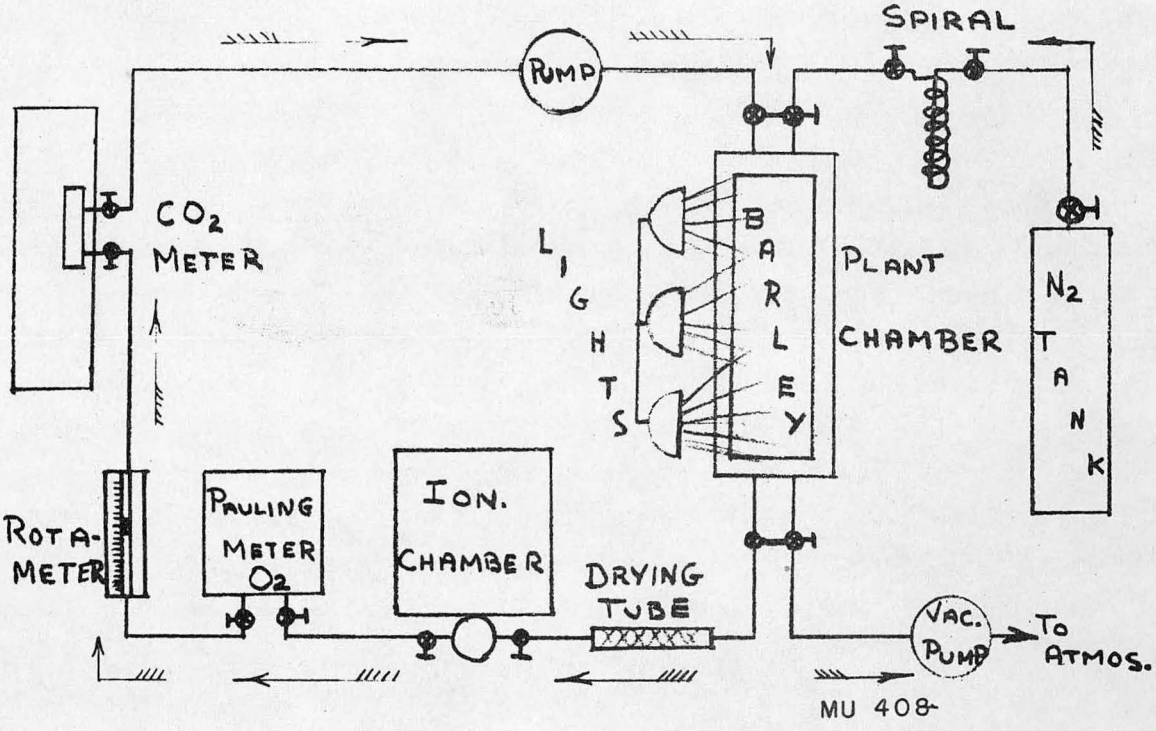

Figure 3

Diagram of Layout

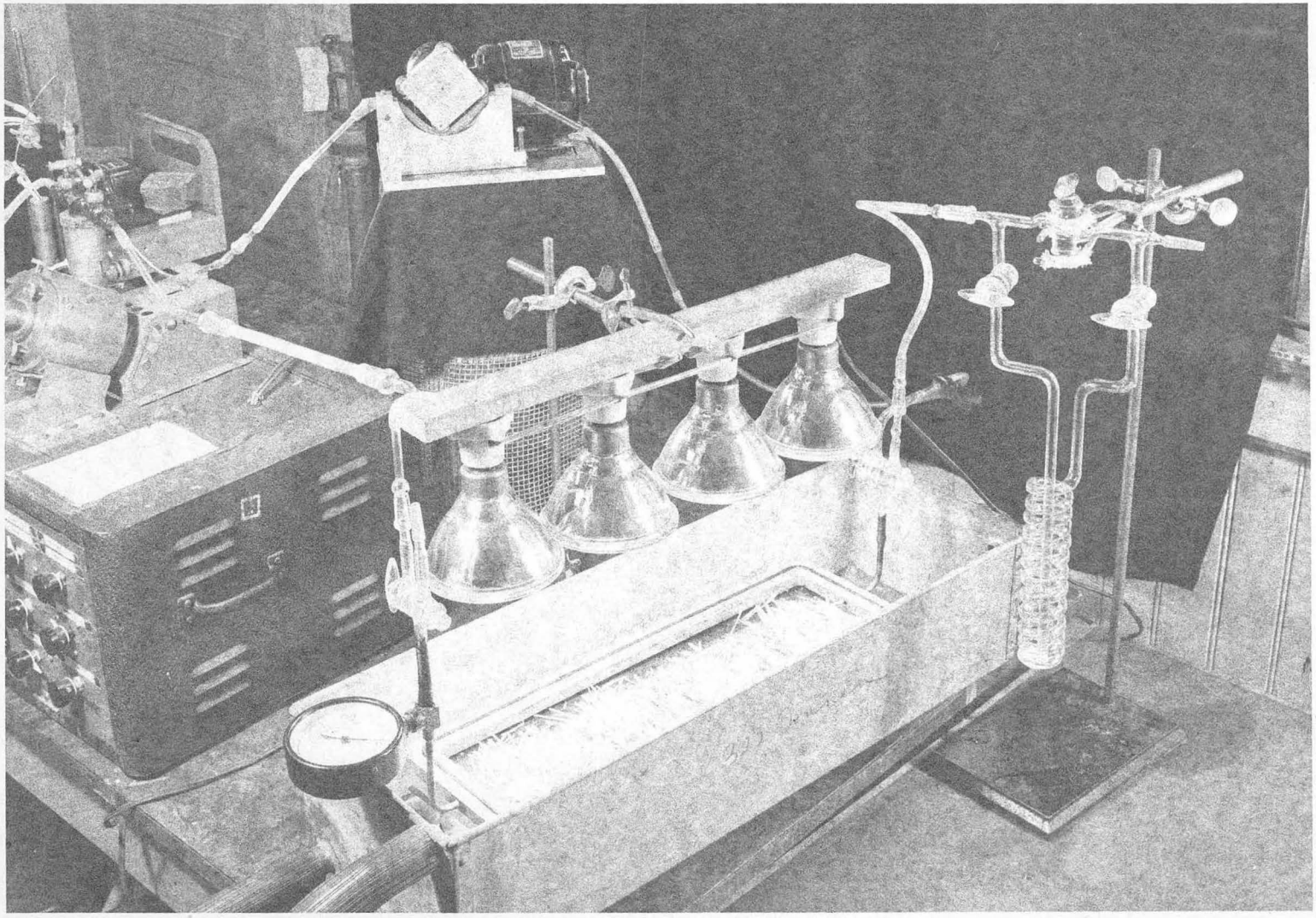

PLANT CHAMBER, LIGHTS, $C^{*}O_2$ SPIRAL, RUBBER TUBING PUMP

FIG. 4

OZ 926

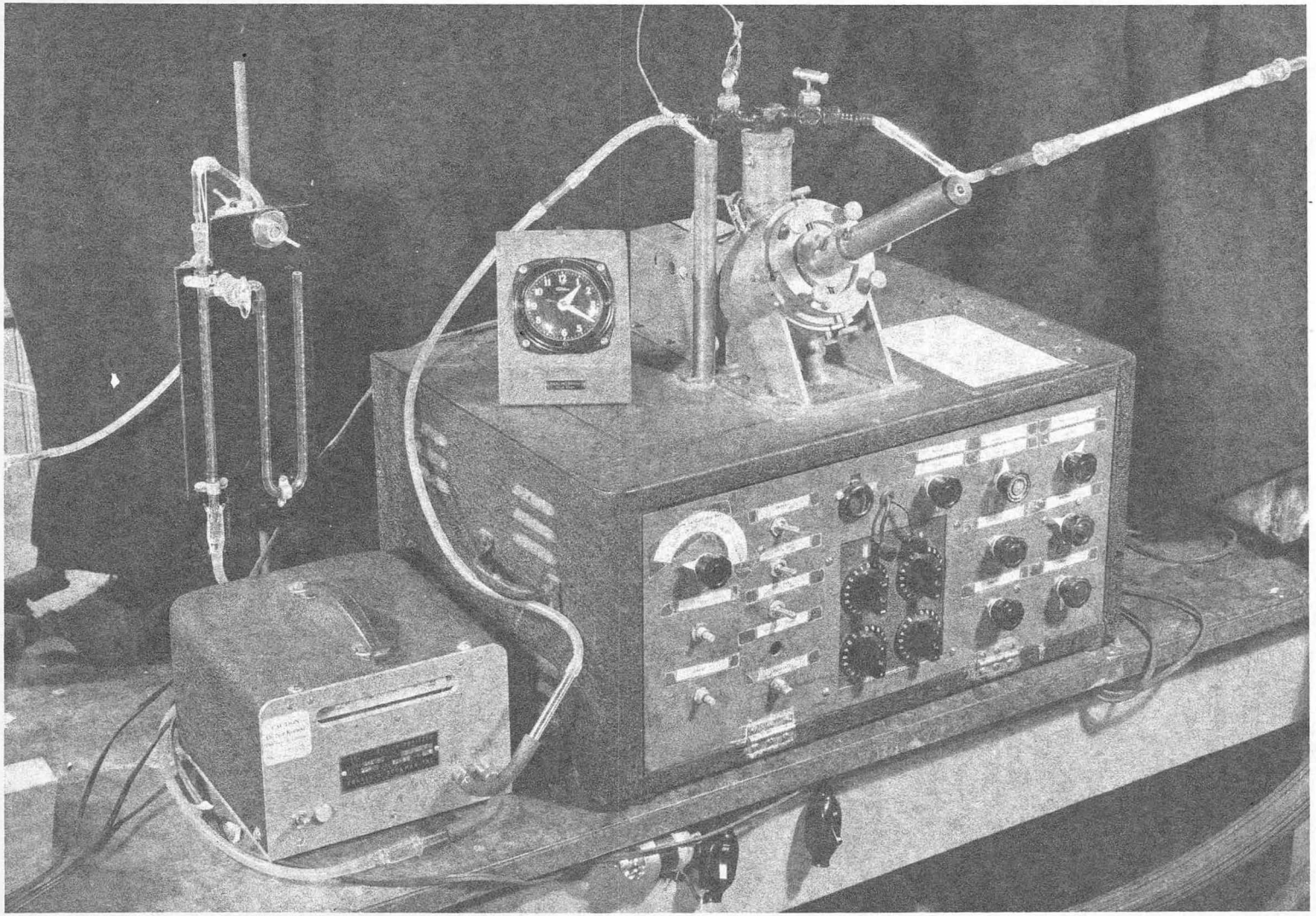

ROTAMETER, PAULING OXYGEN ANALYZER
SMALL IONIZATION CHAMBER AND ELECTROMETER

FIG. 5

OZ 923

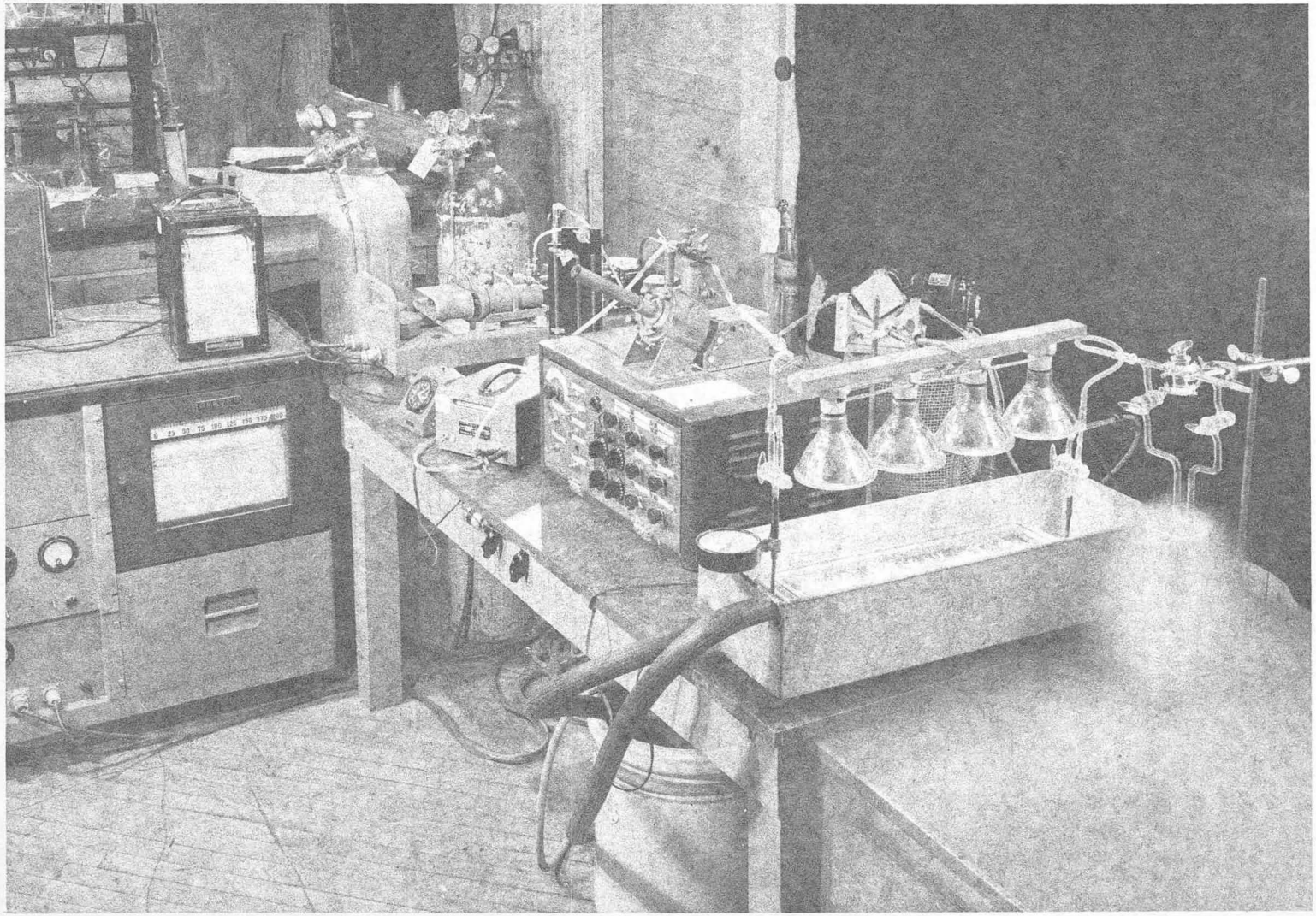

EXPERIMENTAL LAYOUT

FIG. 2

OZ 922

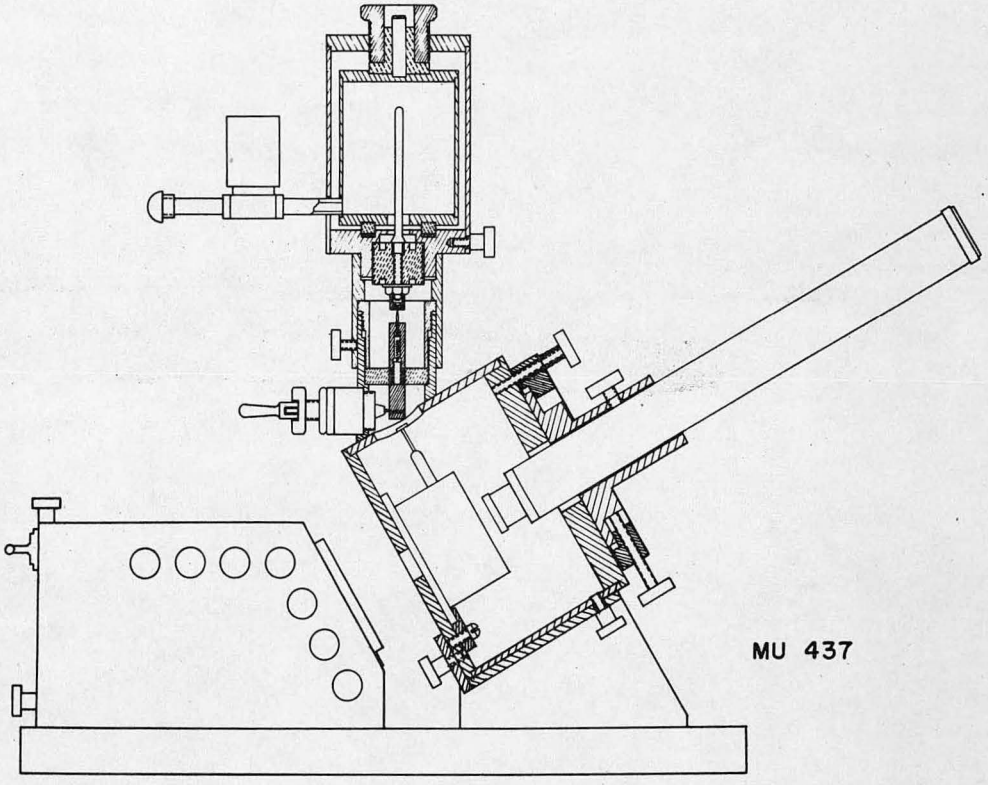

Figure 6

Crossection of Large Ionization Chamber and Electrometer
(after Janney and Moyer, 26)

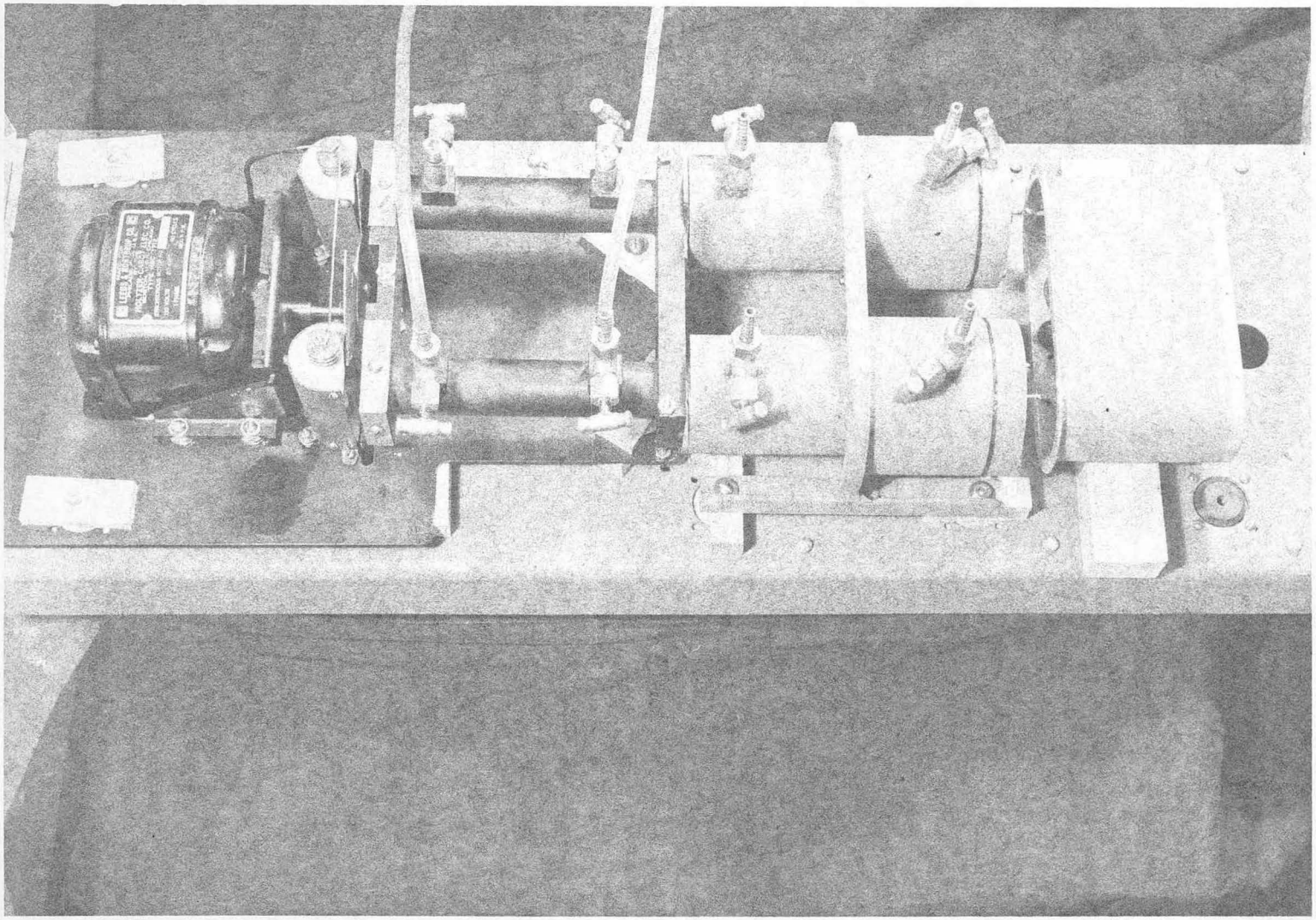

CO_2 ANALYZER, TOP VIEW— SHUTTER MOTOR, SOURCES WITH MIRRORS, SHUTTER, ABSORPTION CELLS WITH PHASING ADJUSTMENT, DETECTOR CELLS, PREAMPLIFIER.

FIG. 7

OZ 924

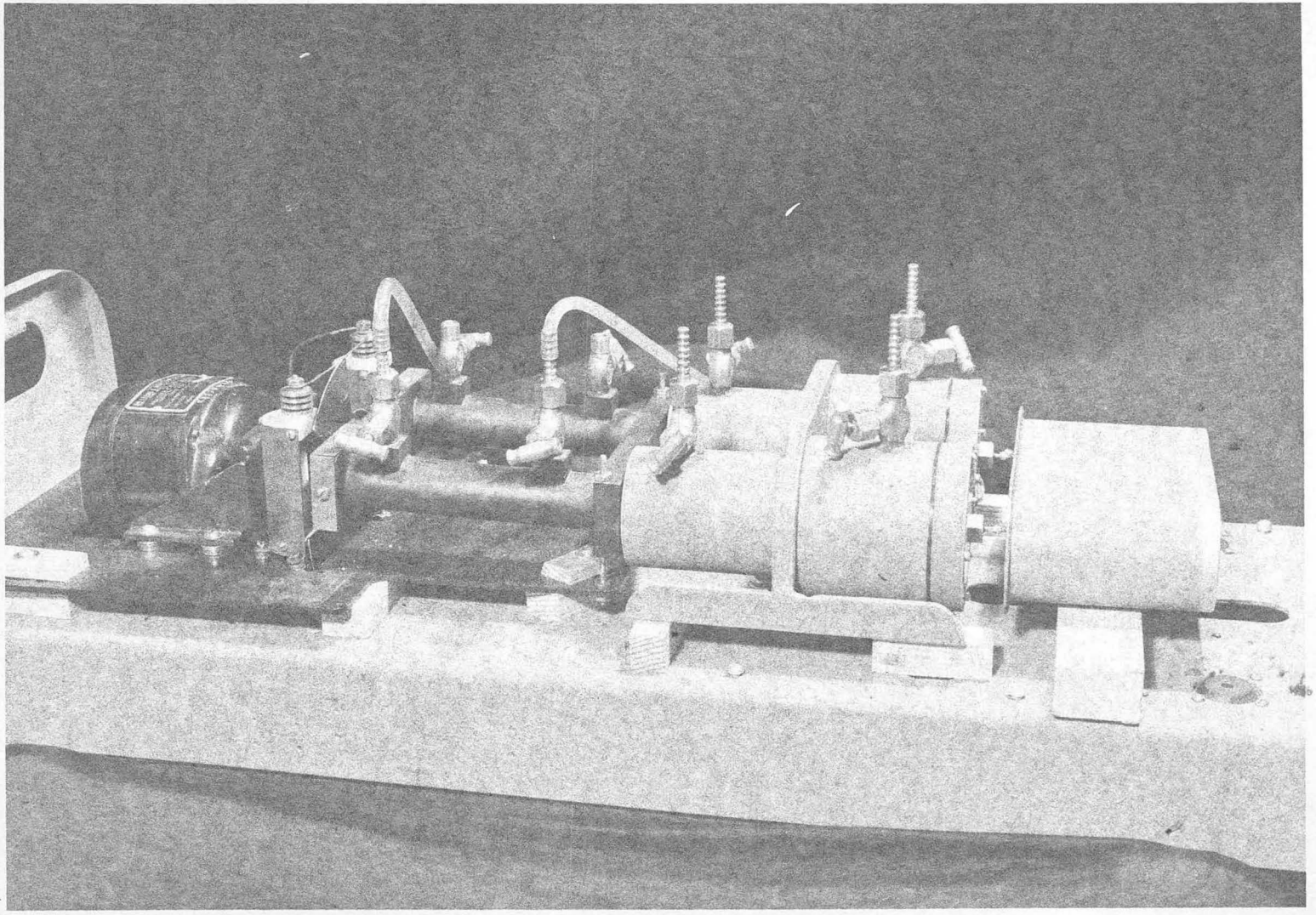

CO_2 ANALYZER, SIDE VIEW

FIG. 8

OZ 925

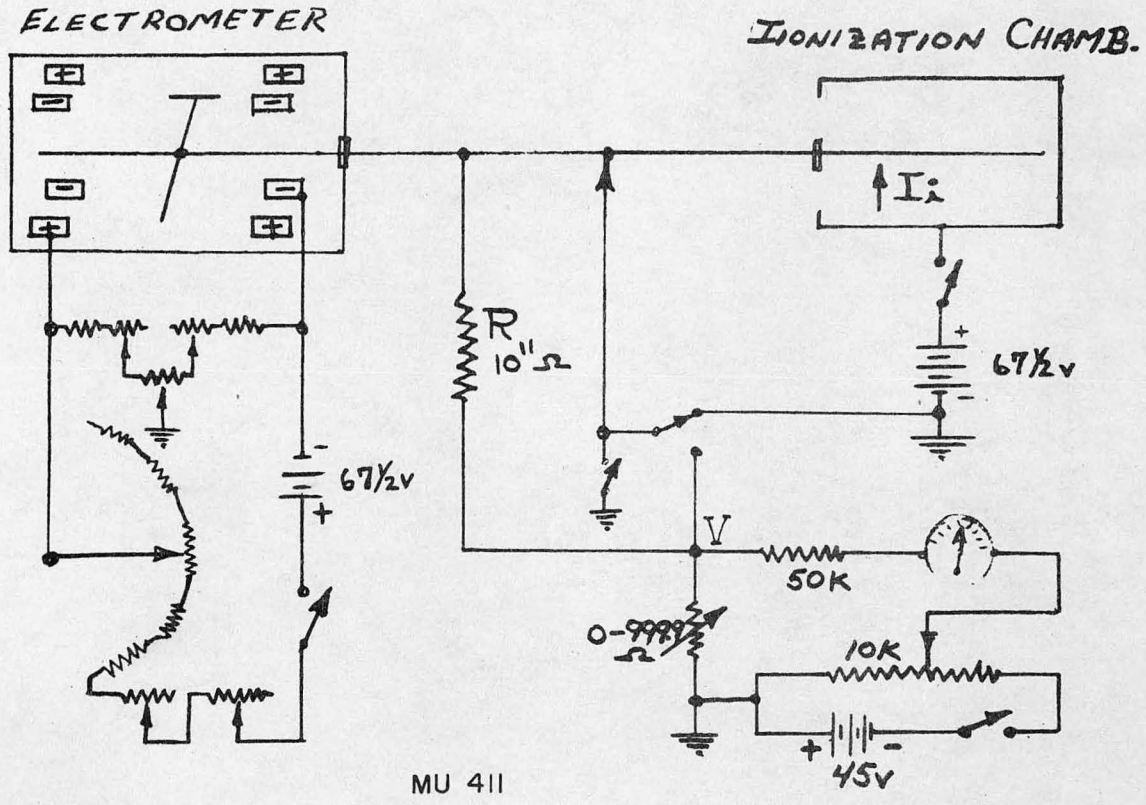

Figure 9

Electrometer Circuit

(modified for instantaneous measurement)

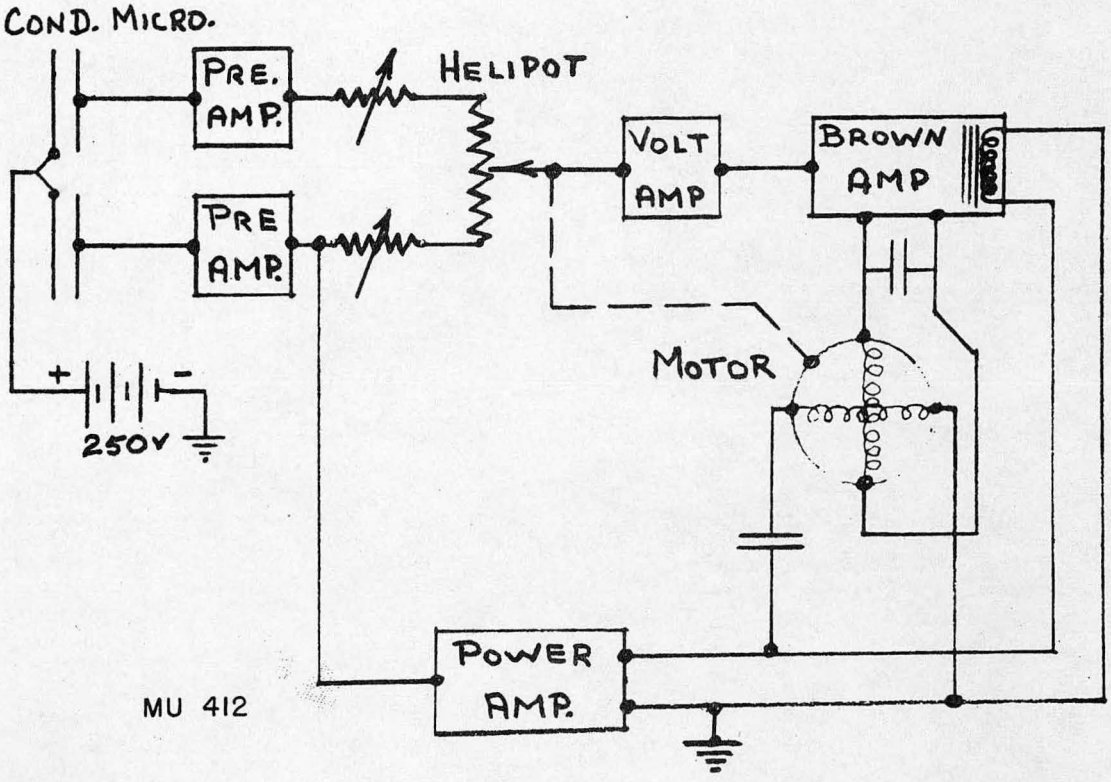

Figure 10

CO_2 Analyzer Circuit, Block Diagram
(Recorder Pen Travels with Pointer on "Helipot" Resistor)

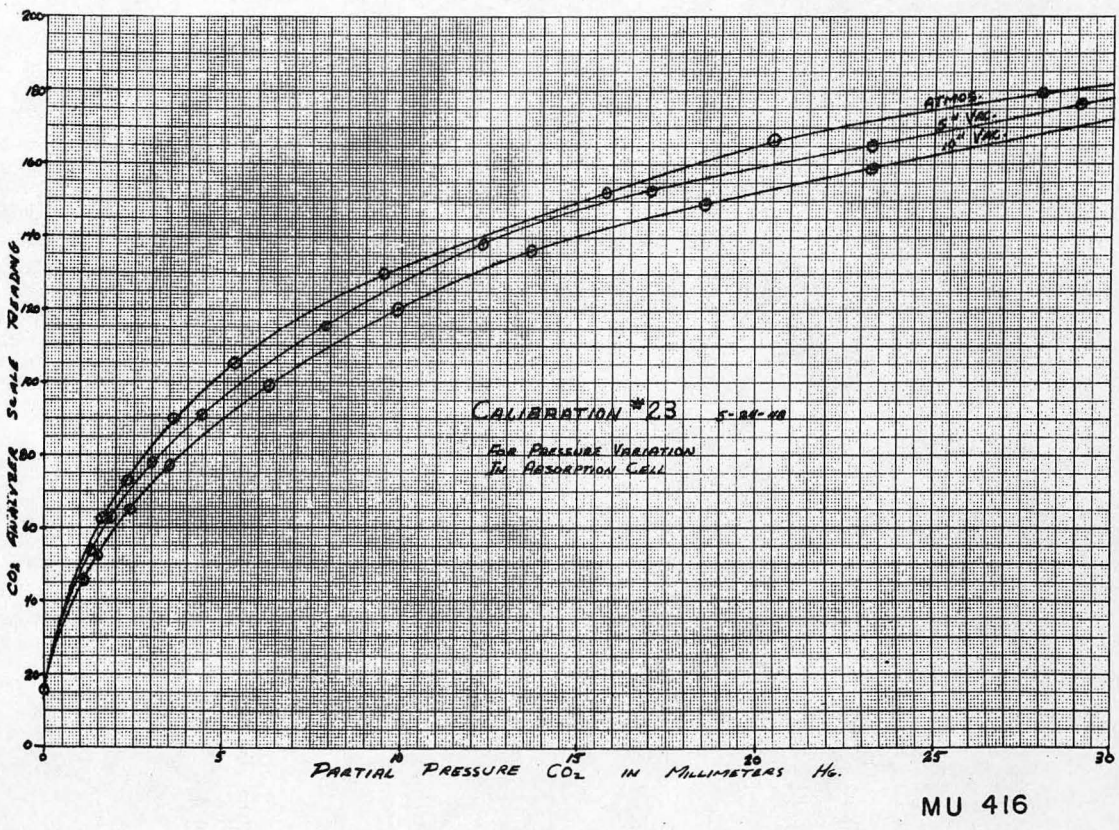
CALIBRATION #23 5-26-48
FOR PRESSURE VARIATION IN ABSORPTION CELL
ATMOS.
5" VAC.
10" VAC.
CO2 ANALYZER SCALE READING
PARTIAL PRESSURE CO2 IN MILLIMETERS Hg.
0
5
10
15
20
25
30
40
60
80
100
120
140
160
180
200
MU 416

Figure 11

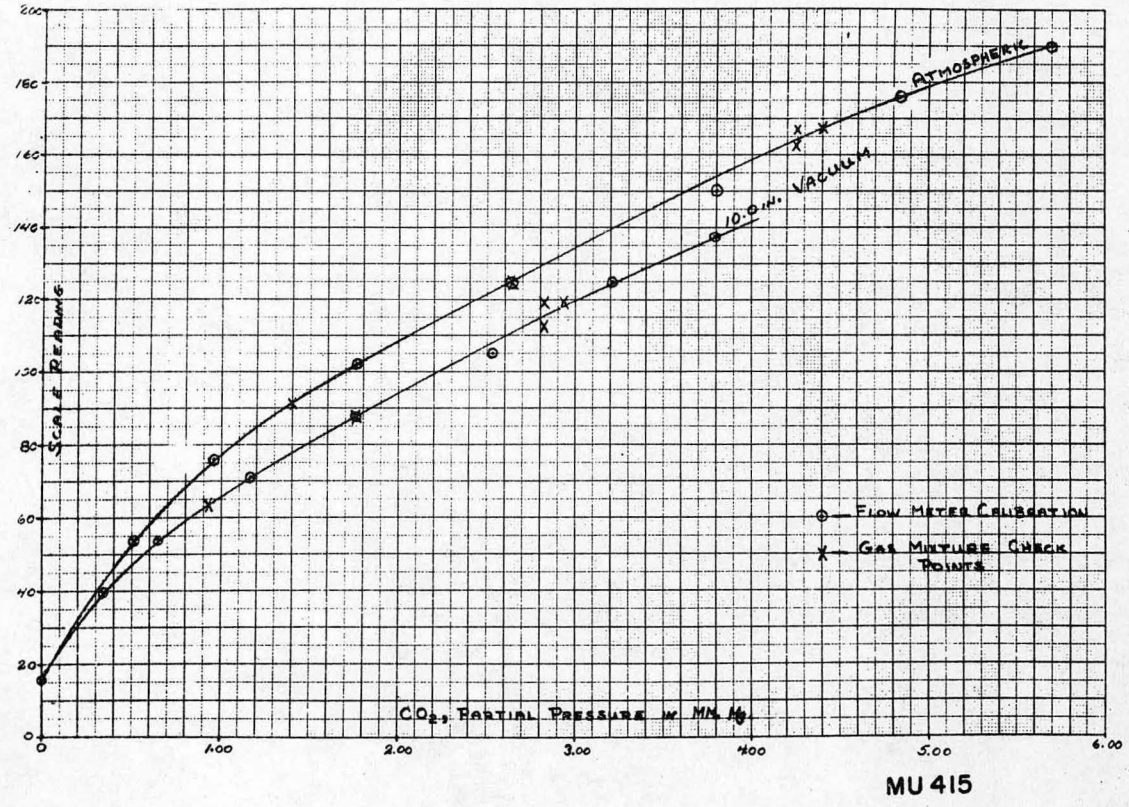
ATMOSPHERIC
VACUUM
10.0 IN.
SCALE READING
⊙— FLOW METER CALIBRATION
X— GAS MIXTURE CHECK POINTS
CO_2, PARTIAL PRESSURE IN MM. Hg.
0
20
40
60
80
100
120
140
160
180
200
1.00
2.00
3.00
4.00
5.00
6.00
MU 415

Figure 12

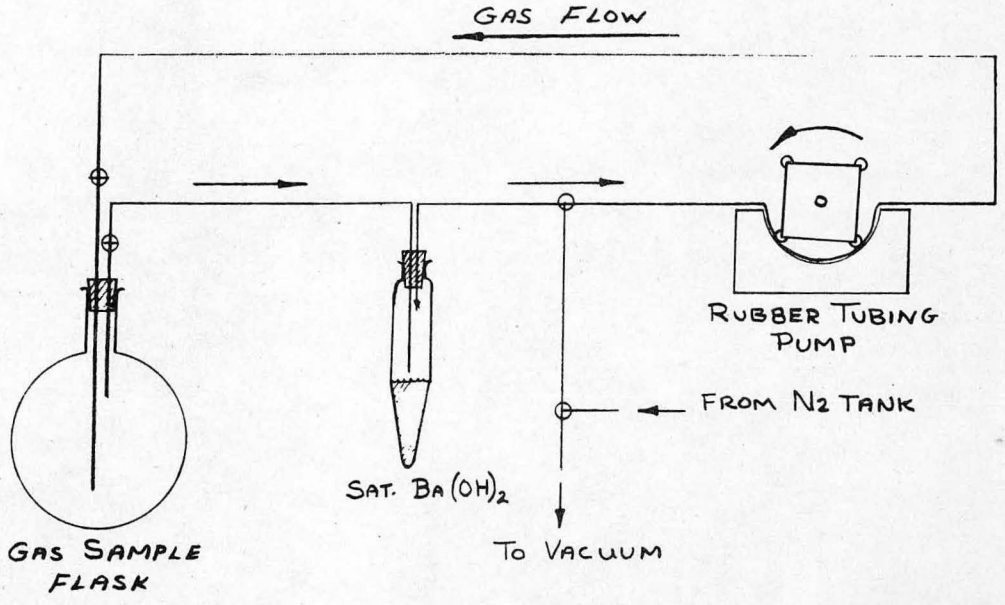

CO_2 PRECIPITATION BY $Ba(OH)_2$

Figure 13

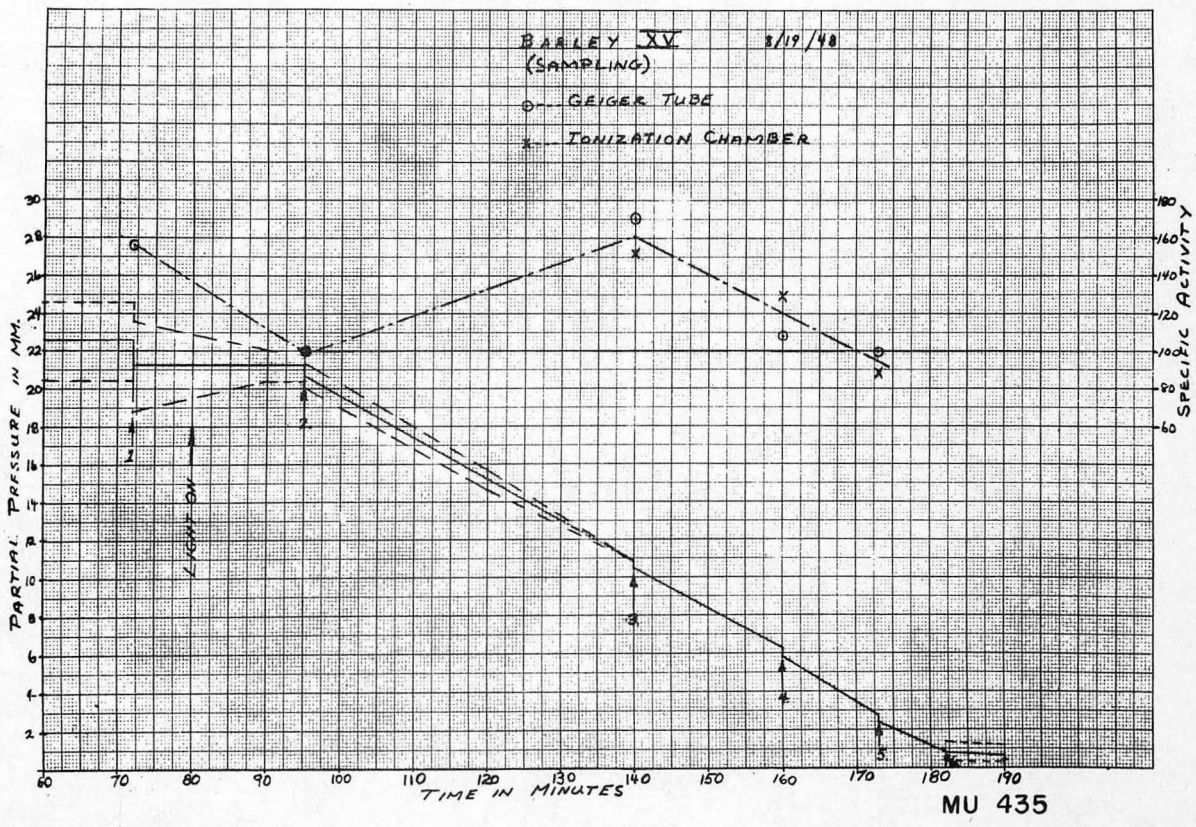
BARLEY XV 8/19/48
(SAMPLING)
⊙ — GEIGER TUBE
x — IONIZATION CHAMBER
PARTIAL PRESSURE IN MM.
SPECIFIC ACTIVITY
TIME IN MINUTES
MU 435

Figure 14

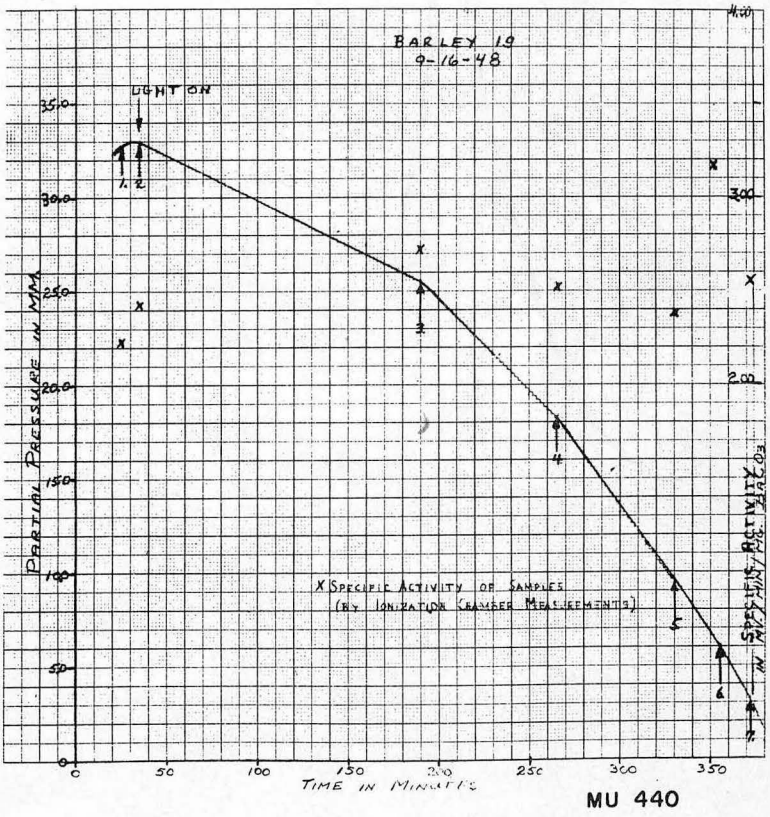
BARLEY 19
9-16-48
LIGHT ON
1
2
3
4
5
6
X SPECIFIC ACTIVITY OF SAMPLES
(BY IONIZATION CHAMBER MEASUREMENTS)
PARTIAL PRESSURE IN MM
TIME IN MINUTES
SPECIFIC ACTIVITY
MU 440

Figure 15

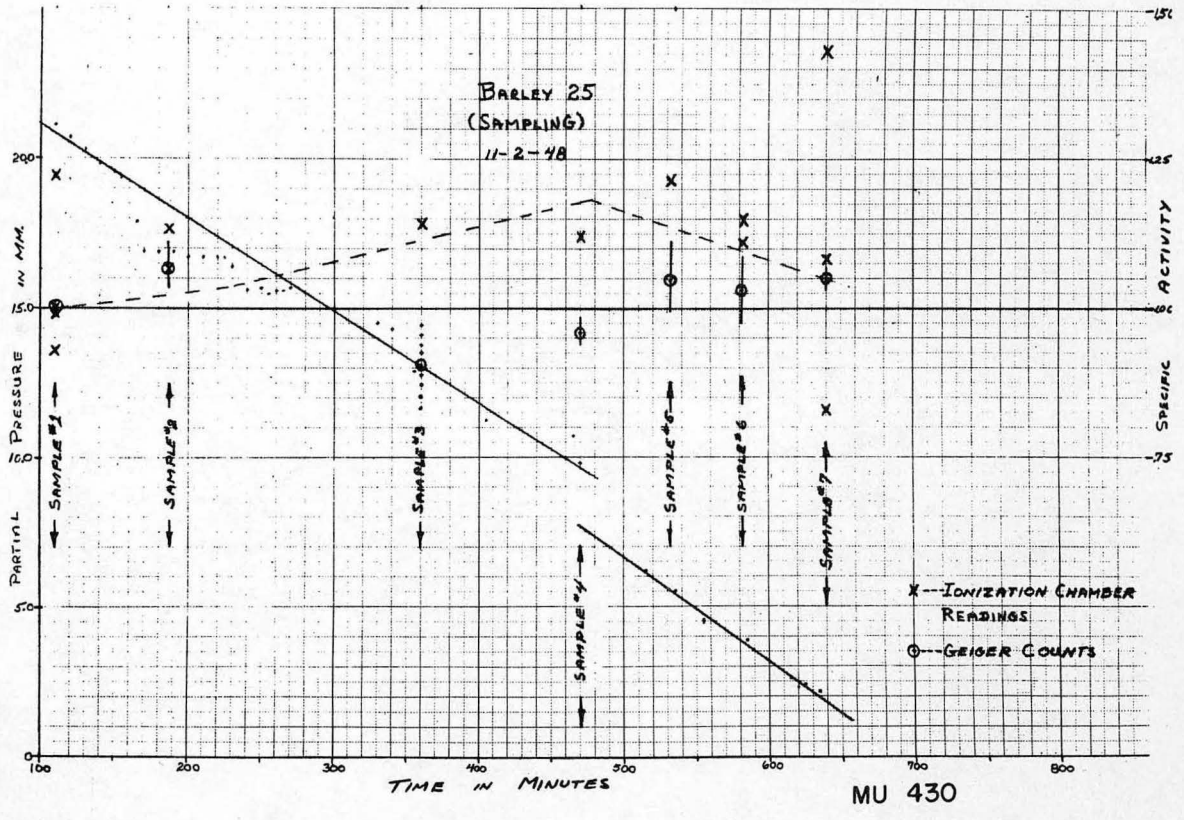
BARLEY 25
(SAMPLING)
11-2-48
PARTIAL PRESSURE IN MM.
SPECIFIC ACTIVITY
SAMPLE #1
SAMPLE #2
SAMPLE #3
SAMPLE #4
SAMPLE #5
SAMPLE #6
SAMPLE #7
X---IONIZATION CHAMBER READINGS
⊙---GEIGER COUNTS
TIME IN MINUTES
MU 430

Figure 16

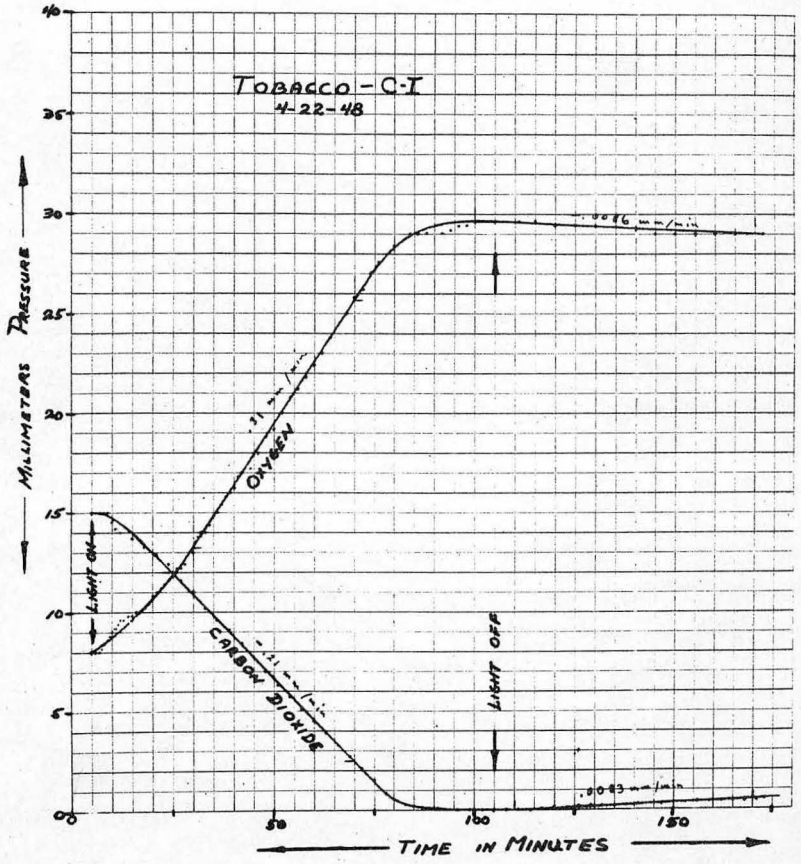
TOBACCO - C-I
4-22-48
MILLIMETERS PRESSURE
TIME IN MINUTES
OXYGEN
CARBON DIOXIDE
LIGHT ON
LIGHT OFF
.0046 mm/min
.0043 mm/min
40
35
30
25
20
15
10
5
0
50
100
150
MU 433

Figure 17

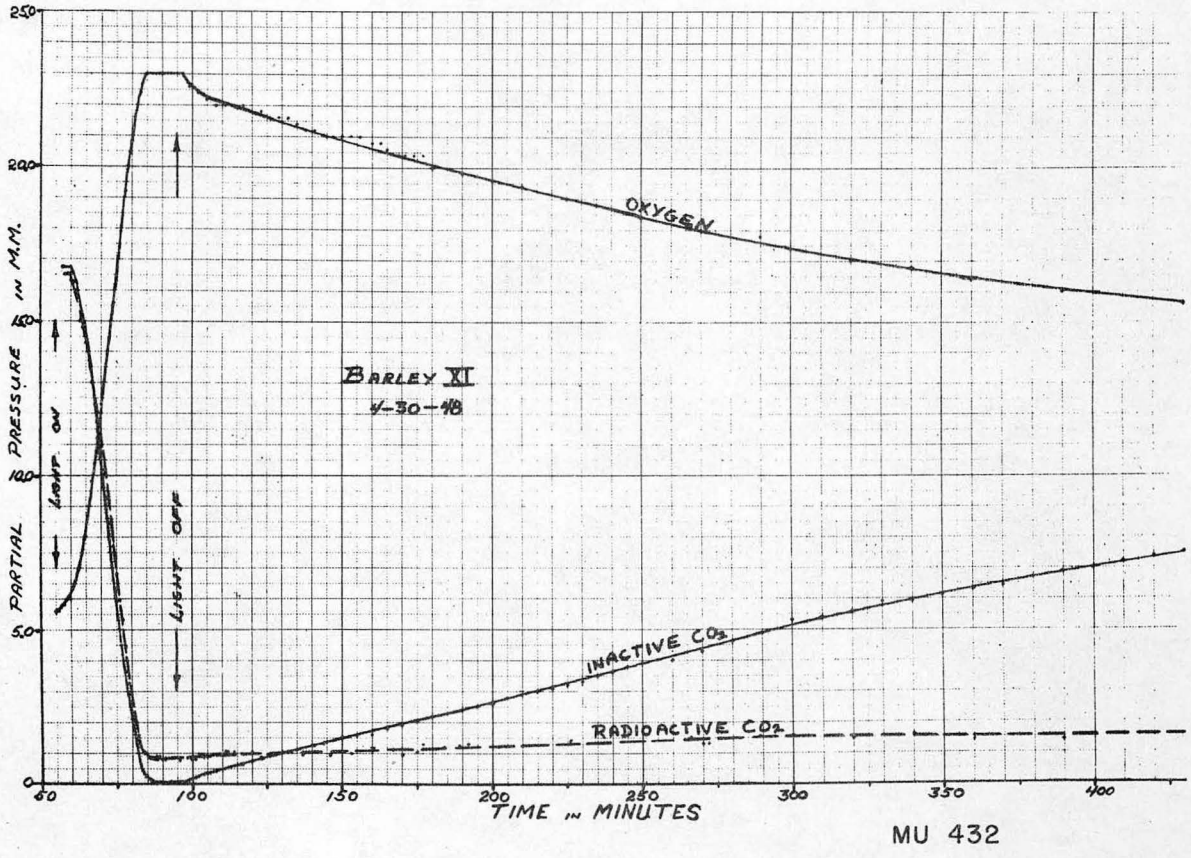
PARTIAL PRESSURE IN M.M.
250
200
150
100
50
0
LIGHT ON
LIGHT OFF
BARLEY XI
4-30-48
OXYGEN
INACTIVE CO2
RADIOACTIVE CO2
60
100
150
200
250
300
350
400
TIME IN MINUTES
MU 432

Figure 18

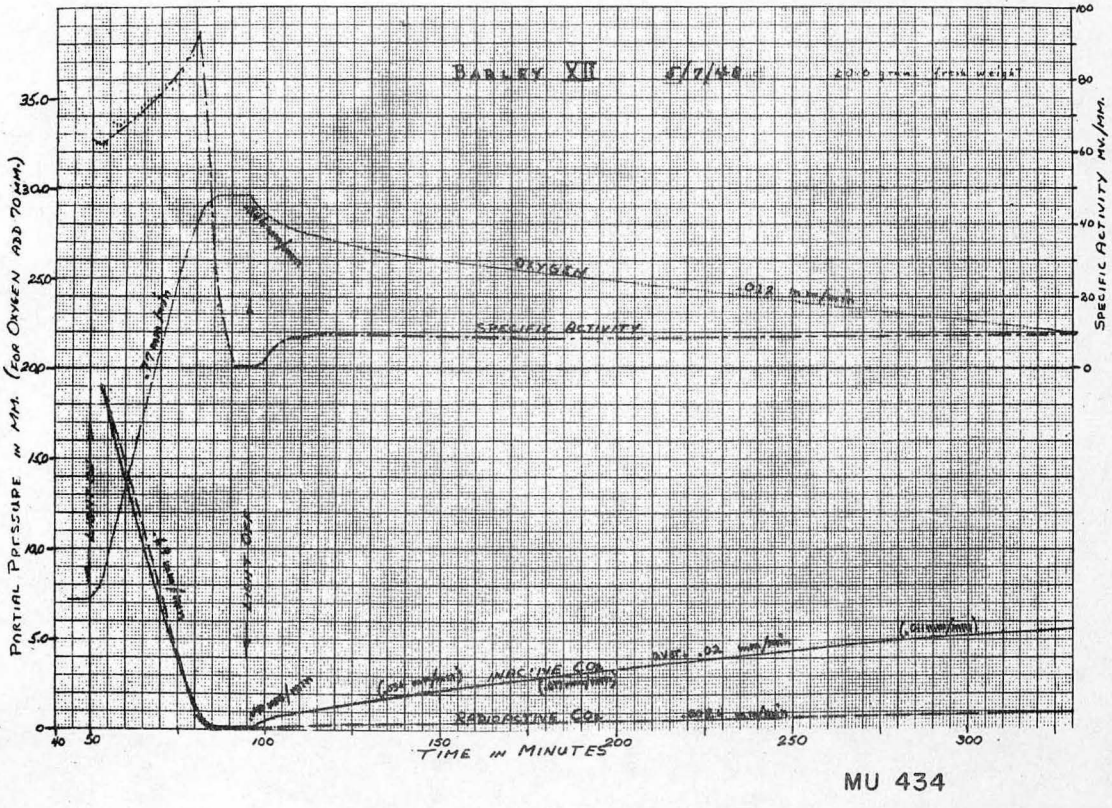
BARLEY XII
OXYGEN
SPECIFIC ACTIVITY
RADIOACTIVE CO2
PARTIAL PRESSURE IN MM. (FOR OXYGEN ADD 70 MM.)
SPECIFIC ACTIVITY MV./MM.
TIME IN MINUTES
MU 434

Figure 19

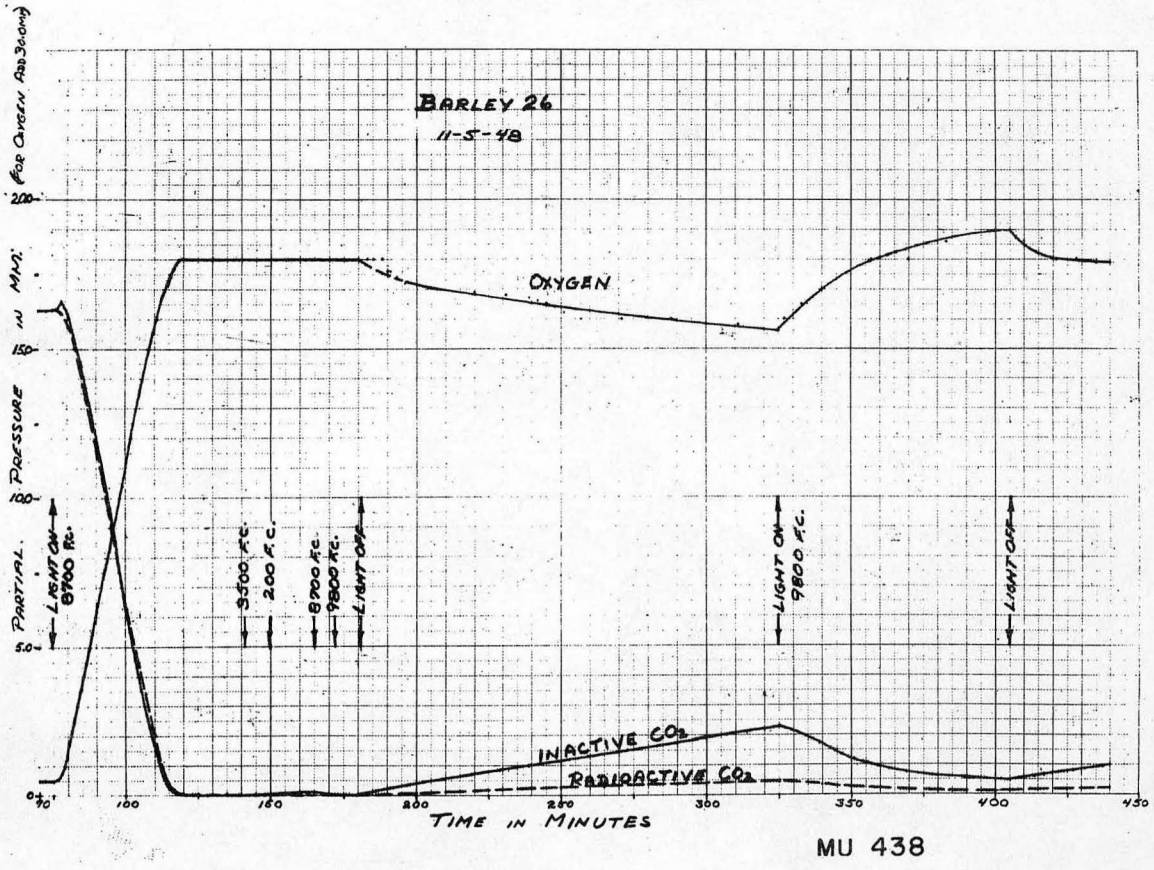
BARLEY 26
11-5-48
OXYGEN
INACTIVE CO2
RADIOACTIVE CO2
PARTIAL PRESSURE IN MM. (FOR OXYGEN ABSORP.)
TIME IN MINUTES
LIGHT ON 8700 FC.
3500 FC.
200 FC.
8700 FC.
9800 FC.
LIGHT OFF
LIGHT ON 9800 FC.
LIGHT OFF
MU 438

Figure 20

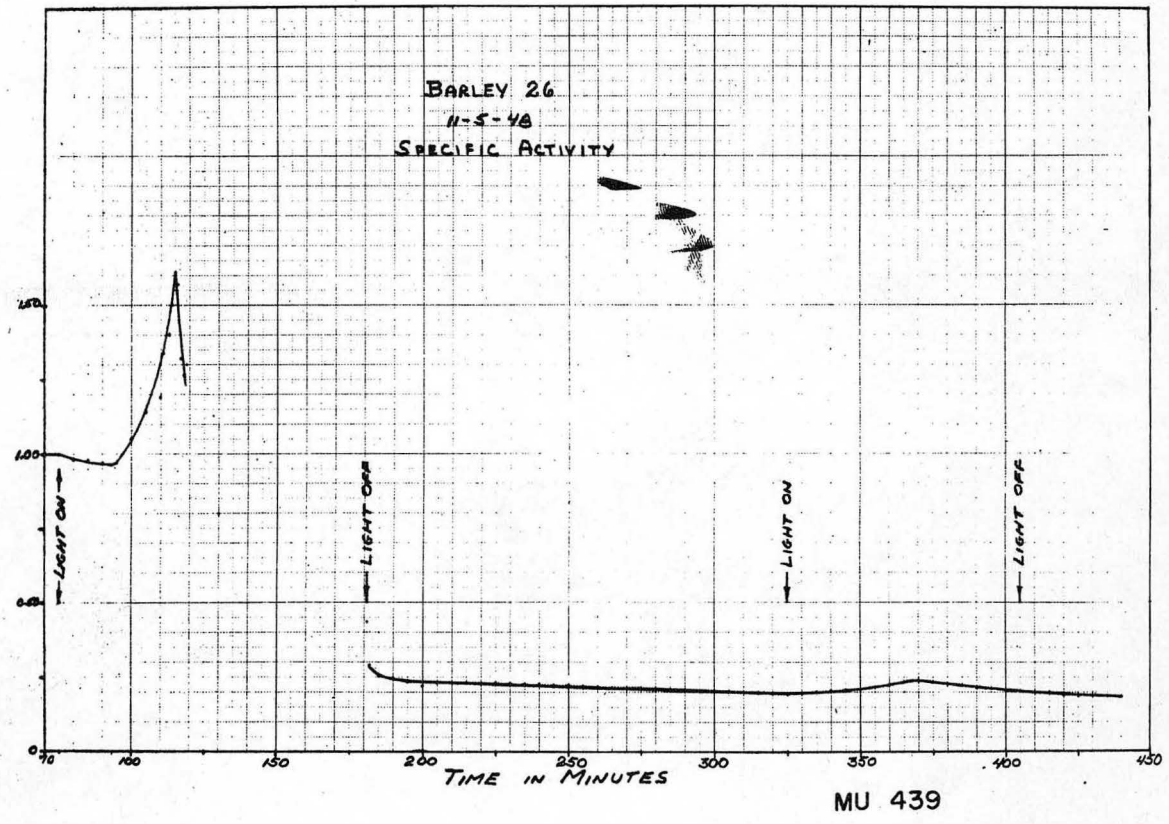
BARLEY 26
11-5-48
SPECIFIC ACTIVITY
1.50
1.00
0.50
0
LIGHT ON
LIGHT OFF
LIGHT ON
LIGHT OFF
70
100
150
200
250
300
350
400
450
TIME IN MINUTES
MU 439

Figure 21

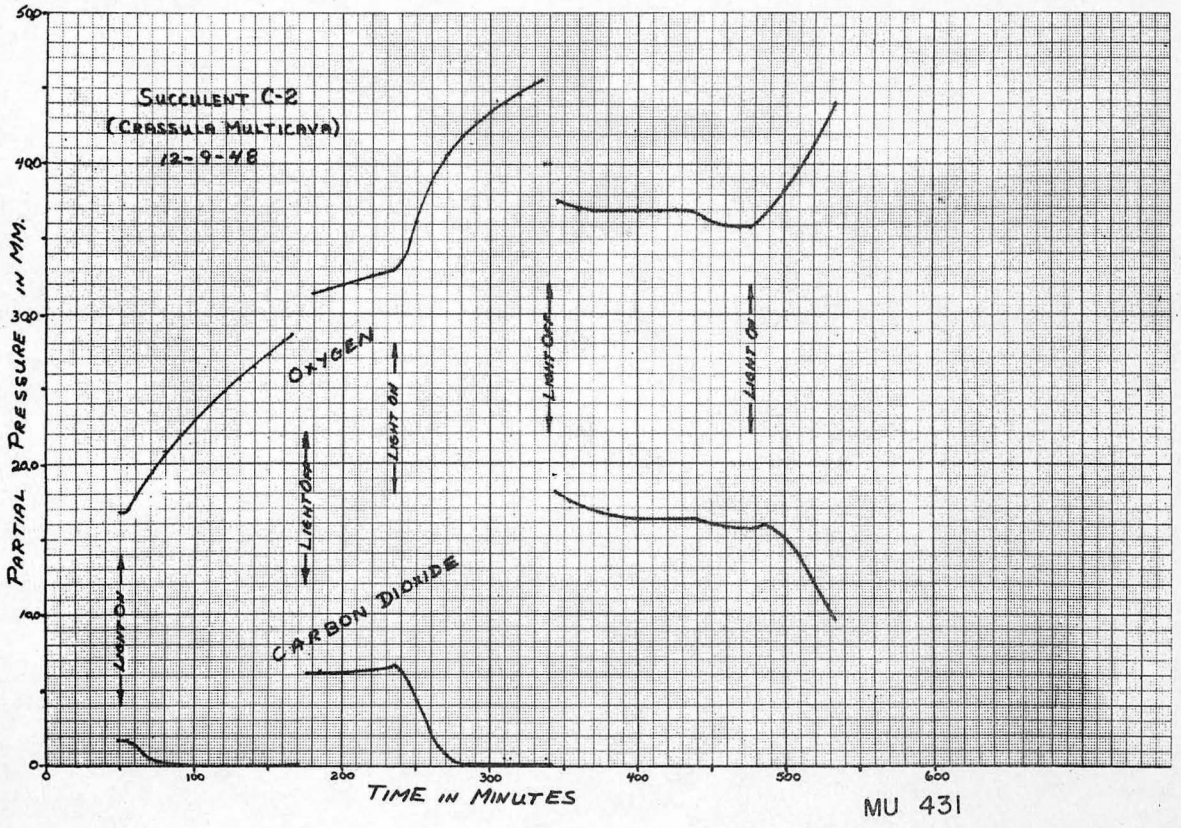
SUCCULENT C-2
(CRASSULA MULTICAVA)
12-9-48
PARTIAL PRESSURE IN MM.
TIME IN MINUTES
OXYGEN
CARBON DIOXIDE
LIGHT ON
LIGHT OFF
LIGHT ON
LIGHT OFF
LIGHT ON
0
100
200
300
400
500
600
MU 431

Figure 22

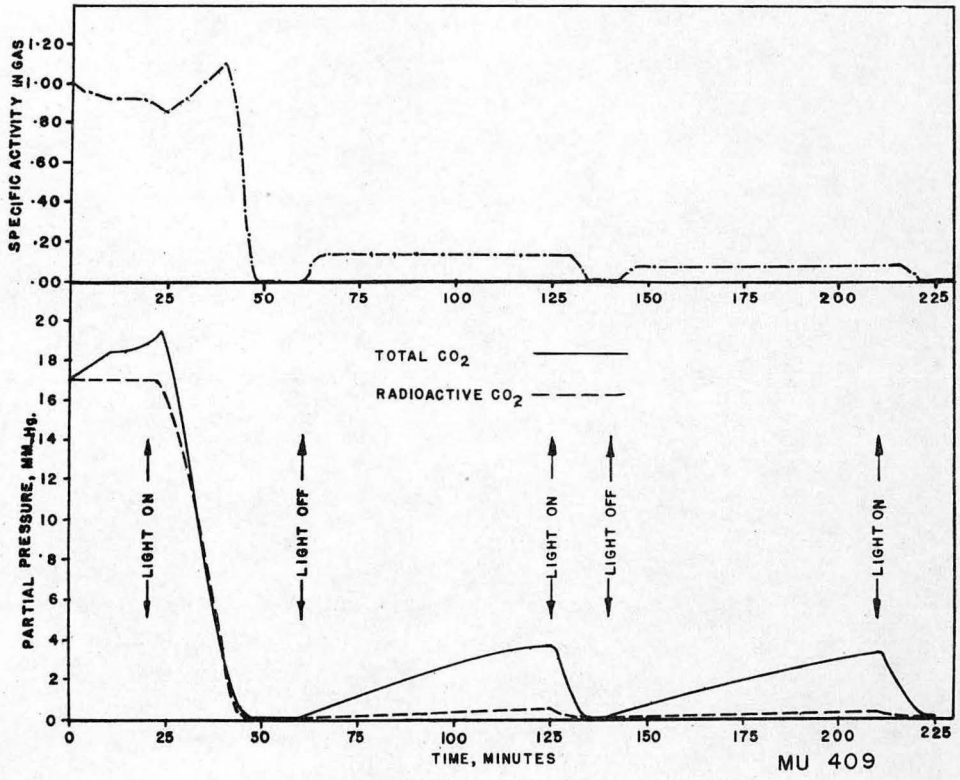

Figure 23

Barley 14

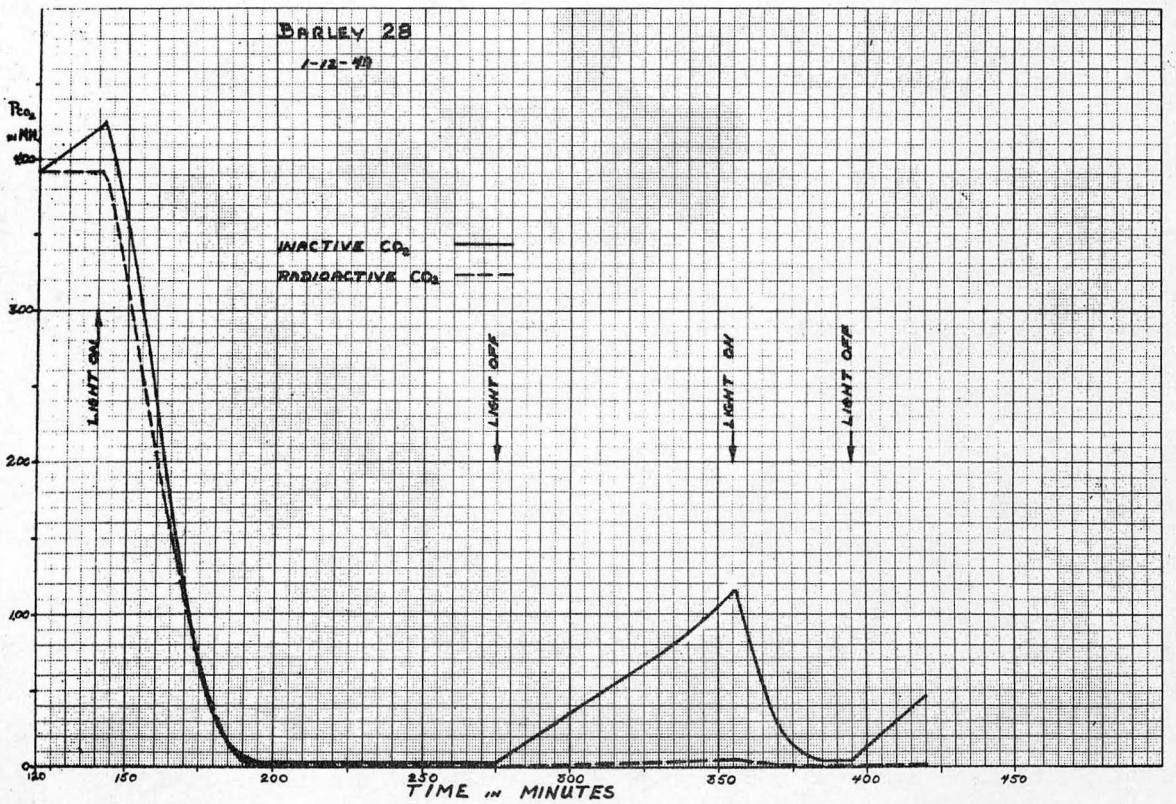
BARLEY 28
1-12-42
P_{CO_2} in MM
INACTIVE CO_2
RADIOACTIVE CO_2
LIGHT ON
LIGHT OFF
LIGHT ON
LIGHT OFF
300
200
100
0
120
150
200
250
300
350
400
450
TIME IN MINUTES
MU 436

Figure 24

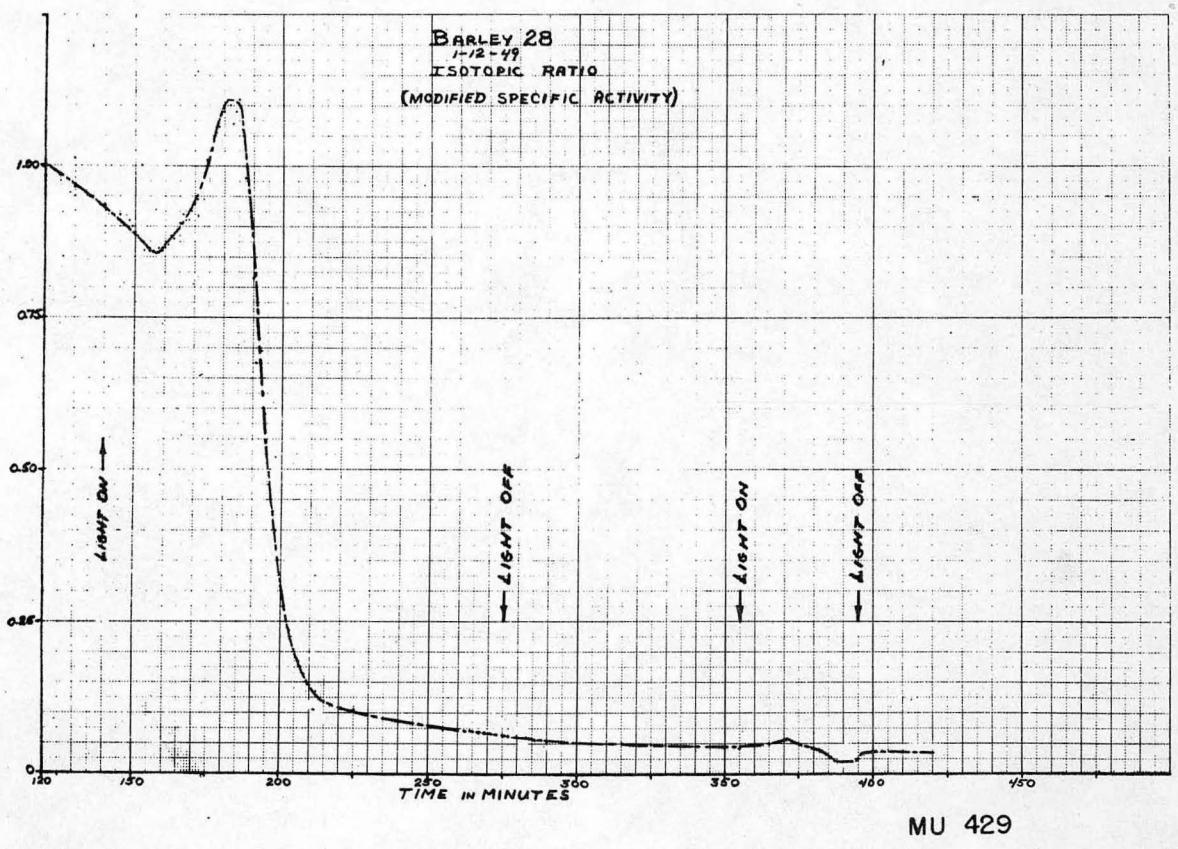
BARLEY 28
1-12-49
ISOTOPIC RATIO
(MODIFIED SPECIFIC ACTIVITY)
1.00
0.75
0.50
0.25
0
LIGHT ON
LIGHT OFF
LIGHT ON
LIGHT OFF
120
150
200
250
300
350
400
450
TIME IN MINUTES
MU 429

Figure 25

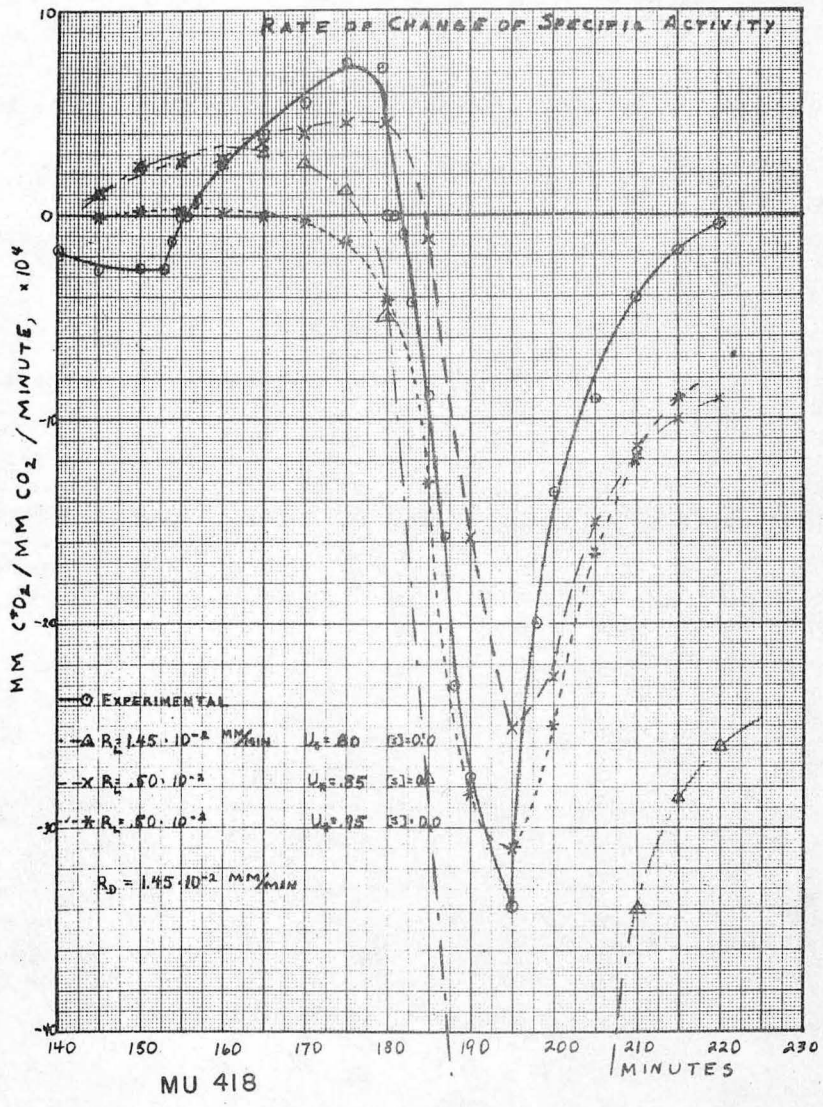

Figure 26

Barley 28

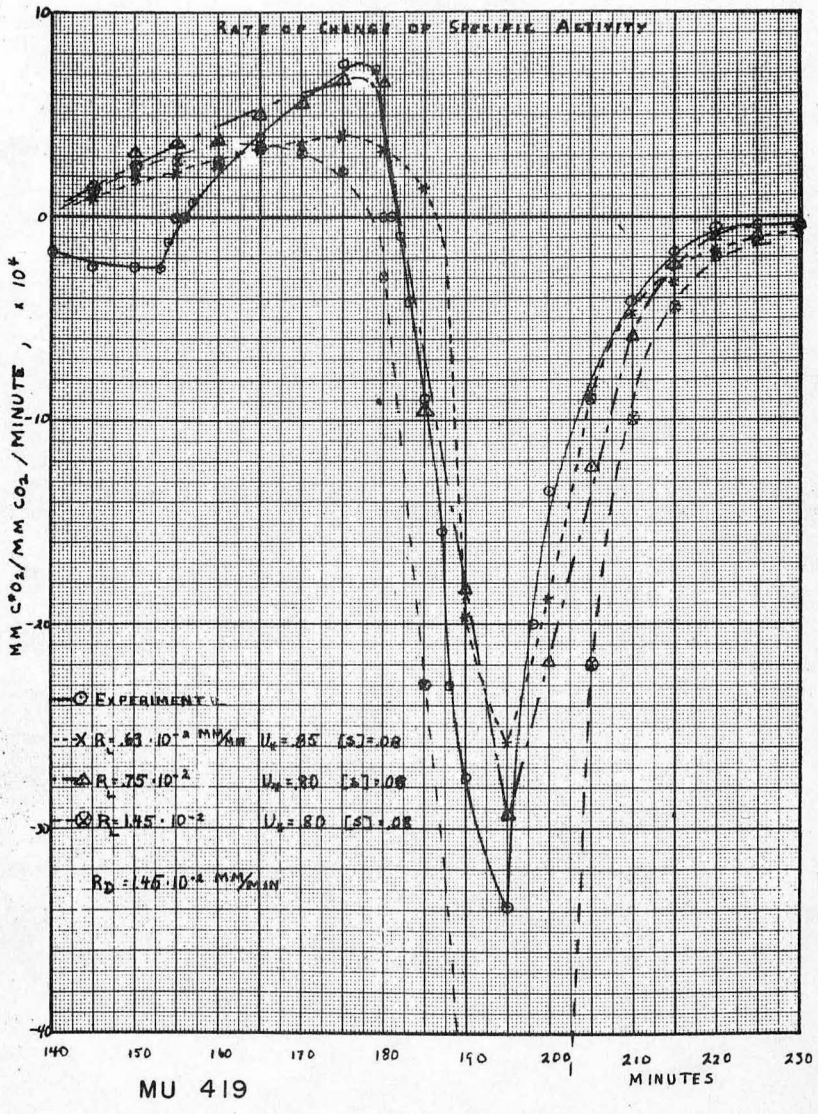

Figure 27

Barley 28

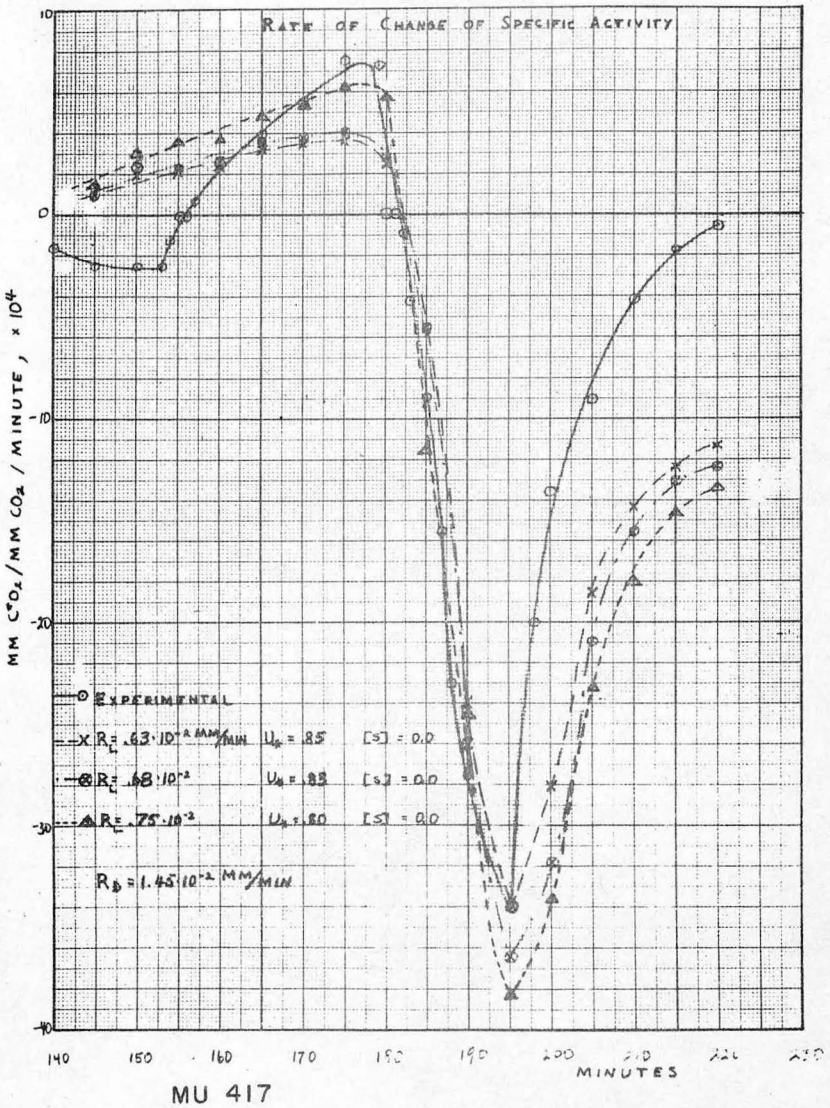

Figure 28

Barley 28

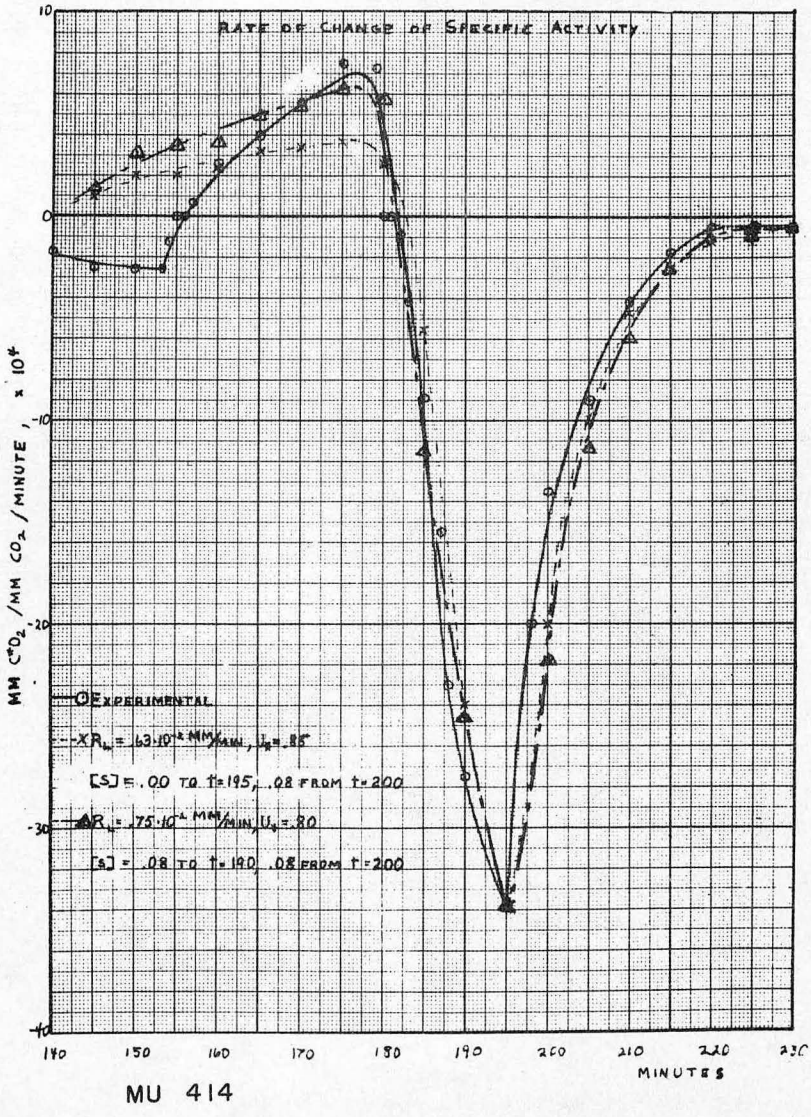

Figure 29

Barley 28

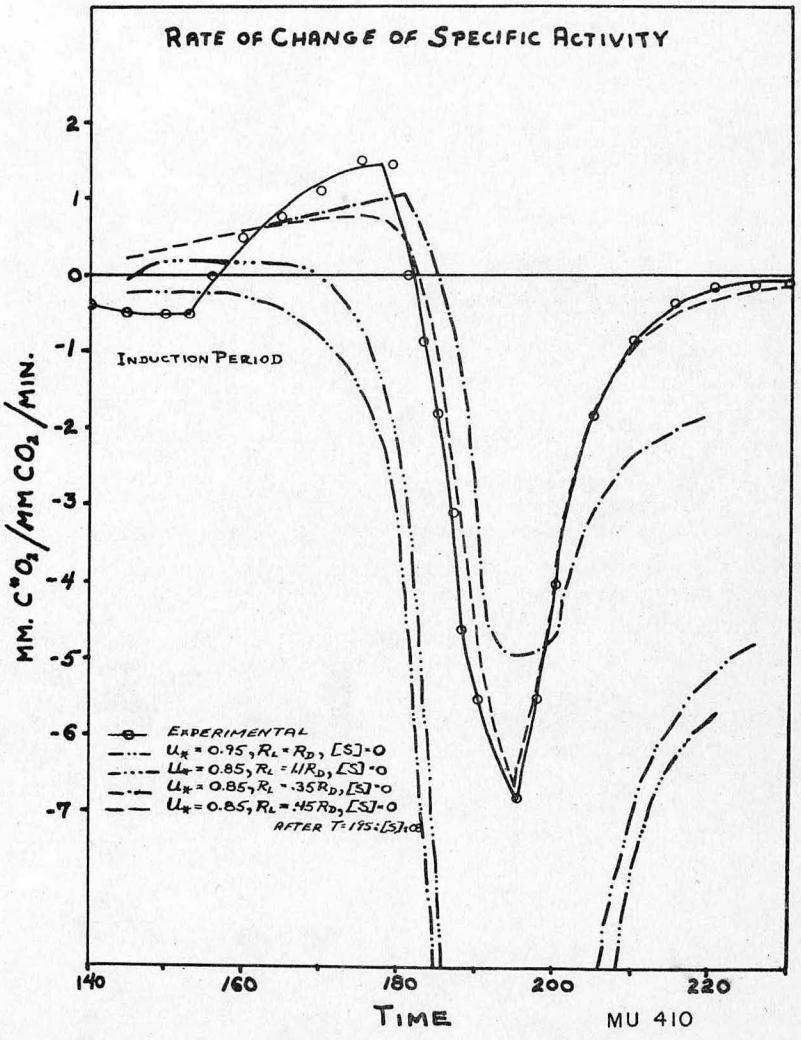

Figure 30

Barley 28

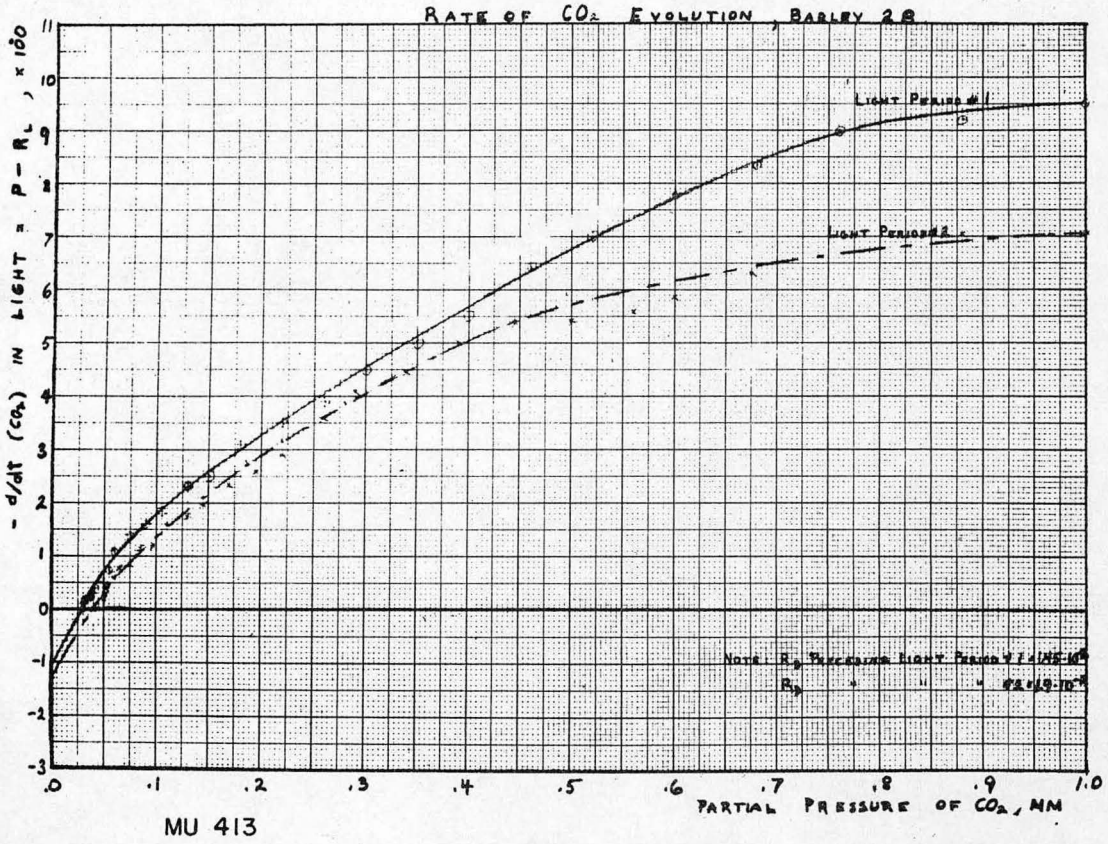
RATE OF CO_2 EVOLUTION, BARLEY 28
$-d/dt\ (CO_2)$ IN LIGHT $= P - R_L$, $\times 100$
LIGHT PERIOD #1
LIGHT PERIOD #2
PARTIAL PRESSURE OF CO_2, MM
MU 413

Figure 31

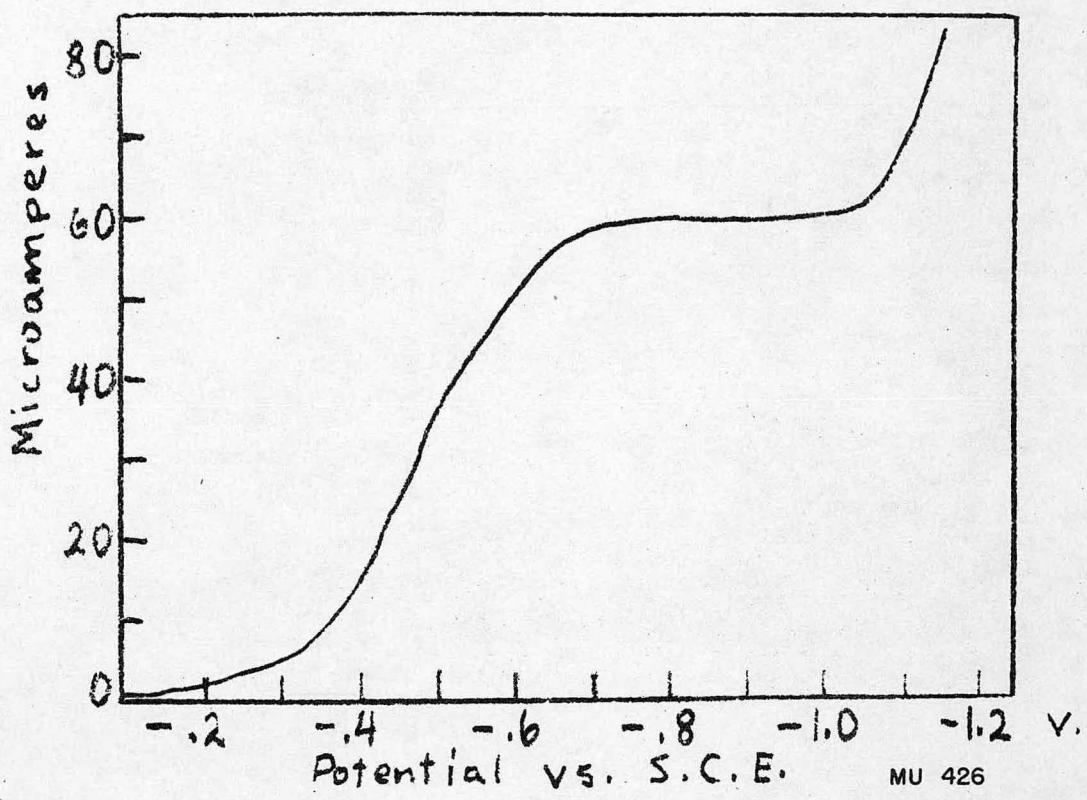

Figure 32

Oxygen Polarogram

(Kolthoff and Lingane, 6)

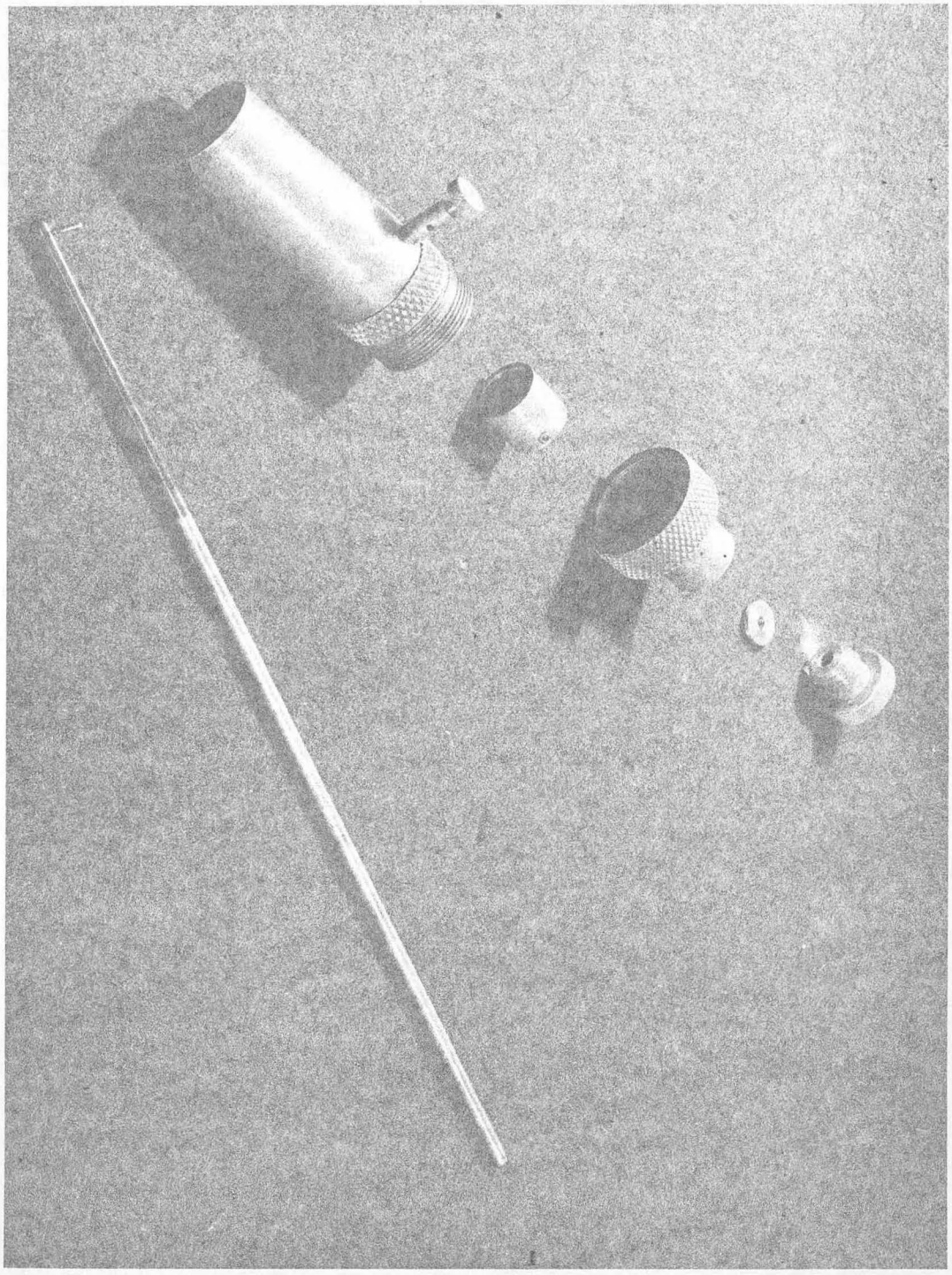

ROTATING MICROELECTRODE (EXPLODED VIEW)
SHAFT WITH PLATINUM WIRE, "OILITE" BEARINGS,
MERCURY CUP, "WILSON" SEAL.

FIG. 33

OZ 929

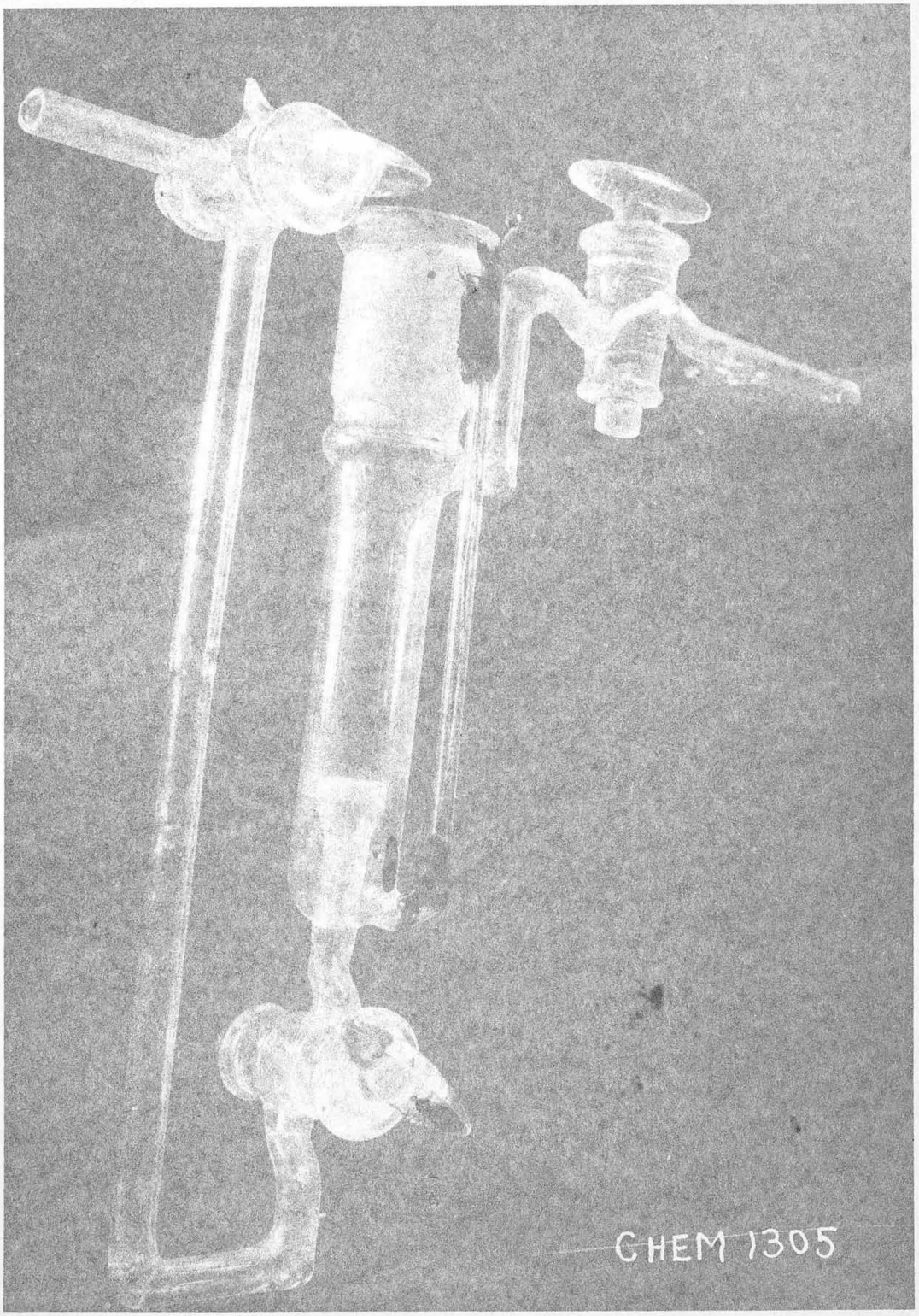

POLAROGRAPH CELL WITH BUBBLER

FIG. 34

OZ 928

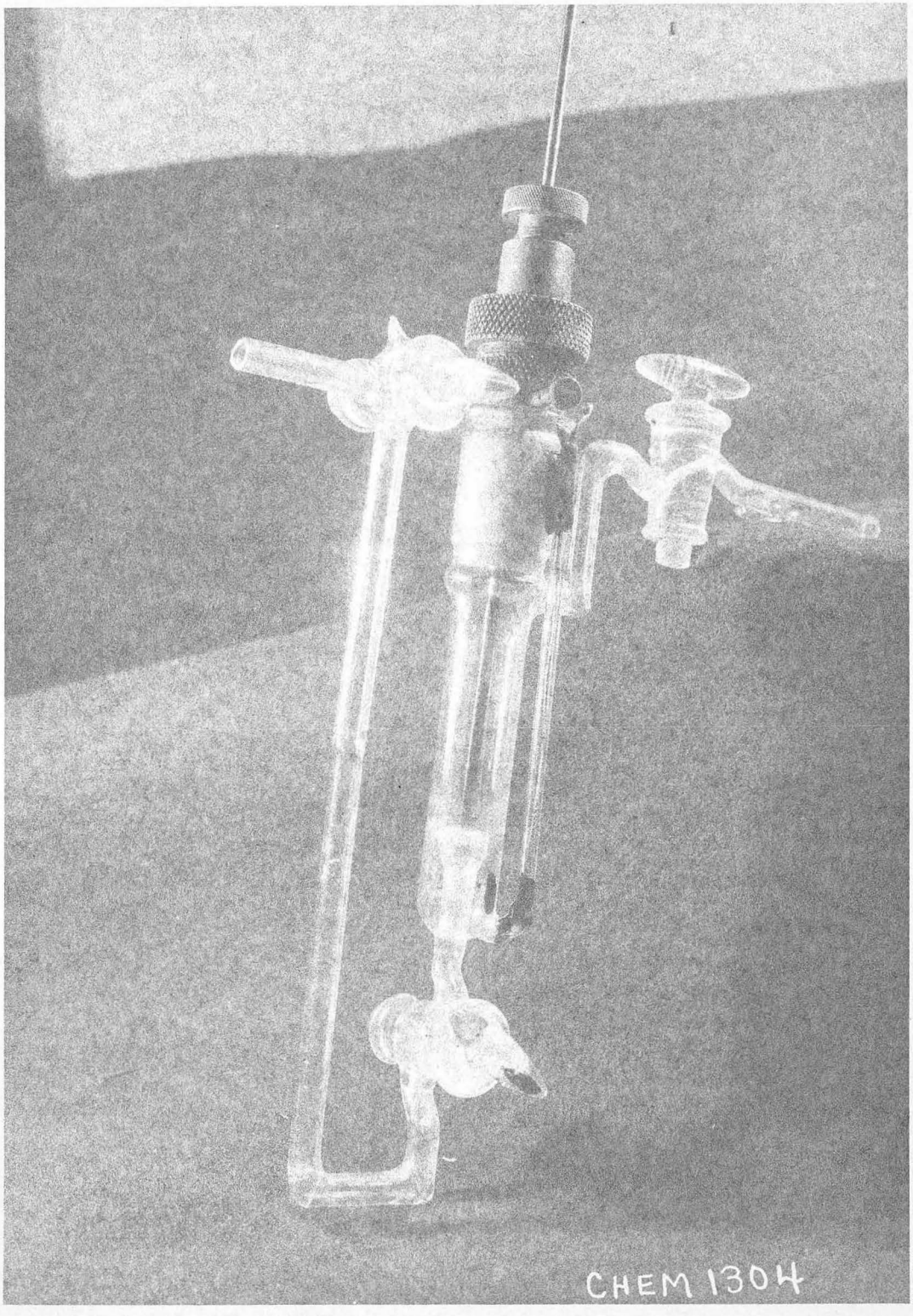

CELL AND ROTOR

FIG. 35

OZ 927

CELL CIRCUIT

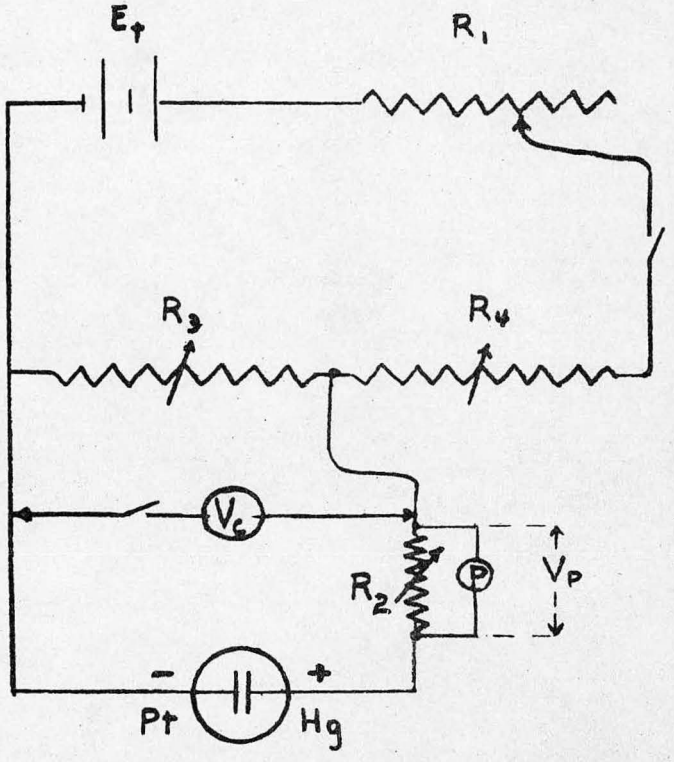

E_t = 6 v E_c = 0 - 1.5 v E_p = 0 - 5 mv

R_1 = 10,000 Ω R_2 = 10^6 Ω R_3 = R_4 = 1000 Ω

I_c = 0 - 100 microamps R_c = 10^4 - 10^6 Ω

Ⓟ is a G.E. recording potentiometer

MU 420

Figure 36

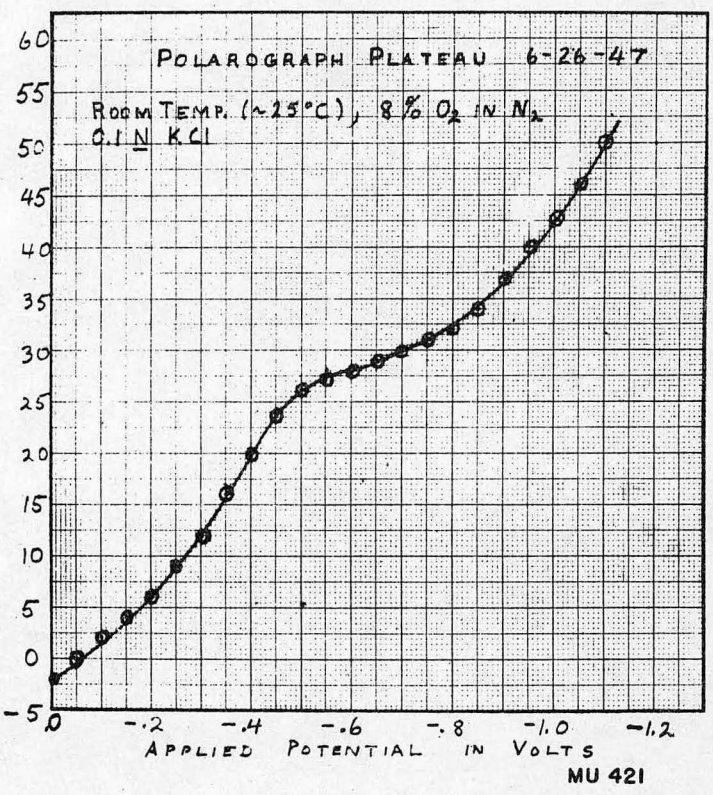
POLAROGRAPH PLATEAU 6-26-47
ROOM TEMP. (~25°C), 8% O_2 IN N_2
0.1 N KCl
60
55
50
45
40
35
30
25
20
15
10
5
0
-5
0
-.2
-.4
-.6
-.8
-1.0
-1.2
APPLIED POTENTIAL IN VOLTS
MU 421

Figure 37

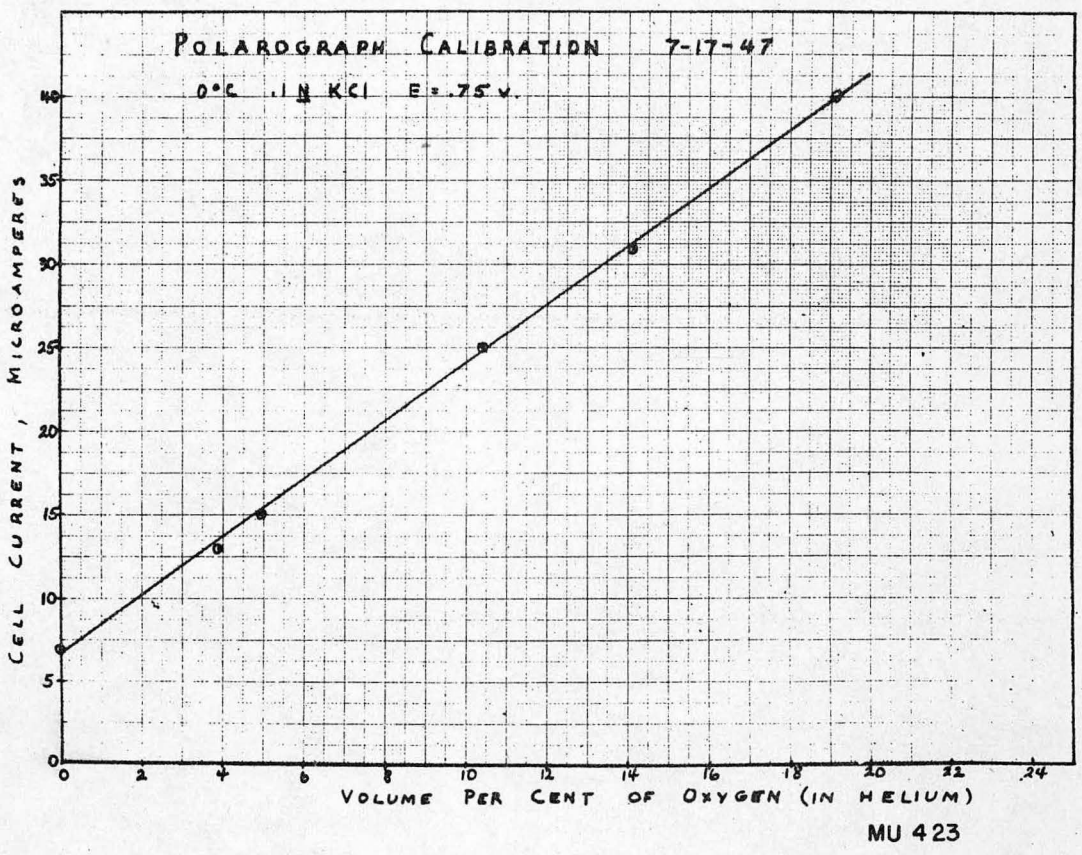
POLAROGRAPH CALIBRATION 7-17-47
0°C .1 N KCl E = .75 v.
CELL CURRENT, MICROAMPERES
0
5
10
15
20
25
30
35
40
0
2
4
6
8
10
12
14
16
18
20
22
24
VOLUME PER CENT OF OXYGEN (IN HELIUM)
MU 423

Figure 38

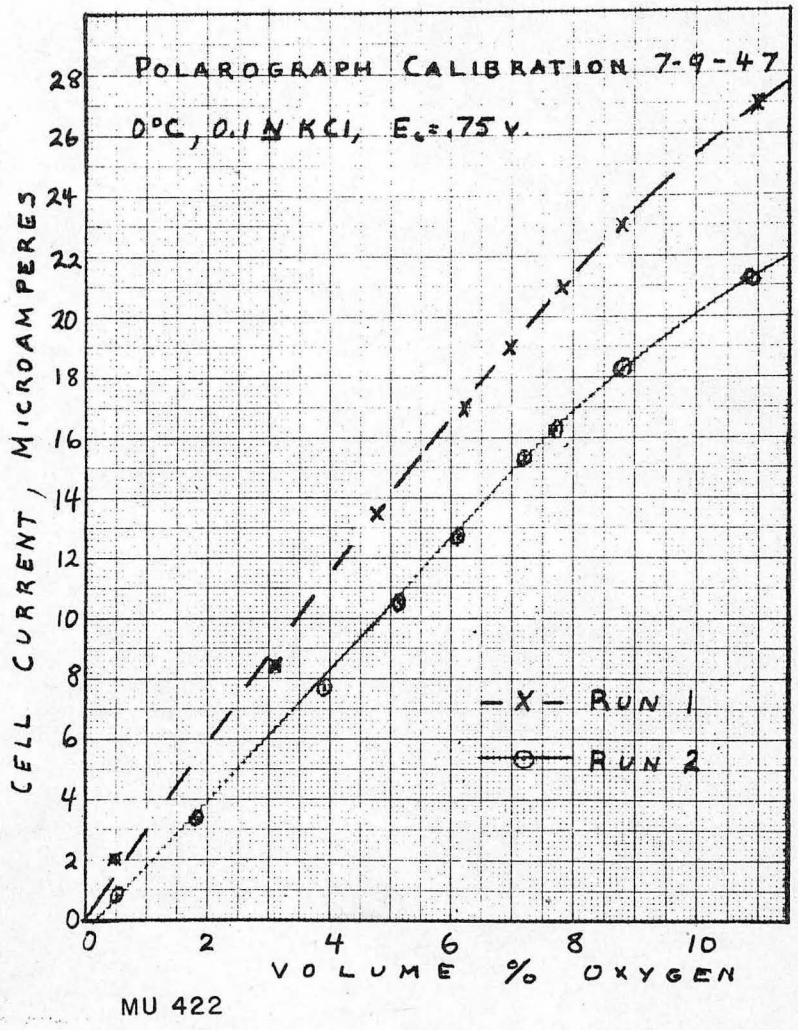
POLAROGRAPH CALIBRATION 7-9-47
0°C, 0.1 N KCl, E = .75 v.
CELL CURRENT, MICROAMPERES
VOLUME % OXYGEN
— X — RUN 1
— ⊙ — RUN 2
0
2
4
6
8
10
12
14
16
18
20
22
24
26
28
MU 422

Figure 39

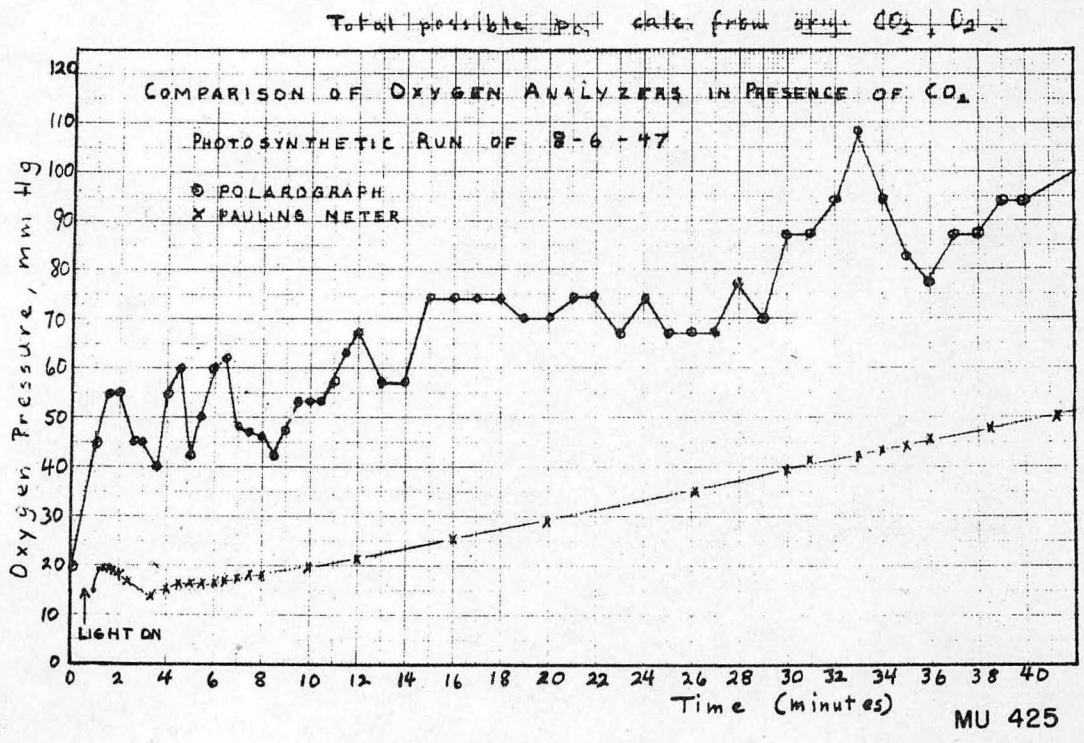
Total possible P_{O_2} calc. from oxy. CO_2 + O_2.
COMPARISON OF OXYGEN ANALYZERS IN PRESENCE OF CO_2
PHOTOSYNTHETIC RUN OF 8-6-47
© POLAROGRAPH
X PAULING METER
Oxygen Pressure, mm Hg
Time (minutes)
LIGHT ON
MU 425

Figure 40

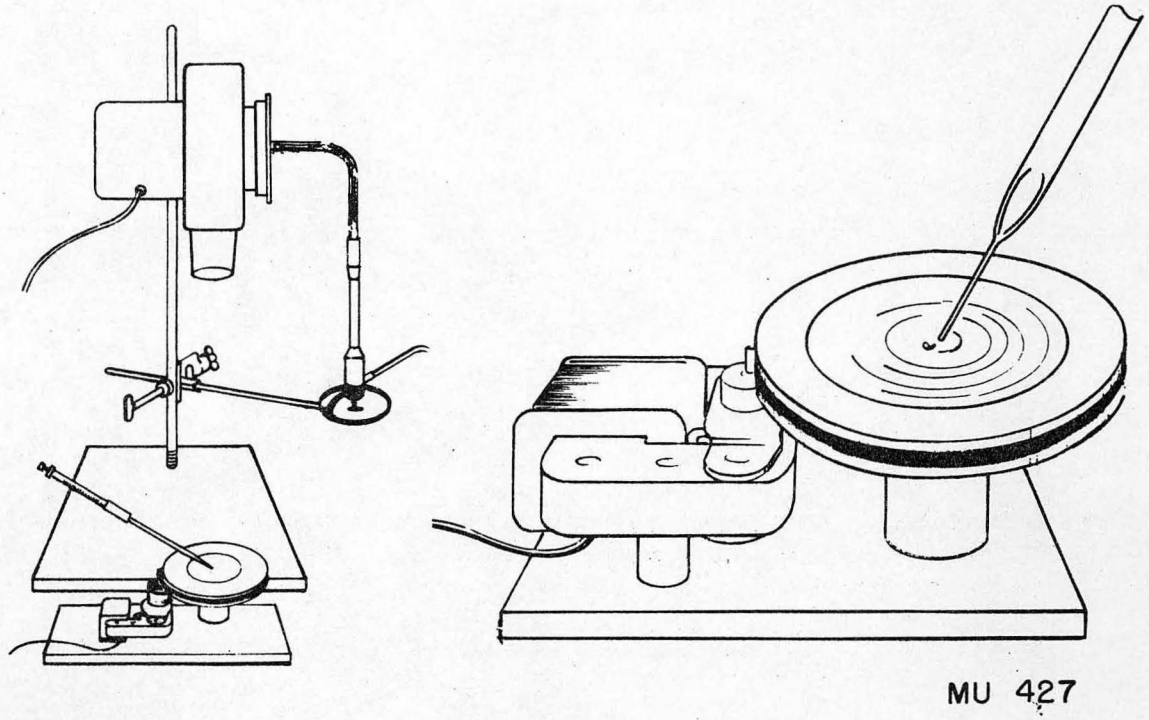

Figure 41

Turntable and Blower for Preparation of "Plates"

(After A. A. Benson, 46)

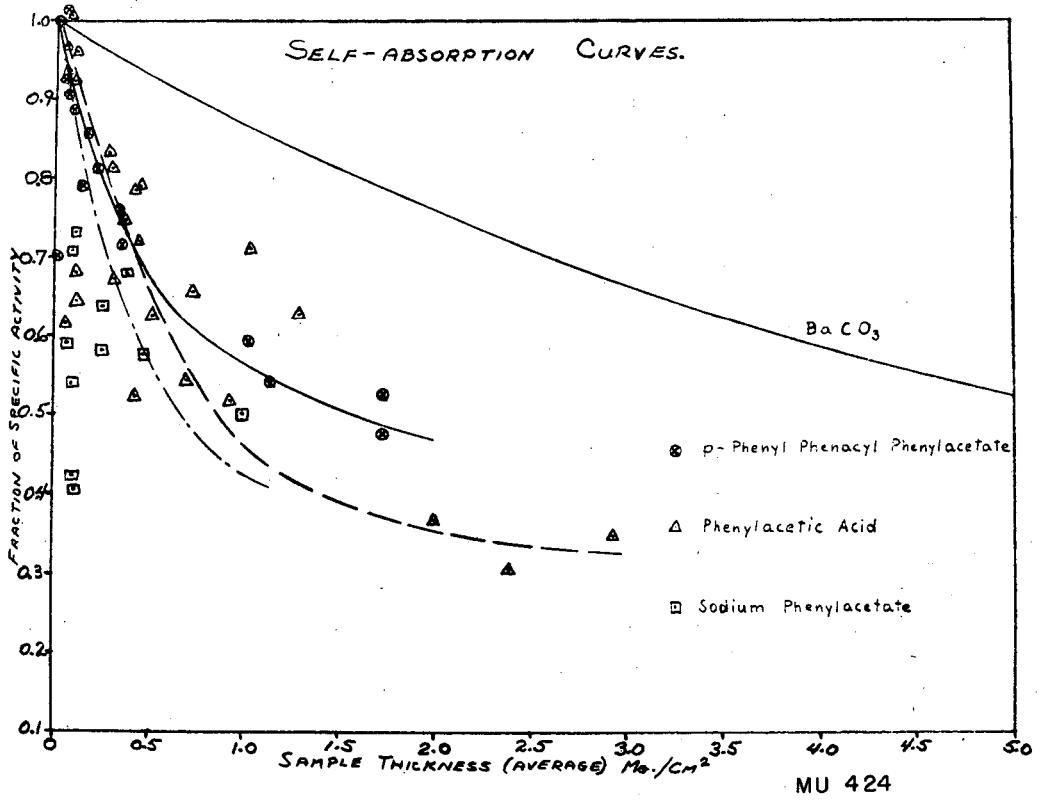
SELF-ABSORPTION CURVES.
FRACTION OF SPECIFIC ACTIVITY
1.0
0.9
0.8
0.7
0.6
0.5
0.4
0.3
0.2
0.1
0
0.5
1.0
1.5
2.0
2.5
3.0
3.5
4.0
4.5
5.0
SAMPLE THICKNESS (AVERAGE) Mg./CM²
BaCO₃
p-Phenyl Phenacyl Phenylacetate
Phenylacetic Acid
Sodium Phenylacetate
MU 424

Figure 42

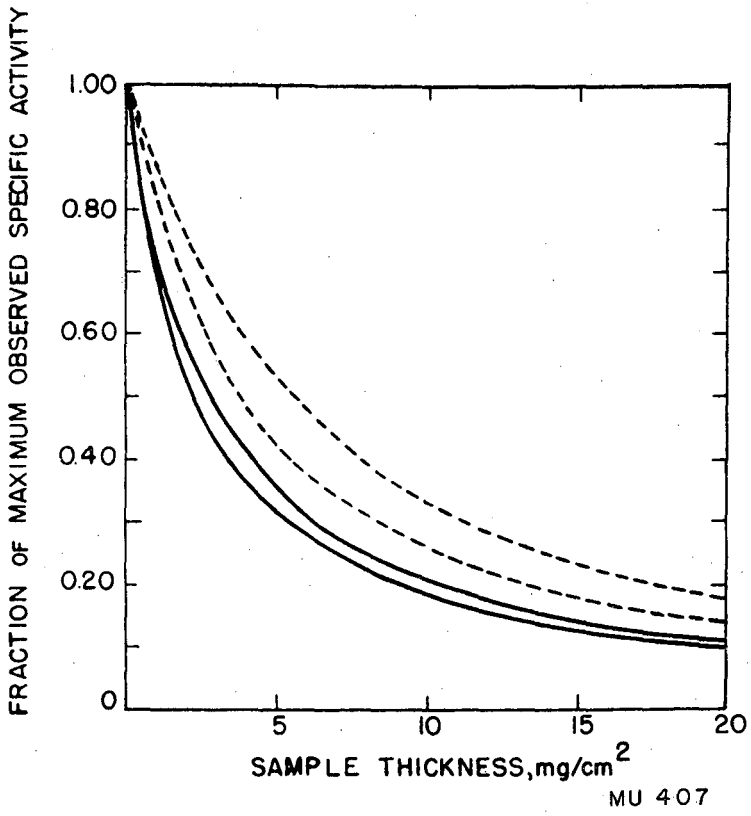

Figure 43

----------Thin-window Geiger counter at 30% geometry

Nucleometer at 50% efficiency

In each case, upper curve is for BaC^*O_3, lower curve for wax.

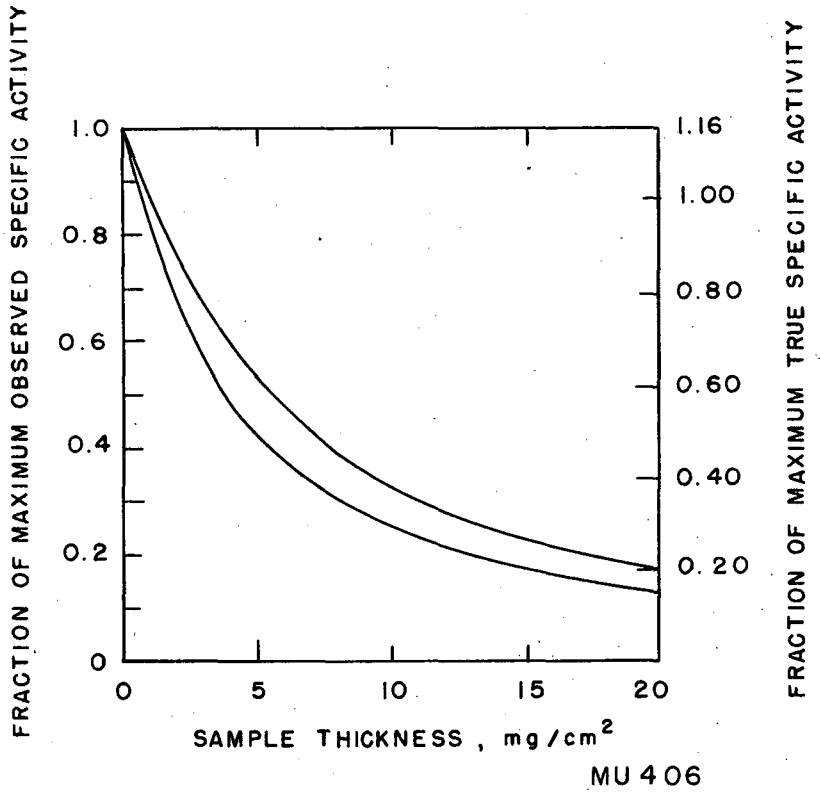

Figure 44

Self-absorption correction curves for barium carbonate and wax samples mounted on aluminum, as functions of sample thickness. (Data obtained at 30% geometry.) J is fraction of maximum specific activity. (Same as dotted lines of Figure 43.)